

Contents

1	Chapter1: Introduction	8
1.1	Background	8
1.1.1	Schizophrenia	8
1.1.2	Evidence for PFC dysfunction in schizophrenia	9
1.1.3	Evidence for altered excitation/inhibition balance in schizophrenia	11
1.1.4	Neurodevelopmental basis of schizophrenia	14
1.1.5	Identification of DISC1 as a psychiatric risk gene	15
1.1.6	Cellular function of DISC1	17
1.1.7	Summary of DISC1 mouse model behavioral findings	23
1.1.8	Cognitive impairment as an endophenotype of DISC1 genetic variation	26
1.2	Summary of performed experiments	30
2	Cell type-specific effects of reduced DISC1 expression	32
2.1	Introduction	32
2.2	Methods	35
2.2.1	Animals	35
2.2.2	Stereotaxic surgery	36
2.2.3	Viral constructs	36
2.2.4	Electrophysiological recordings of miniature events	37
2.2.5	Electrophysiological recording of GABA PPR	38
2.2.6	Data analysis and statistics	39
2.3	Results	40

2.3.1	Changes in spontaneous inhibitory transmission onto pyramidal neurons .	40
2.3.2	Age-dependent changes in spontaneous inhibitory transmission in DISC1 HET and WT mice	40
2.3.3	Postnatal DISC1 knockdown	43
2.3.4	Changes in spontaneous transmission onto PV+ interneurons	43
2.3.5	Changes in spontaneous transmission onto SST+ interneurons	45
2.3.6	Altered short-term plasticity at PV-PN synapse in DISC1 HET mice. . .	47
2.3.7	Short-term plasticity at the SST-PN synapse is unaltered in DISC1 HET mice	50
2.3.8	Distinct decay kinetics of GABA transmission from PV vs. SST interneu- rons	52
2.3.9	Conclusions	54
3	Feedforward inhibition in the MD-mPFC projection	58
3.1	Introduction	58
3.1.1	The role of PV+ INs in thalamocortical projections	60
3.1.2	General anatomy/connectivity of MD	62
3.1.3	MD dysfunction in schizophrenia	68
3.1.4	MD function	69
3.1.5	Evidence for MD recruitment of PV interneurons	73
3.2	Methods	74
3.2.1	Animals	74
3.2.2	Stereotaxic surgery, viral constructs, and perfusion	74
3.2.3	Electrophysiology	76
3.2.4	PV monosynaptic rabies tracing from mPFC	77
3.2.5	Data analysis	77
3.3	Results	78
3.3.1	PV monosynaptic rabies tracing from mPFC	78
3.3.2	Anatomical organization of the MD-PFC circuit	79
3.3.3	Optogenetic activation of MD-dACC circuit	83

3.3.4	MD-evoked IPSCs are likely disynaptic, mediated by PV INs	85
3.3.5	Thalamocortical transmission onto PV INs and PNs	88
3.3.6	Relative timing of MD-evoked EPSCs and IPSCs	94
3.3.7	Chemicogenetic inhibition of PV+ interneurons during MD axon stimulation	99
3.3.8	Optogenetic silencing of PV+ interneurons during MD axon stimulation .	102
3.3.9	Suppressing SST interneurons while stimulating MD terminals	104
3.3.10	PV halorhodopsin effect on PN PSPs	106
3.3.11	E/I balance in the MD-mPFC pathway	108
3.3.12	Conclusions	111
4	Discussion	116
4.0.13	PV interneuron function in DISC1 LI model	116
4.0.14	Future perspectives	121
	Appendices	147
.1	Supplementary figures	147
.2	List of abbreviations	149

List of Figures

1.1	Proposed model of EI balance in schizophrenia	13
1.2	DISC1 chromosomal translocation: Scottish pedigree and gene structure	20
1.3	DISC1 animal models summary	25
1.4	Thesis map	29
2.1	Spontaneous excitatory & inhibitory transmission onto layer II/III PN in mPFC	42
2.2	Spontaneous excitatory transmission onto PV+ INs in mPFC	44
2.3	Spontaneous excitatory transmission onto SST+ INs in mPFC	46
2.4	Spontaneous inhibitory transmission onto SST+ INs in mPFC.	47
2.5	Altered short-term plasticity at PV-PN synapse in DISC1 HET mice	49
2.6	Short-term plasticity at the SST-PN synapse is unaltered in DISC1 HET mice .	51
2.7	Distinct short-term plasticity and decay kinetics of GABA transmission from PV vs. SST interneurons	53
3.1	Summary of existing MD-mPFC anatomical data	64
3.2	Retrograde tracing from dACC and PrL reveals topographical separation of tha- lamic projection	67
3.3	mPFC PV rabies tracing reveals dense input from MD	80
3.4	Retrograde tracing from MD to mPFC	81
3.5	MD axons colocalize with superficial PV+ INs in dACC	82
3.6	MD axon stimulation recruits excitation & inhibition	84
3.7	Evidence for disynaptic nature of MD-evoked IPSCs	86
3.8	Feedforward IPSCs resemble IPSCs directly mediated by PV INs	87

3.9	MD directly activates PV interneurons in layer 3 dACC	90
3.10	Consistent MD response properties in DISC1 WT and HET mice	93
3.11	Reliable timing of MD-evoked IPSCs	96
3.12	MD-evoked IPSC latency is consistent with disynaptic feedforward inhibition . .	98
3.13	Chemicogenetic inhibition of PV+ INs during MD axon stimulation	101
3.14	Optogenetic silencing of PV+ INs during MD axon stimulation	103
3.15	Optogenetic silencing of SST+ INs during MD axon stimulation	105
3.16	Halorhodopsin expression	107
3.17	PV+ IN optogenetic silencing effect on MD-evoked PSPs	108
3.18	Reduced feedforward inhibition onto DISC1 HET pyramidal neurons	110
1	Generation of DISC1 locus impairment mouse	147
2	BLA to mPFC projection	148

Acknowledgments

I'd like to thank my PhD advisor Bo Li for the support and guidance he's given me over the last 4 years. I'm especially grateful for the freedom I've had to pursue my interests within the lab. Jones Laboratory is a unique place to do science, not just because it's a 120 year old building, but because it's inhabited by some of the most passionate scientists I've met. I'd like to thank the members of the Li and Shea lab past and present who have been my scientific companions, who have offered assistance and guidance and constantly broadened my scientific perspective. It's been remarkable to watch the lab grow, and I look forward to reading Li lab papers for years to come.

This thesis wouldn't have been possible without the guidance and feedback from my committee members: Steve Shea, Josh Huang, and Tony Zador. I would also like to thank Barry Connors for agreeing to be my external examiner and the tremendously constructive feedback that he provided.

I would like to thank Steve Shea, my academic mentor, who has been a great source of encouragement throughout my PhD. Whether educating me about 90s indie rock or sitting down to chat after in-house about some crisis I was having, he has made my time at Cold Spring Harbor more enriching and enjoyable. I hope to encounter people who are as generous as he is in my next step, and will strive to offer that generosity to my future colleagues.

I would like to thank the WSBS administration - Dawn, Leemor, Kim G, Alyson, Keisha, Kim C, Carrie and Alex for organizing the recruitment weekend that brought me here for the first time, to managing our hectic first year schedule, and always being there for help and advice. Thank you for making the school run so smoothly, even when experiments didn't.

I'm grateful to my family who have always encouraged and supported me in life. From my fellow biologist sister, who I had the pleasure of working with at CSHL for a short while and visiting her at her current research post in Panama, to my computer scientist brother who keeps offering to help teach me to program (I should really take him up on that), I'm thankful to you for keeping me grounded, and I cherish the time we have together more with each passing year. None of this would have been possible without my parents, who offered me so many

opportunities growing up.

I'd also like to thank the scientific mentors I've had along the way, from Mrs. Carlson in A.P. Bio, to Dr. Ed Stricker, my unforgettable professor for Intro to Neuroscience, to Dr. Robert Sweet, my undergraduate mentor who encouraged my early ventures in critical scientific thinking, and the colleagues I've had at CSHL, especially Mario Penzo and Haohong Li, whom I consider my scientific mentors. I'm also grateful for the many research opportunities I had as an undergraduate, supported by the Center for Neuroscience at the University of Pittsburgh (CNUP), the SURE summer program at Emory University, and the NIMH research fellowship that exposed me to the clinical psychiatric setting and has left a lasting impression on me.

I wouldn't have survived the first year at WSBS without my classmates. We danced on Fridays in Bush Hall with "meetings people" and traveled the world together, while still managing to get some science done. I think you're all remarkable people, and I marvel at your accomplishments. I can't wait to see what you do in the future.

Last but not least I'd like to thank Colin, the most supportive and complementary (complimentary too) partner I can imagine.

Chapter 1

Chapter1: Introduction

1.1 Background

1.1.1 Schizophrenia

Schizophrenia (SZ) is a mental disorder that profoundly alters the way in which people perceive their external and “internal” worlds, and in turn, how they interact with them. “Positive” symptoms refer to behaviors that are present in an individual with SZ that are absent from the normal population and include delusions, hallucinations, and disorganized speech. Conversely, the “negative” symptoms refer to normal behaviors that are absent in patients with schizophrenia and include social withdrawal, diminished emotional expression, and avolition (Tandon *et al.*, 2013). While cognitive deficits are a prominent feature of SZ psychopathology, cognitive impairment is not a diagnostic criteria in the DSM-5, as it doesn’t sufficiently distinguish schizophrenia from other psychotic disorders (Barch & Keefe, 2010).

Schizophrenia affects more than just mental health; factors such as personal care neglect (Hayes *et al.*, 2012), antipsychotic drug side effects such as weight gain (Sicras-Mainar *et al.*, 2008), comorbid addiction (Winklbaur *et al.*, 2006) (as high as 90% of people with schizophrenia are smokers) (Kelly & McCreadie, 2000), and increased lifetime risk of suicide ($\sim 5\%$) (Hor & Taylor, 2010) all contribute to the ~ 15 years reduction in average lifespan seen in people with

SZ (Wahlbeck *et al.*, 2011). Individuals with SZ are overrepresented among some of the most marginalized groups in society including the homeless, unemployed, unmarried, incarcerated, and chronically hospitalized (Carpenter & Koenig, 2008). As a result, SZ is often associated with dependence, placing emotional and financial strain on families and substantial economic burden on society at large (Lewis & Sweet, 2009). In order to improve the outlook for individuals with SZ, new therapeutics need to be designed that adequately treat negative and cognitive symptoms in addition to positive symptoms, while causing minimal adverse side-effects.

Schizophrenia has a strong genetic component, although its genetic underpinnings are complex and poorly understood. Monozygotic twins have a concordance rate of approximately 50%; an over 70-fold enrichment above the .7% prevalence of SZ among the general population (Kellendonk *et al.*, 2009). Most of the genetic risk factors identified are common allelic variants that individually confer only a small risk (Consortium, 2009). However, other studies have identified structural variants such as copy number variants (CNVs)– either duplications or deletions of large genomic regions– that confer a greater disease liability. The picture that has emerged is that schizophrenia may be both a “common disease-common allele” and “common disease-rare allele” genetic disorder (Arguello & Gogos, 2012; Walsh *et al.*, 2014). However, a major barrier to uncovering a genetic basis for the disorder is that “schizophrenia” may be an umbrella term for a “diverse set of very rare genetic conditions that happen to share similar symptoms” (Mitchell, 2012). While it’s unclear how many cases of schizophrenia rare structural variants may account for, their high penetrance make them a good candidate for study in animal models.

1.1.2 Evidence for PFC dysfunction in schizophrenia

Cognitive symptoms are increasingly recognized as a core symptom of SZ – impairments in working memory (WM), attention, and executive function are present prior to the onset of psychosis and are a mainstay throughout the course of the disease. Working memory has been described as a “mental workspace” where items of information are held, shifted around, and associated to other ideas and incoming information (Goldman-Rakic & Selemon, 1997). The contents of WM are constantly updated and used to guide actions that accord with one’s internal

goals across time. Efficient WM relies on the ability to buffer temporarily stored representations against interference from either internal noise or external distractors (Manoach, 2003; Murray *et al.*, 2014). Impaired attention, the inability to filter out irrelevant stimuli, may contribute to WM impairments by increasing such interference. Working memory is necessary for interpreting chains of events in a rational way, and deficits in WM may contribute to the positive symptoms of SZ such as delusions and hallucinations. Executive function is believed to play a supervisory role over several cognitive domains in order to implement higher order processes such as response inhibition, problem-solving, planning, and rule switching (Arguello & Gogos, 2006). Studies in nonhuman primates and humans have identified the prefrontal cortex (PFC) as a critical node in WM and executive function (Castner *et al.*, 2004).

The processes of WM and executive function are important for accomplishing every day life tasks. Unfortunately, the current medications used to treat SZ do not address the cognitive impairments. Even the latest second-generation antipsychotic drugs are largely ineffective at treating cognitive symptoms (Keefe *et al.*, 2007), a harsh reality considering that cognitive function is a key predictor for the long-term quality of life for people with SZ (Green *et al.*, 2000). Intriguingly, a period of relative cognitive decline from childhood to adulthood may predict the psychotic phase of SZ (Kremen *et al.*, 2010). Furthermore, cognitive impairment is commonly seen in first degree relatives of individuals with SZ (Cannon *et al.*, 2000; Myles-Worsley & Park, 2002; Snitz *et al.*, 2006), suggesting that certain cognitive functions, and perhaps the brain structures and circuits that subserve them, are highly heritable. Because cognitive impairment is a strong determinant of the functional disability associated with schizophrenia, it's become a prime target for drug development (Carter *et al.*, 2008). In order to remediate cognitive defects in the future, it will be important to understand the nature of cognitive circuitry perturbations associated with SZ.

In *Dementia Praecox and Paraphrenia* Dr. Kraepelin speculated that lesions of the frontal cortex could produce the symptoms of dementia praecox (schizophrenia):

On various grounds it is easy to believe that the frontal cortex, which is specially well developed in man, stands in closer relation to his higher intellectual abilities, and these are the faculties which in our patients invariably suffer profound loss in

contrast to memory and acquired capabilities. (1916, p. 219)

In line with Kraepelin’s intuitions, much of schizophrenia research today has focused on the structure and function of the prefrontal cortex. As mentioned previously, patients with SZ perform poorly in cognitive tasks that depend on efficient PFC processing, and functional imaging studies find abnormal patterns of PFC activation in SZ patients during working memory tasks (Callicott *et al.*, 2000; Goldman-Rakic & Selemon, 1997; Manoach, 2003). Postmortem studies have found various alterations in the prefrontal cortex, such as subtle changes in the neuronal density, soma volume, and spine numbers (Lewis & Sweet, 2009). In addition, there is a growing body of literature that suggests that SZ is associated with impaired GABAergic transmission in the prefrontal cortex, which I will review below.

1.1.3 Evidence for altered excitation/inhibition balance in schizophrenia

Data from postmortem human studies suggests that schizophrenia pathology involves impairments in GABAergic transmission. One of the most reproducible findings is a reduction of the GABA synthetic enzyme GAD67 mRNA and protein levels in the dorsolateral prefrontal cortex (DLPFC) of subjects with SZ. However, this finding is not specific to the prefrontal cortex and is seen in other cortical regions (Curley *et al.*, 2011; Gonzalez-Burgos *et al.*, 2011). In addition, ~50% of PV mRNA-positive neurons lacked detectable levels of GAD67 in schizophrenia relative to matched control subjects (Hashimoto *et al.*, 2003). The expression of PV mRNA itself is reduced in schizophrenia, while the total number of neurons that label for either PV mRNA or protein are not (Tooney & Chahl, 2004; Woo *et al.*, 1997). Taken together, these data suggest that the number of PV+ INs aren’t reduced in patients with schizophrenia, but the function of PV+ INs may be impaired.

Gamma-band oscillations, which reflect synchronized firing of principal neurons in the 30-80 Hz range, are induced during working memory tasks. In fact, gamma-band power increases as a function of working memory load (Howard *et al.*, 2003). Optogenetic studies have demonstrated that gamma-band oscillations can be driven by selectively activating PV INs (Cardin *et al.*, 2009; Sohal *et al.*, 2009). GABA $\alpha 1$ receptors are found at the postsynapse of

PV basket cells, and a developmentally-related increase in GABA α 1 expression correlates with faster unitary IPSC decay times (Doischer *et al.*, 2008). Furthermore, the emergence of these faster IPSC decay times correlates with the emergence of gamma band oscillations (Doischer *et al.*, 2008). Patients with SZ have been shown to exhibit reduced DLPFC gamma-band power during several phases of working memory tasks including the encoding, maintenance, and retrieval of stored information (Haenschel *et al.*, 2009). In addition, patients with SZ exhibit reduced frontal lobe gamma power during cognitive control tasks that test the subject’s ability to manipulate the content of working memory in order to flexibly adapt thought and behavior to achieve goals (Cho *et al.*, 2006; Minzenberg *et al.*, 2010). Furthermore, DLPFC GABA levels measured by MRS have been shown to correlate with peak gamma power in DLPFC during a working memory task (Chen *et al.*, 2014). The picture that emerges is that patients with SZ exhibit postmortem and electrophysiological signatures of impaired GABAergic transmission, particularly as mediated by PV INs.

In addition to reduced markers of GABAergic transmission, it’s been observed that patients with schizophrenia have reduced dendritic spine density in layer III DLPFC (Lewis & Gonzalez-Burgos, 2008). One interpretation of the concomitant alterations in excitatory and inhibitory circuit components, put forward by David Lewis and colleagues, is that an upstream deficit in dendritic spines leads to compensatory downregulation of inhibition onto pyramidal cells **Fig1.1** (Lewis *et al.*, 2012). However, the limitations of postmortem studies prevent the disambiguation of primary impairments versus secondary compensatory changes. Nevertheless, studies have demonstrated that reduced GABA transmission in mPFC is linked to alterations in executive function. GABA_A antagonism in rodents and nonhuman primates (Enomoto *et al.*, 2011; Sawaguchi *et al.*, 1989), postnatal genetic ablation of NMDA receptors from corticolimbic PV INs (Belforte *et al.*, 2010; Carlen *et al.*, 2012; Korotkova *et al.*, 2010) or loss of PV INs in the MAM G17 lesion model (Lodge *et al.*, 2009) all produce cognitive deficits that resemble those observed in schizophrenia and diminish gamma oscillations (Carlen *et al.*, 2012; Lodge *et al.*, 2009).

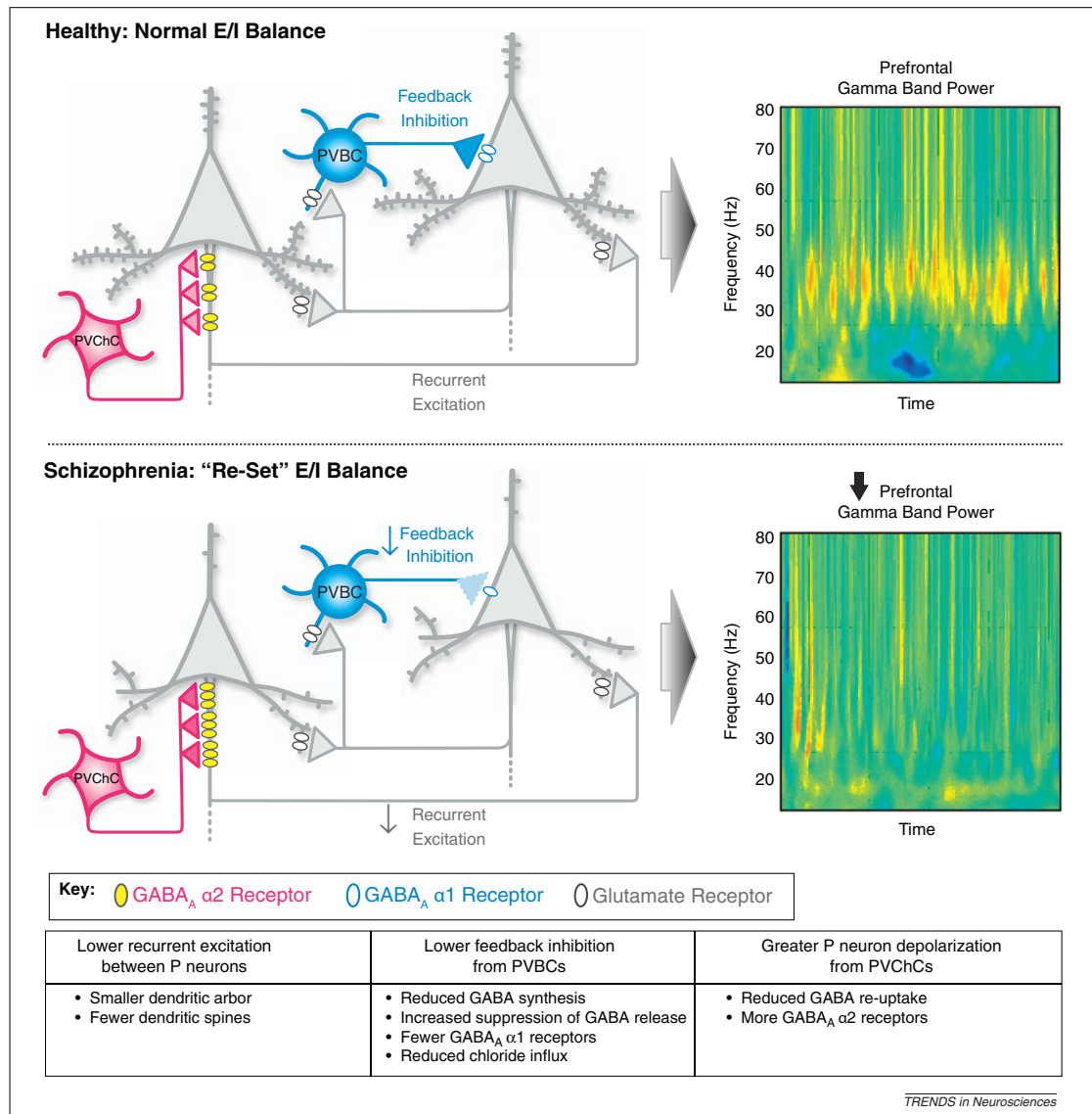


Figure 1.1: **Postmortem human data suggests altered EI balance in schizophrenia.** The top panel shows the healthy situation, in which axon collaterals from pyramidal neurons (PNs) drive recurrent excitation onto other pyramidal neurons and recruit feedback inhibition from connected parvalbumin positive basket cells (PVBCs) in the cortex. The connections between PNs and PVBCs are critical for generating gamma oscillations, and the relative strength of PN-PVBC and PVBC-PN connections could be tuned to maintain a set E/I balance that can optimally generate gamma. In schizophrenia, it is hypothesized that reduced spine density in layer III lowers network excitation, which results in a compensatory downregulation of inhibitory mediators (see table). As a result, the new, lower E/I set point reduces the network's ability to generate gamma, particularly as cognitive load increases and gamma power should normally ramp up. Reproduced from Lewis *et. al* 2012.

1.1.4 Neurodevelopmental basis of schizophrenia

Today, schizophrenia is thought to be a disorder that is the consequence of abnormal brain development. When schizophrenia was first described, it was believed to be a form of rapid neurodegeneration but no evidence of gliosis in the brains of people with SZ exists to support this claim (Woods, 1998). One piece of evidence for the neurodevelopmental basis of schizophrenia is the overlap of genetic risk factors for schizophrenia with childhood onset brain disorders such as autism (Walsh *et al.*, 2014). This overlap includes many genes that function in developmental processes such as neuronal proliferation, neuronal migration, axonal outgrowth, myelination, and synapse development (Fatemi & Folsom, 2009). In addition, epidemiological studies indicate that environmental stress during pre- and perinatal periods increases the risk of developing schizophrenia (Cannon *et al.*, 2002a). Prospective studies of “high risk” cohorts have repeatedly found that the children of parents with schizophrenia exhibit delayed developmental milestones and perform more poorly on neuropsychological tests than other children (Cannon *et al.*, 2000; Davies, 2007; Erlenmeyer-Kimling *et al.*, 2000; Kremen *et al.*, 2010). A critical period for the onset of schizophrenia appears to be adolescence, a time during which glutamatergic synapses are pruned, myelination increases, and dopaminergic and inhibitory circuits reach maturity (Insel, 2010; Jaaro-peled *et al.*, 2009). A challenge for researchers is to understand how schizophrenia lies relatively dormant for the first 1.5 to 3 decades before the onset of psychosis when the disease becomes full-blown and rapidly debilitating (Lewis & Lieberman, 2000). One idea is that the previously mentioned adolescence-related developmental processes somehow unmask the early abnormalities in brain structure and connectivity. In this way, schizophrenia might be thought of as a progressive neurodevelopmental disease (Cannon *et al.*, 2002b; Woods, 1998).

With no clear etiology, it has historically been difficult to study schizophrenia in model organisms. Researchers have previously relied on psychoactive drugs that produce psychopathology that is similar to what is seen in patients with SZ (e.g. PCP) (Arguello & Gogos, 2006) or lesions made in early in development that produce phenotypic changes at adolescence that are relevant to schizophrenia (Lodge & Grace, 2010). However, these models fail to capture the underlying cause of schizophrenia or recapitulate the diversity of impairments seen

in schizophrenia. However, recent advances in psychiatric genetics have identified promising genetic susceptibility factors for SZ that may hold the key to understanding how genes can affect neurodevelopment, brain circuit function, and ultimately behavior. Below, I will describe one such genetic risk factor examined in this thesis, Disrupted-in-Schizophrenia 1.

1.1.5 Identification of DISC1 as a psychiatric risk gene

The story of DISC1 begins, of all places, in a Scottish youth penitentiary. A cytogenetic survey conducted by researchers identified an 18-year-old boy who carried a chromosomal translocation between chromosome one and eleven ((1;11)(q42.1;q14.3)) (Jacobs *et al.*, 1970) **Fig1.2A**. Work over the next couple decades pieced together the Scottish pedigree (St. Clair *et al.*, 1990) and identified DISC1 (Disrupted-in-Schizophrenia-1) as the the open reading frame of a gene that was disrupted by the translocation breakpoint (Millar *et al.*, 2000) **Fig1.2B**. In addition to DISC1, a noncoding RNA on the antisense strand to DISC1 (DISC2) is also disrupted (Millar *et al.*, 2000). Within the Scottish pedigree, the DISC1 translocation was reported to cosegregate with schizophrenia and other psychiatric illness with a maximum logarithm of the odds (LOD) score of 3.6 when the disease was restricted to schizophrenia and 7.1 when relatives with recurrent major depression, bipolar disorder, and schizophrenia were included (Blackwood *et al.*, 2001). This is the highest LOD score ever reported for a genetic association with schizophrenia, however, DISC1’s status as a “proven” risk factor for SZ has come under fire (Sullivan, 2013), primarily because variation in DISC1 did not associate with psychiatric disease in a GWAS mega-analysis (Consortium, 2013). However, variation in DISC1 has been associated with schizophrenia in a separate Finnish cohort (Ekelund *et al.*, 2004), and several studies have reported that rare nonsynonymous mutations within DISC1 are enriched in SZ cases compared to controls (Song *et al.*, 2008). These findings lend credence to DISC1’s wider relevance to schizophrenia. Finally, it should be noted that by design, genome-wide association studies cannot detect rare events, and therefore GWAS isn’t a suitable validation for this particular gene (Sullivan, 2013). Consequently, DISC1 may not be a *prevalent* genetic risk factor for schizophrenia but biology supports the notion that it is a hub for signaling pathways that contribute to schizophrenia pathology.

It is known that specific cognitive impairment is a common feature of individuals with schizophrenia. Intriguingly, cognitive functions such as short-term and long-term memory are reliably impaired in non-schizophrenic relatives (Snitz *et al.*, 2006) as a function of relatedness (Cannon *et al.*, 2000). In keeping with this, there is evidence that the DISC1 translocation is associated with subclinical cognitive effects in the Scottish pedigree. $t(1;11)(q42.1;q14.3)$ translocation carriers display increased latency and reduced amplitude of the P300 event related potential (Blackwood *et al.*, 2001), a measure of the speed and efficiency of information processing that is consistently reduced in individuals with SZ (Begleiter & Porjesz, 1986). Reduced P300 amplitude has been correlated with reduced perfusion of the anterior cingulate cortex (ACC) in patients with SZ and their relatives (Blackwood *et al.*, 1999). In addition, blood RNA levels of DISC1 and its interacting proteins partners were reported to correlate with the performance of healthy controls in a PFC-dependent working memory task (Rampino *et al.*, 2014). So far there have been no postmortem studies of members of the Scottish pedigree. Therefore, it's unknown whether their brains exhibit patterns of changes (such as reduced PV or GAD67 expression) that are consistent with observations from postmortem studies of individuals with SZ. This may be a key point for determining the generalizability of DISC1 pathophysiological mechanisms to schizophrenia more generally. However, the evidence for high heritability of cognitive phenotypes with the DISC1 translocation at least suggests that cognitive impairment is a promising disease aspect to study within a DISC1 mouse model.

Common variants of the DISC1 gene have been associated with reduced gray matter volume (particularly prefrontal and temporal regions) and increased ventricular volume in psychiatric patients and controls (Brauns *et al.*, 2011; Duff *et al.*, 2013; Mata *et al.*, 2010; Trost *et al.*, 2013) and were even reported to predict frontal lobe volume at birth (Knickmeyer *et al.*, 2013). Other studies have found that certain haplotypes that spanned DISC1 and the neighboring TRAX gene were overrepresented among individuals with schizophrenia (Cannon *et al.*, 2005; Palo *et al.*, 2007). Furthermore, DISC1 haplotypes have been associated with prefrontal gray matter reductions and short- and longterm memory impairments (Cannon *et al.*, 2005; Carless *et al.*, 2011; Hennah *et al.*, 2005; Palo *et al.*, 2007). Interestingly, reduced cortical thickness in the ACC was associated with two DISC1 haplotypes (Carless *et al.*, 2011), and

the ACC is a region that has been observed to have reduced volume in people in individuals with schizophrenia and those who are at very high risk for developing it (Fornito *et al.*, 2009; Jung *et al.*, 2011). These studies highlight the association between DISC1 function and early brain development. Moreover, a common missense variant in the DISC1 gene, Ser704Cys (rs821616) was found to be associated with reduced information transfer efficiency (Li *et al.*, 2013) and increased MD-PFC functional connectivity but reduced anatomical connectivity in healthy controls (Liu *et al.*, 2013). The authors argued that the increased functional connectivity in the face of reduced anatomical connectivity could represent a compensatory effect achieved in healthy controls but not individuals with schizophrenia, who exhibit both reduced mediodorsal thalamus- prefrontal cortex functional and anatomical connectivity.

1.1.6 Cellular function of DISC1

DISC1 is a large, multifunctional scaffolding protein that facilitates the formation of protein complexes. DISC1 has no known enzymatic activity itself, but is believed to regulate the activity and localization of its protein binding partners. Over 200 protein interaction partners have been identified by yeast two-hybrid studies (Camargo *et al.*, 2007; Millar *et al.*, 2003; Morris *et al.*, 2003) many of which have been biochemically confirmed (Kim *et al.*, 2009; Morris *et al.*, 2003; Ozeki *et al.*, 2003; Wang *et al.*, 2010). Therefore, DISC1-related cognitive effects likely arise from the dysregulation of a wide-array of protein-protein interactions across development (Bradshaw & Porteous, 2012). Adding to the complexity, it's been reported that there are as many as 50 different DISC1 splice isoforms in the human brain that are dynamically regulated across development (Nakata *et al.*, 2009). The DISC1 gene is made up of 13 exons and its genetic structure is well-conserved, particularly within the C-terminal domain, across multiple species including mice **Fig1.2C** (Chubb *et al.*, 2008). The C-terminus encodes a coiled-coiled domain predicted to facilitate DISC1 protein-protein interactions, and the t(1;11) translocation is predicted interfere with C-terminus protein binding. Interestingly, many of the protein-binding partners of DISC1 are also involved in neurodevelopmental processes, and several (*PDE4B*, *FEZ1*, *PCM1*, *NDE1*) have been identified as independent risk factors for major mental illness (Bradshaw & Porteous, 2012; Camargo *et al.*, 2007; Chubb *et al.*, 2008).

Therefore, the high penetrance of the DISC1 translocation in the Scottish pedigree may be due to the fact that DISC1 is a hub that lies in many pathways involved in neurodevelopment and synaptic transmission (Porteous *et al.*, 2014).

The temporal expression pattern of DISC1 mRNA highlights its role in brain development as well as its potential role in postnatal brain maturation. DISC1 mRNA reaches its peak expression embryonically at E13.5, underscoring its important role in neurodevelopmental processes like neurogenesis and migration (Schurov *et al.*, 2004). A similar temporal pattern of expression has been observed in human brain (Lipska *et al.*, 2006). DISC1 is most highly expressed in the dentate gyrus but is also expressed at high levels in the olfactory bulb, cortex, and cerebellum (Schurov *et al.*, 2004). In addition, DISC1 mRNA exhibits a second peak of expression that corresponds to the onset of puberty in mice (P35) (Schurov *et al.*, 2004). Interestingly, one study that looked at inducible expression of a truncated human form of DISC1 (hDISC1) found differential neurobehavioral effects of hDISC1 expression whether it was restricted to the pre- or postnatal period (Ayhan *et al.*, 2010).

DISC1 is not only expressed in the brain, but is found in other tissues such as placenta and heart (Millar *et al.*, 2000). DISC1 is found in multiple subcellular locations, including mitochondria, cytoplasmic puncta/stress granules, the nucleus, centrosome, and actin filaments (Brandon *et al.*, 2005; James *et al.*, 2004; Miyoshi *et al.*, 2003; Morris *et al.*, 2003; Ozeki *et al.*, 2003; Sawamura *et al.*, 2005). Within neurons, DISC1 is found in dendritic spines, where it colocalizes with the post-synaptic density (Hayashi-Takagi *et al.*, 2010; Kirkpatrick *et al.*, 2006) and also at the presynapse (Wang *et al.*, 2010). In addition to expression within excitatory PNs, DISC1 has also been shown to be present in medial ganglionic eminence (MGE) derived neurons, which include parvalbumin (PV) and somatostatin (SST) INs, (Steinecke *et al.*, 2012) and colocalizes with GAD67 (Meyer & Morris, 2008).

Animal models of DISC1 have mainly focused on two hypothesized consequences of the t(1;11)(q42.1;q14.3) translocation: either loss-of-function knockdown or deletion models or gain-of-function expression of a truncated dominant-negative form of DISC1 **Fig1.2D**. A non-exhaustive list of DISC1 mouse models that have been generated include shRNA knockdown mice (Hayashi-Takagi *et al.*, 2010; Kamiya *et al.*, 2005; Niwa *et al.*, 2010) transgenic models

that express a putative dominant-negative human DISC1 fragment (Hikida *et al.*, 2007; Li *et al.*, 2007; Pletnikov *et al.*, 2008), a transgenic mouse lacking exons 1-3 (Kuroda *et al.*, 2011), chemical mutagen-induced point mutants (Clapcote *et al.*, 2007), and mice with a naturally occurring micro deletion in exon 6 (Koike *et al.*, 2006). Koike *et al.* found that C57Bl/6J mice that were heterozygous for the 129 DISC1 variant performed significantly worse compared to C57Bl/6J mice in a working memory task, suggesting that DISC1 is haploinsufficient with respect to this PFC-dependent phenotype (Koike *et al.*, 2006). This is interesting in relation to the cognitive impairments seen in unaffected DISC1 translocation carriers and the fact that DISC1 expression is approximately 50% lower in lymphoblastoid cell lines of t(1:11) translocation carriers **Fig1.2D** (Millar *et al.*, 2005). In my thesis project, I studied a loss-of-function model (unpublished) generated by Dr. Hannah Jaaro-Peled at Johns Hopkins University. In this mouse, multiple genetic perturbations were introduced into the DISC1 locus including a 40-kb genomic deletion covering exons 1-3 of DISC1, in addition to the 25 bp deletion in exon 6, with the goal of eliminating as many DISC1 isoforms as possible.

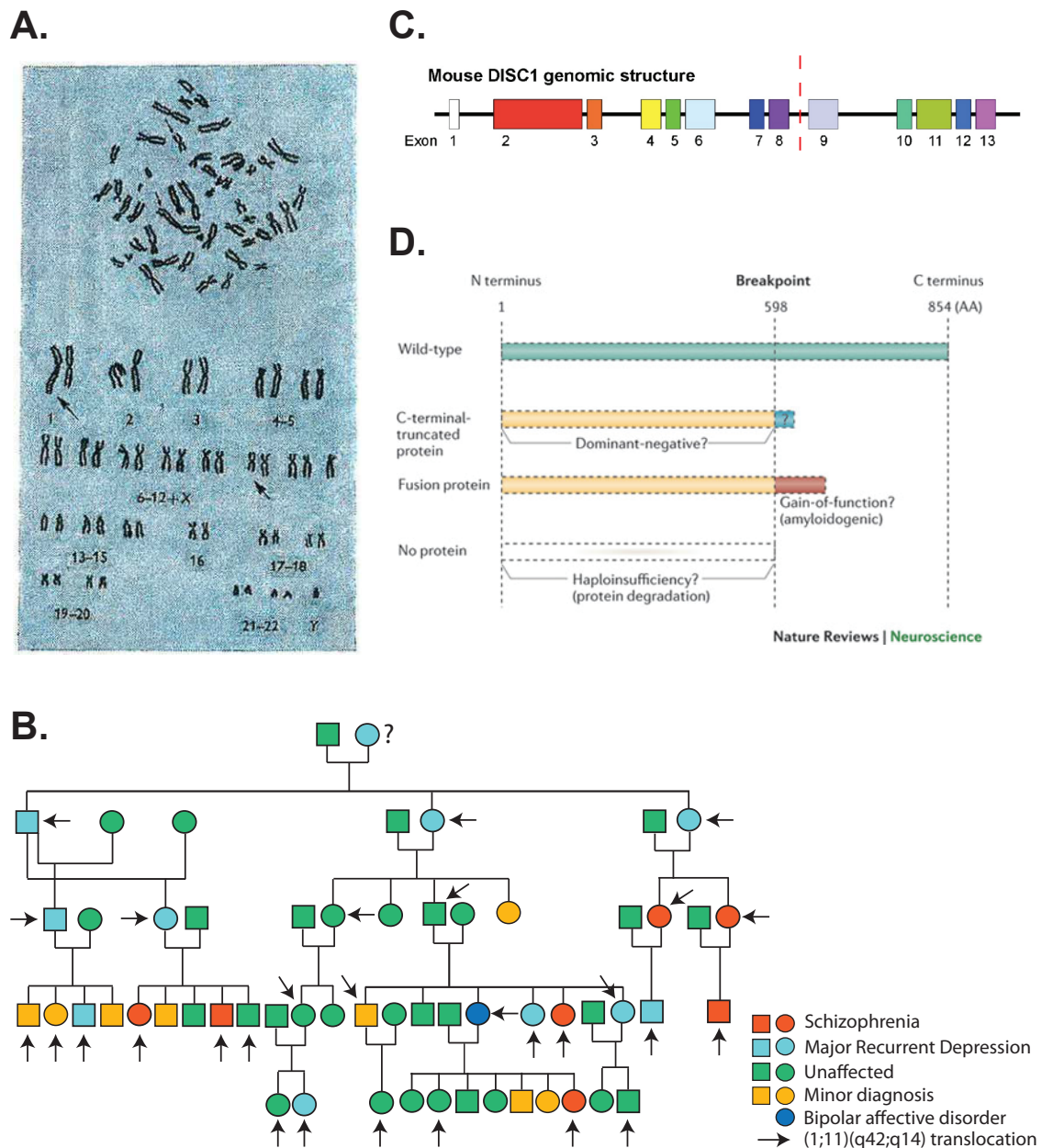


Figure 1.2: **DISC1 chromosomal translocation: Scottish pedigree and gene structure** A. A karyotype of a propositus of the Scottish pedigree in the original Jacobs *et al.* paper. Arrows indicate the translocation event. B. Scottish pedigree in which a balanced translocation between chromosome 1 and 11 was discovered. The breakpoint of this translocation was between exons 8 and 9 of a previously unidentified gene DISC1. Note that the translocation segregates with a variety of major psychiatric diagnoses within the family. C. Structure of the mouse ortholog of DISC1, a 13 exon gene with many splice isoforms. Red dashed line indicates the breakpoint in the Scottish pedigree. D. Models of different biological consequences of DISC1 translocation, including a truncated form of the protein, a fusion protein, or the model of protein loss and haploinsufficiency. Figure A. from (Jacobs *et al.*, 1970) B. adopted from (Brandon & Sawa, 2011), Figure C. from (Duan *et al.*, 2007), and Figure D. from (Brandon & Sawa, 2011).

Role for DISC1 in early brain development

DISC1 plays an important role in neuronal migration. DISC1 knockdown was first reported to impair neurite outgrowth and delay neuronal migration, leading to fewer RNAi-transfected neurons in the superficial layers of cortex at P14 (Kamiya *et al.*, 2005). In addition, DISC1 RNAi-transfected neurons had less extensive dendritic arbors that appeared to be misoriented with respect to the pial surface (Kamiya *et al.*, 2005). The role of DISC1 in radial migration has been replicated several times (Ishizuka *et al.*, 2011; Kubo *et al.*, 2010; Niwa *et al.*, 2010; Singh *et al.*, 2010). In addition to cortical development, DISC1 regulates the migration and dendritic arborization of newborn granule cells in the adult and neonatal hippocampus (Duan *et al.*, 2007; Enomoto *et al.*, 2009; Kim *et al.*, 2009; Meyer & Morris, 2009; Tomita *et al.*, 2011). *In utero* DISC1 knockdown impaired the migration of granule cells in the hippocampus, similar to the phenotype produced in the cortex. However, when DISC1 was knocked down in adult-born granule cells it produced the opposite phenotype, such that neuronal migration was accelerated, and granule cells exhibited precocious elaboration of dendritic arbors and synapse formation (Duan *et al.*, 2007). Given that dentate gyrus develops in an “outside-in” fashion as opposed to the “inside-out” pattern of cortical layers during embryonic development, these results suggests that DISC1 plays a role in relaying extracellular positional cues to intracellular migratory machinery. Finally, DISC1 has also been shown to regulate the tangential migration of MGE-derived interneurons (Lee *et al.*, 2013b; Steinecke *et al.*, 2012). The proposed mechanism of DISC1’s control of migration is through its interactions with many microtubule-associated motor complex proteins such as NDE1, NDEL1, PCM1, and LIS1 (Camargo *et al.*, 2007). DISC1’s ability to anchor these proteins to the centrosome may organize the microtubule network for interkinetic nuclear migration and radial migration.

In addition to regulating migration, DISC1 is important for two aspects of corticogenesis: proliferation of neuronal progenitors and the switch from proliferation to differentiation. DISC1 knockdown *in utero* leads to reduced neural progenitor proliferation, resulting in early cell cycle exit and ultimately fewer neurons (Mao *et al.*, 2009). This is because when DISC1 is present, it binds to GSK3 β to prevent it from phosphorylating β -catenin, which stabilizes β -catenin and promotes neural proliferation. Furthermore, another DISC1 binding protein,

Dixdc1, cooperates with DISC1 to regulate GSK3 β . When Cdk5 phosphorylates Dixdc1, it promotes the binding of the Dixdc1/DISC1 complex to Ndel1 (Singh *et al.*, 2010), and DISC1 interaction with Ndel1 at the centrosome promotes the centrosome-microtubule dynamics required for neuronal migration (Kamiya *et al.*, 2005). Finally, more recently it was shown that phosphorylation of DISC1 itself reduces DISC1's affinity for GSK3 β and promotes its binding to the dynein motor-related protein BBS1, highlighting another way in which DISC1 can regulate the proliferation/migration transition (Ishizuka *et al.*, 2011).

Related to DISC1's function in microtubule dynamics in neuronal migration, DISC1 has been shown to regulate neurite outgrowth, which involves microtubule dynamics and remodeling of the actin cytoskeleton. *In vitro* expression of a truncated form of DISC1 resulted in fewer outgrowths and shorter neurites (Hattori *et al.*, 2010; Ozeki *et al.*, 2003). Finally, DISC1 recruits its binding partner Ndel1 to the distal part of the axon where it forms a complex with LIS1 and 14-3-3 ϵ . DISC1 also binds Kinesin-1, apparently serving as a cargo receptor to link the motor protein to the Ndel1-LIS1-14-3-3 ϵ complex. The knockdown of DISC1 inhibited the accumulation of this complex and impaired axon elongation (Taya *et al.*, 2007). DISC1's regulation of NDEL1's subcellular localization for different developmental processes (migration and axon elongation) highlights its role in regulating the function of its protein binding partners either spatially (as in the case of NDEL1) or by inhibiting their enzymatic function (as in the case of GSK3 β).

DISC1 at the synapse

DISC1 has been shown to regulate spine size through its interaction with kalirin-7 a member of the Rho-family of small G-proteins. DISC1 knockdown *in vitro* leads to a rapid increase in the volume of spines and surface expression of GluR1 and increases the frequency of mEPSCs onto DISC1 RNAi-transfected neurons. This process occurs due to kalirin-7's increased access to Rac1, a GDP/GTP exchange factor (GEF) that is known to regulate spine morphology and plasticity in association with neuronal activity (Penzes & Jones, 2008). Interestingly, longterm DISC1 knockdown *in vivo* causes spines to shrink, suggesting that Rac1 gain-of-function increases spine growth in the short term but has deleterious effects on spines in the long term

(Hayashi-Takagi *et al.*, 2010). Another DISC1 interacting partner identified in the large yeast 2-hybrid screen (Camargo *et al.*, 2007) that is found at the PSD is TNIK. DISC1 specifically binds to the kinase domain of TNIK and prevents TNIK-mediated degradation of postsynaptic proteins such as Glur1 and PSD95 (Wang *et al.*, 2010). These findings suggest that DISC1 is involved in regulating cytoskeletal dynamics that affect spine structure and postsynaptic composition primarily by titrating the activity levels of its protein binding partners. It is difficult to anticipate how short-term knockdown experiments can translate to genomic models of DISC1 deficiency.

1.1.7 Summary of DISC1 mouse model behavioral findings

Despite the variation in the genetic models of DISC1 (discussed previously), there is a reassuring overlap in behavioral alterations. For example, frontal deficits that are characterized by impairments in working memory (assessed by the DNMTTP task) and latent inhibition are present in all DISC1 models tested thus far (Brandon & Sawa, 2011). In contrast, spatial learning and memory are not perturbed. Meanwhile, the effects on social behavior and anxiety are more mixed (Ayhan *et al.*, 2010; Clapcote *et al.*, 2007; Hikida *et al.*, 2007; Ibi *et al.*, 2010; Li *et al.*, 2007; Lipina *et al.*, 2010; Pletnikov *et al.*, 2008). In addition, many models show deficits in pre-pulse inhibition (Clapcote *et al.*, 2007; Hikida *et al.*, 2007; Lipina *et al.*, 2010; Niwa *et al.*, 2010) a measure of sensory-motor gating that is considered to be a reliable endophenotype in schizophrenia (Amann *et al.*, 2010).

In terms of brain structural changes, several studies have identified increased ventricular volume/reduced cortical volume (Ayhan *et al.*, 2010; Kvaajo *et al.*, 2008; Pletnikov *et al.*, 2008) and have noted reductions in dendritic spine number and/or dendritic complexity (Kvaajo *et al.*, 2008; Lee *et al.*, 2011; Li *et al.*, 2007; Niwa *et al.*, 2010; Pletnikov *et al.*, 2008), and reduced parvalbumin staining in the mPFC (Ayhan *et al.*, 2010; Hikida *et al.*, 2007; Ibi *et al.*, 2010; Lee *et al.*, 2013a; Niwa *et al.*, 2010; Shen *et al.*, 2008). Increased ventricular volume/reduced cortical volume is predicted from the described roles of DISC1 in regulating neural proliferation and migration. Similarly, reductions in dendritic length may be ascribed to DISC1's function in neurite outgrowth, while spine reduction is consistent with the findings of Hayashi-Takagi

et al. of DISC1's regulation of kalirin-7 activity. In addition, the mispositioning of pyramidal neurons due to delayed migration may affect their integration into the local cortical circuit and therefore lead to reduced synapse formation and hence fewer spines. However, the robust finding of reduced parvalbumin expression has no predicted cellular mechanism. The co-occurrence of working memory impairment and reduced PV expression is of course intriguing in light of human SZ data. While working memory impairments are observed in DISC1 t(1;11) carriers, due to a lack of postmortem data it is not known whether they exhibit reduced markers of inhibitory transmission in the PFC. Therefore, one possibility is that reduced PV expression is a downstream consequence of a dysfunctional prefrontal cortical circuit caused by abnormal neurodevelopment in DISC1 mouse models. While the mechanism underlying reduced PV expression is likely complex and difficult to test, it is possible to examine the physiological function of PV INs in DISC1 mouse models which may provide insight into the link between DISC1 and working memory impairment.

	Mutants	Dominant-negative transgenic model					Knockdown
		Q31L	L100P	Δ25 bp and stop codon	Constitutive	Inducible	
					BAC-DN	CaMK-DN	CaMK-cc
Neurogenesis	↓(CTX)	↓(DG)	↓(CTX)				
Pyramidal neurons (CTX, HP)	Misposition, ↓dendrites, ↓spine						↓Dendrite
Granule neurons (DG)	Alteration						
Interneurons (mPFC)				→PV, CB	↓PV	↓PV	↓PV
Dopamine						↓DA, DOPAC (CTX)	↓TH, DA (CTX)
Amphetamine hypersensitivity					Yes	Yes	Yes
MK-801 hypersensitivity					Yes*		
Sensorimotor gating (PPI)	Yes	Yes	No		Yes	No/no*	Yes
Latent inhibition	Yes	Yes		Yes			
Short-term memory (Y maze)					No/yes*	No/no*	
Working memory (DNMTP)	Yes	Yes	Yes			Yes	Yes
Spatial learning and memory (MWM)	No	No	No		No	No/no*	
Fear conditioning				No	Yes*		
Antidepressive effects (FST)	Yes	No		Yes	Yes	No/yes*	Yes
Sociability	Yes	No			Yes*	No/yes*	Yes
Anxiety (EPM)	No	No			No	No/yes*	No
References	92,113,158	92,113,158	99,152	88	150,156	149,157,159	151
							153

*Indicates the behavioural outcome when the environmental stressor polyribosin polyribocytidylic acid (poly(C)) is added to the genetic model. The down arrow (↓) indicates a reduction, the up arrow (↑) indicates augmentation and the right-hand arrow (→) indicates no change. BAC, bacterial artificial chromosome; CaMK, calcium/calmodulin-dependent protein kinase; CB, calbindin; cc, carboxy-terminal fragment of DISC1; CTX, cortex; DA, dopamine; DG, dentate gyrus; DOPAC, 3,4-dihydroxyphenylacetic acid; DN, dominant-negative; DNMTP, delayed non-matching to place; EPM, elevated plus maze; FST, forced swim test; HP, hippocampus; MK-801, (5S,10R)-(+)-5-methyl-10,11-dihydro-5H-dibenz[*a,d*]cyclohepten-5,10-imine maleate; mPFC, medial prefrontal cortex; MWM, Morris water maze; PPI, prepulse inhibition; PV, parvalbumin; STR, striatum; TH, tyrosine hydroxylase.

Figure 1.3: **Working memory deficits and reduced parvalbumin expression are commonly observed in DISC1 animal models.** PV reduction in mPFC and impairments in DNMTP, a working memory task, performance are highlighted as the most reproducible findings across models. From (Brandon & Sawa, 2011)

1.1.8 Cognitive impairment as an endophenotype of DISC1 genetic variation

As humans, we are highly social animals who are remarkably sensitive to small deviations from “normal” behavior. To date, the diagnosis for SZ still relies solely on the recognition of abnormal behaviors like hallucinations, delusions, or flat affect. An interesting question is what type of variation the brain can buffer before disturbances reach the level of detectability. For highly heritable psychiatric diseases, it’s predicted that family members may exhibit subclinical symptoms that aren’t easily observable. This is essentially the concept of endophenotypes: that there are measurable phenotypes that lie beneath the surface of overt syndromic behaviors. Endophenotypes lie somewhere between the cognitive and behavioral manifestations of, for instance, schizophrenia, and its elusive genetic and environmental underpinnings (Gottesman & Gould, 2003). Studying specific endophenotypes may make the problem of understanding complex diseases more tractable by narrowing the focus to establishing links between genes and specific endophenotypes as opposed to genes and the disease as a whole. In a similar formulation by Gordon and Moore, if we think of understanding the neurobiology of schizophrenia as charting a course, there are many starting points (e.g. genetic or environmental causes) and waypoints (pathophysiological theories, e.g. dopamine hypothesis) on the path to understanding the symptoms of schizophrenia (Gordon & Moore, 2012). In the same way, an endophenotype can be thought of as a waypoint on the course to understanding the biology of schizophrenia. This framework has been adopted by the NIMH Research Domain Criteria (RDoC) initiative whose stated goal is to understand the neurobiological mechanisms that underly specific symptom domains, irrespective of clinical diagnosis (Cuthbert & Insel, 2013).

Gottesman and Gould laid out five criteria for identifying useful endophenotypes in psychiatry: (1) the endophenotype should be associated with illness in the population; (2) it should be heritable; (3) the endophenotype should be primarily state independent; (4) within families, the endophenotype and the illness should co-segregate; and (5) it should be found in nonaffected family members at a higher rate than in the general population (Gottesman & Gould, 2003; Snitz *et al.*, 2006). To extend these criteria to identifying useful mouse models of

endophenotypes: (1) the gene of interest should be highly homologous (2) the endophenotype should involve a brain region whose conserved function is relevant to cognitive or behavioral symptoms that are seen in the disease population (Arguello & Gogos, 2012). I believe that the cognitive impairments observed within the DISC1 pedigree (and in the larger SNP-association studies) meet endophenotype criteria, particularly in the sense that DISC1 has been associated with working memory performance and PFC structure/activation in unaffected DISC1 translocation carriers and healthy controls who carry certain DISC1 polymorphisms. By modeling DISC1 loss-of-function in the mouse, we can probe more deeply into the function of the prefrontal cortex to understand how DISC1 genetic variation can lead to changes in cognitive performance.

The goal of my thesis was to understand how disruption of the DISC1 gene might alter cognitive-related circuitry that underlies the cognitive tasks that DISC1 has been shown to modify. Rather than focusing on the impact of DISC1 loss-of-function at the molecular or behavioral level, I focused my studies at the synaptic to circuit level in the prefrontal cortex. In this way, I used the DISC1 heterozygous deletion mouse as a starting point to assess the potential pathophysiological mechanisms that link DISC1 genetic variation to cognitive dysfunction. Given that there are a myriad of gene by environmental interactions that can give rise to phenotypes that psychiatrists categorize as “schizophrenia”, the common feature of the many “schizophrenias” should be altered function in brain areas that subserve the cognitive and behavioral domains that contribute to the schizophrenia phenotype. I believe that uncovering the points of convergence of brain circuit alterations across various genetic and environmental animal models of SZ will shed light on the central pathophysiology of the disease.

As described in the second chapter of my thesis, within the mPFC, DISC1 deletion appears to primarily alter inhibitory transmission, particularly that mediated by the parvalbumin (PV) interneurons. The observed reduction in action potential-independent inhibitory transmission and increased GABA paired-pulse ratio from PV INs led me to evaluate one current hypothesis of schizophrenia pathology: altered excitation to inhibition (EI) balance. This thesis reports 1) the synaptic effects of DISC1 deletion on pyramidal and inhibitory interneuronal populations in the prefrontal cortex 2) the characterization of a previously hypothesized direct

projection from the mediodorsal thalamus to PV INs in the anterior cingulate cortex 3) altered EI balance in the MD-ACC projection of DISC1 HET mice that is due to reduced feedforward inhibition from PV INs.

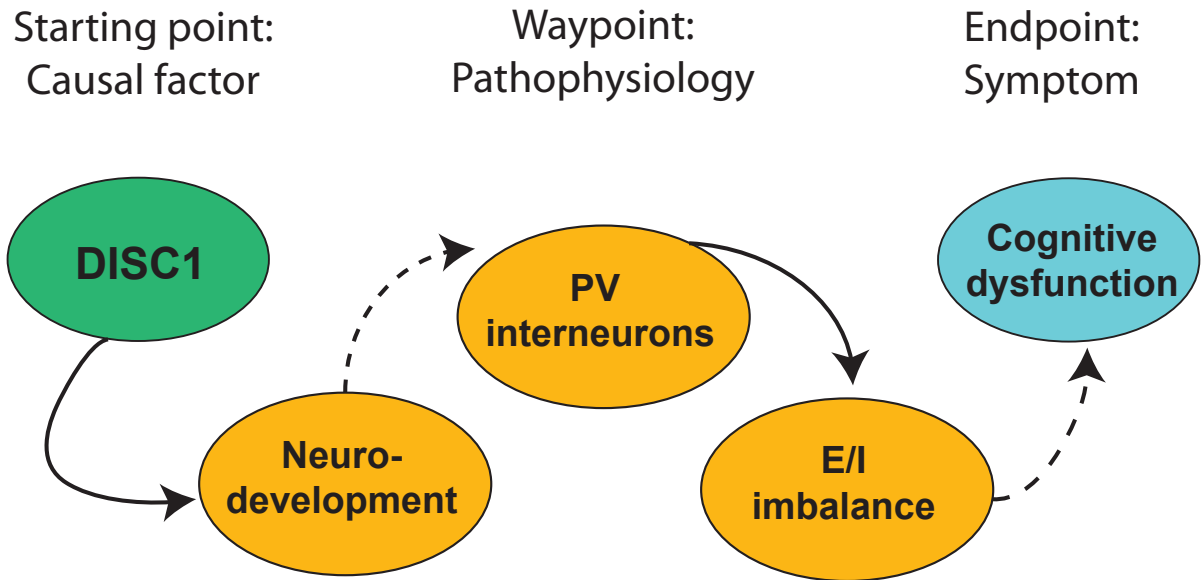


Figure 1.4: **Summary “thesis roadmap”** Based on a figure from (Gordon & Moore, 2012), I’ve outlined my thesis project in terms of charting a course; with the starting point being the genetic risk factor DISC1 and the endpoint being understanding the neurobiological basis of cognitive dysfunction in carriers of DISC1 variants and, more broadly, individuals with schizophrenia. This thesis project focused on DISC1 mediated changes of prefrontal cortical function as a potential pathophysiological cause of cognitive dysfunction. Solid lines represent strong causal links, while dotted lines are still hypothetical. In many studies, DISC1 has been shown to be important for neurodevelopment and many DISC1 animal models show reduced parvalbumin in the prefrontal cortex. However, the neurodevelopmental mechanism for this change is unknown. In addition, studies have shown that PV INs are the main interneuron subtype that controls excitation to inhibition (EI) balance in the cortex. However, only preliminary evidence has linked altered EI balance to cognitive dysfunction. In my thesis, I primarily worked at the waypoint, first identifying a synaptic alteration at the PV-PN synapse in the mPFC of DISC1 mice and then working to understand how this synaptic change could alter EI balance in a thalamocortical circuit that is relevant to cognition and has been implicated in the pathophysiology of schizophrenia.

1.2 Summary of performed experiments

I first performed whole-cell patch clamp electrophysiological recordings from superficial pyramidal neurons in the dorsal portion (ACC and PL region) of the mPFC in adult mice. I recorded miniature excitatory and inhibitory postsynaptic currents (mEPSCs and mIPSCs) that arise from action potential independent fusion of single synaptic vesicles. By comparing the mEPSC and mIPSC measurements onto pyramidal neurons, I was able to survey the net inhibitory vs. excitatory input onto pyramidal neurons in mice heterozygous for DISC1 deletion and their wildtype littermates. I found that mEPSCs were consistent across genotypes, while the frequency of mIPSCs was significantly reduced in DISC1 HET mice. Meanwhile, mEPSC recordings onto PV and SST INs revealed that excitatory transmission onto INs was either normal or enhanced in the DISC1 HET background. Together, these data suggested that presynaptic GABA release is impaired in DISC1 HET mice. To further characterize GABA release from presynaptic inhibitory neurons, I selectively expressed Cre-dependent ChR2 in the two major populations on inhibitory INs in the mPFC, PV and SST INs. I measured the paired-pulse ratio (PPR) of PV+ or SST+ ChR2-evoked IPSCs in DISC1 HET or WT mice and found that the PPR of PV-mediated but not SST-mediated IPSCs was significantly increased in DISC1 HET mice.

In the second set of experiments, I characterized a brain circuit that strongly recruits PV INs. Cre-dependent monosynaptic rabies tracing revealed that a dense population of neurons in the mediodorsal nucleus of the thalamus (MD) project to PV INs in the mPFC. Through *in vitro* optogenetic electrophysiology experiments, I confirmed that PNs and PV INs receive monosynaptic excitatory input from the MD and that MD stimulation drives disynaptic inhibitory currents onto layer III PNs. In addition, I confirmed that MD-driven IPSCs were mediated by PV INs. I performed a combined *in vitro* optogenetic stimulation and silencing experiments to suppress firing in either PV or SST INs while simultaneously activating MD fibers. I found that silencing PV INs significantly reduced, and in some cases abolished, feedforward inhibition in the MD-mPFC pathway. Meanwhile, SST silencing never reduced MD-evoked IPSCs and in fact significantly enhanced feedforward IPSCs. Our PV inactivation experiments support the

idea that PV INs mediate feedforward inhibition, and effectively shunt excitatory input onto layer III pyramidal neurons, thus narrowing the window of time over which excitatory currents can be integrated. Finally, I measured the functional output of the MD-mPFC feedforward inhibitory circuit in DISC1 HET mice. Given that I observed increased GABA PPR from PV INs in DISC1 HET, and PV interneurons were then determined to be the major mediators of MD-driven inhibition, I conclude that PV mediated GABA release is impaired in the MD-dACC feedforward circuit of DISC1 HET mice.

Chapter 2

Cell type-specific effects of reduced DISC1 expression

2.1 Introduction

The prefrontal cortex, particularly the DLPFC, has been a prime locus of schizophrenia (SZ) related pathology that is believed to contribute to cognitive impairment. While the rodent mPFC is not as complex as the primate PFC, it still retains many of the functional and anatomical characteristics. Therefore, the study of homologous prefrontal regions within experimentally-tractable rodents are an important tool for understanding SZ-related cognitive impairment. The most widely accepted definition of the rodent PFC today is that it is the projection zone of the mediodorsal nucleus of the thalamus (MD) (Divac, 1993; Heidbreder & Groenewegen, 2003; Rose & Woolsey, 1948). By this definition, the prefrontal cortex involves all of the cortex of the dorsolateral, orbital and medial frontal lobe rostral to the precentral motor cortex (Öngür & Price, 2000). However, because the rodent frontal cortex completely lacks a granular zone, it is difficult to determine whether rodents have a homolog of the primate DLPFC. The main part of the prefrontal cortex lies along the medial wall, anterior and dorsal to the knee of the corpus callosum. The mPFC can be further divided into four cytoarchitectonically distinct areas dorsal to ventral: the medial precentral area (PrCm, also called M2), the anterior cingu-

late cortex (ACC), the prelimbic cortex (PrL), and the infralimbic cortex (IL) (Heidbreder & Groenewegen, 2003). Heidbreder and Groenewegen proposed that the mPFC could be divided into dorsal-ventral streams, whereby the dorsal mPFC areas have distinct connections with sensorimotor and association areas that ventral mPFC lacks, while ventral mPFC has more interconnections with temporal and limbic structures. These patterns suggest that dorsal mPFC areas are more involved in the planning of behavioral sequences, while the ventral mPFC may be more involved in integrating internal state with environmental cues to guide behavior (Heidbreder & Groenewegen, 2003). All of the mPFC structures are likely to contribute to executive function, which involves sensory integration, the sensing of internal states, motor planning, and action evaluation.

As mentioned previously, the rodent prefrontal cortex is agranular and thus lacks a layer IV. Therefore the thalamic input to mPFC terminates within layer III. Pyramidal neurons within layers II/III of the cortex are reciprocally connected with neurons in other cortical areas, while deeper layers project to subcortical targets. Projection neurons in layer V can be subdivided into intratelencephalic (IT) neurons that project to the cortex and striatum, and pyramidal tract (PT) neurons that are restricted to layer Vb and project to the brainstem and spinal cord (Shepherd, 2013). Finally, layer VI contains corticothalamic projection neurons. The majority (70-80%) of the neurons in the cortex are glutamatergic (DeFelipe & Farinas, 1992) while the remaining (20-30%) are inhibitory interneurons (Markram *et al.*, 2004). Of these inhibitory interneurons, almost all are accounted for by three markers: parvalbumin, somatostatin, and 5HT3a (Rudy *et al.*, 2010). The two major interneuron populations (PV and SST) are exclusively derived from the medial ganglionic eminence (Xu *et al.*, 2004).

PV and SST INs have distinct properties that confer them with different modes of inhibitory control in the cortex. Fast-spiking PV INs include basket and chandelier cells that target the soma/basilar dendrites and axon initial segment, respectively. Chandelier cells are thus poised to gate action potential generation (Howard *et al.*, 2005), and apparently promote or inhibit spiking in a state-dependent manner (Woodruff *et al.*, 2011). PV INs have been shown to be important for shaping spike timing and the dynamic range of cortical activity (Cardin *et al.*, 2009; Cruikshank *et al.*, 2007; Gabernet *et al.*, 2005; Pouille & Scanziani, 2001; Sohal *et al.*,

2009). In addition, they've been shown to mediate gain control in the cortex (Atallah *et al.*, 2012). Postmortem SZ studies have found consistent alterations to PV INs, such as reduced PV expression, and selective reduction of GAD67 in PV INs compared to other INs (Curley *et al.*, 2011; Hashimoto *et al.*, 2003; Tooney & Chahl, 2004; Woo *et al.*, 1997). Meanwhile, SST INs have been typically associated with Martinotti cells, GABAergic INs whose ascending axons ramify in layer I and spread horizontally to target distal dendrites of pyramidal neurons (Rudy *et al.*, 2010). Recently, SST INs have also been shown to inhibit PV INs in thalamorecipient layer IV (Xu *et al.*, 2013). SST INs display heterogeneous firing patterns and can be classified as regular or burst spiking (Kawaguchi, 1996). Strong facilitating excitatory inputs onto SST INs can recruit strong feedback inhibition (Silberberg & Markram, 2007), and SST IN targeting of distal dendrites places them in a position to influence dendritic integration (Gentet *et al.*, 2012). In postmortem SZ studies, transcriptome analysis found that SST mRNA levels were lower in SZ vs. controls (Hashimoto *et al.*, 2008).

To date, there have been no studies in DISC1 animal models assessing the synaptic properties of inhibitory IN populations. Because a variety of DISC1 animal models exhibit impaired working memory and reduced PV expression, we hypothesized that there is an mPFC circuit dysfunction in DISC1 loss-of-function and dominant negative models. In order to begin to understand how mPFC circuit function might be impaired in the DISC1 locus impairment (LI) mouse, we first assessed spontaneous transmission onto the major players of the mPFC: pyramidal neurons (PNs), parvalbumin (PV) interneurons, and somatostatin (SST) interneurons. The results of our 'mini survey' led us to interrogate the function of PV INs in more depth. In this chapter we report the effects of DISC1 genomic deletion and cell type-specific knockdown on mEPSC and mIPSC transmission in the mPFC. Furthermore, we assess the effect of DISC1 genomic deletion on short-term plasticity at the PV-PN and SST-PN synapses.

2.2 Methods

2.2.1 Animals

All mice were bred and maintained in on-campus animal facilities, and all experimental procedures involving animals were approved by the Institute Animal Care and Use Committees of Cold Spring Harbor Laboratory and carried out in accordance with US National Institutes of Health standard. Mice were group-housed under a 12-h light-dark cycle (7 a.m. to 7 p.m. light) with ad libitum access to standard pellet food and water.

In order to study the effects of reduced DISC1 protein expression on prefrontal cortical circuit function, we utilized an unpublished DISC1 “locus impairment” mouse model generated by Dr. Hanna Jaaro-Peled in the lab of Dr. Akira Sawa at Johns Hopkins University. This mouse line has a 40 kb deletion that spans exons 1 through 3 of murine DISC1, together with a 250 bp microdeletion in exon 6. It was demonstrated to deplete the major full-length 100 kD isoform of DISC1, and was designed to eliminate as many DISC1 splice isoforms as possible. Briefly, a BAC-based genomic library generated from C57Bl/6J-129SvEv-hybrid embryonic stem cell lines was screened to identify a DISC1-containing clone. This clone was subsequently modified by a RecA-mediated recombination strategy so that the 40 kb genomic region was replaced with a neomycin selection cassette. Embryonic stem cell clones that were successfully targeted with the modified BAC were injected into C57Bl/6J blastocysts, and generations of backcrossing into the C57Bl/6J line standardized the genetic background. In our studies, DISC1 mice that retained 1 functional copy of DISC1 were used because homozygous knockout mice exhibit obvious physical defects such as runting and motor impairments. Furthermore, loss of a single functional copy of DISC1 more closely mimics the predicted effect of the chromosomal translocation observed in the Scottish pedigree.

In order to assess the effects of reduced DISC1 protein expression on inhibitory interneuron subtypes within the mPFC, we crossed the DISC1 HET mouse line onto the *SST-IRES-Cre* and *PV-IRES-Cre* transgenic reporter lines. These transgenic reporter lines drive expression of Cre-recombinase downstream of the somatostatin (Taniguchi *et al.*, 2011) or parvalbumin pro-

moter, respectively (Hippenmeyer *et al.*, 2005). Cell type-restricted Cre-recombinase expression was utilized in my project in two ways: Cre recombinase mediated the excision of a *loxP* site flanked STOP codon (lox-STOP-lox) upstream of a sequence of interest packaged in virus or, alternatively, when crossed onto the *Ail4* reporter mouse line mediated the excision of a lox-STOP-lox sequence upstream of the TdTomato red fluorescent protein (Madisen *et al.*, 2010). These two strategies allowed us to manipulate or visualize distinct populations of inhibitory interneurons in the mPFC within the context of the DISC1 locus impairment.

2.2.2 Stereotaxic surgery

Standard surgical procedures were followed. Mice were anesthetized with ketamine (100 mg/kg body weight) supplemented with xylazine (10 mg/kg body weight), and secured in a stereotaxic frame using serrated non-rupture ear bars. The injection frame was linked to a digital mouse brain atlas to define injection coordinates and guide the injection pipette to the target location (Leica ANGLE TWO, MyNeuroLab.com). 1 uL of Cre-dependent DISC1 shRNA or scrambled hairpin virus was delivered into the mPFC (A/P 1.94 mm; M/L .34 mm; D/V 2.0 mm vertical from the cortical surface) through a small burr hole in the skull (1-2 mm²) via pressure application (5-12 psi, Picospritzer III, General Valve). Mice were returned to their home cage and placed on a heating pad where they were allowed to recover for 12-24 hours. Neosporin was applied to the sutured skin and mice were provided recovery diet gel (ClearH₂O). Mice were monitored once per day for activity level and surgical site appearance for at least three days post-surgery. For DISC1 shRNA experiments, DISC1 HET and WT animals crossed to *SST-IRES-Cre* or *PV-IRES-Cre* mice were injected at P45 and recorded at P64-76. For GABA PPR experiments, Cre+ DISC1 HET and WT littermates were injected unilaterally with 0.5 uL of AAV-DIO-ChR2(H134R)-GFP at P54 and recorded approximately 2 weeks later.

2.2.3 Viral constructs

For DISC1 knockdown experiments, we utilized a shRNA sequence that has been extensively characterized (Ishizuka *et al.*, 2011; Kamiya *et al.*, 2005): the 5'-GGCAAACACTGTGAAGTGC-

3' sequence was packaged into an AAV construct that contains a floxed STOP codon cassette that enables Cre-dependent shRNA and GFP expression (Kuhlman & Huang, 2008). The control shRNA construct was also Cre-dependent but expressed a scrambled target sequence without homology to any known messenger RNA as well as GFP downstream of the floxed STOP codon. The lox-STOP-lox DISC1 shRNA AAV and lox-STOP-lox scrambled shRNA-AAV were generously gifted by the Sawa lab at Johns Hopkins University. Dr. Saurav Seshadri of the Sawa lab performed immunohistochemistry experiments to validate the specificity of shRNA/GFP expression and DISC1 knockdown *in vivo* (Seshadri *et al.* 2014, *submitted*).

2.2.4 Electrophysiological recordings of miniature events

Mice were anesthetized with isoflurane and decapitated, and their brains were quickly removed and chilled in ice-cold dissection buffer. (110.0 mM choline chloride, 25.0 mM NaHCO₃, 1.25 mM NaH₂PO₄, 2.5 mM KCl, 0.5 mM CaCl₂, 7.0 mM MgCl₂, 25.0 mM glucose, 11.6 mM ascorbic acid and 3.1mM pyruvic acid, gassed with 95% O₂ and 5% CO₂). Coronal sections containing mPFC were cut at 300 μ m thickness in dissection buffer, using a HM650 vibrating microtome (MICROM International GmbH), and transferred to a storage chamber containing ACSF (118 mM NaCl, 2.5 mM KCl, 26.2 mM NaHCO₃, 1 mM NaH₂PO₄, 20 mM glucose, 2 mM MgCl₂ and 2 mM CaCl₂, at 34 C, pH 7.4, gassed with 95% O₂ and 5% CO₂) at 34C for 30 min before it was transferred to room temperature (RT, 20-24C) and allowed to recover for an additional 30 min. Slices were then transferred to a recording chamber where they were constantly perfused with ACSF. All recordings were done without heating, at room temperature.

For pyramidal neuron miniature EPSC/IPSC recording experiments male and female DISC1 HET and WT littermates were recorded at age P70-P80. For SST and PV miniature EPSC/IPSC recording experiments, DISC1 HET or WT *SST-IRES-Cre; Ai14* or *PV-IRES-Cre; Ai14* mice were recorded at P54-P64. Whole cell voltage clamp recordings were obtained from layer II/III pyramidal neurons in the dorsal portion of the mPFC (including ACC and PrL cortex) in DISC1 HET and WT littermates (both male and female) aged P70-P80. The PrL region was identified based on landmarks (forceps minor of the corpus callosum) and

by measuring the distance from the midline and cortical surface. Borosilicate pipettes (3-5 M Ω) were filled with internal solution containing 115 mM cesium methanesulphonate, 20 mM CsCl, 10 mM HEPES, 2.5 mM MgCl₂, 4 mM Na₂-ATP, 0.4 mM Na₃GTP, 10 mM sodium phosphocreatine. Miniature excitatory post synaptic currents (mEPSCs) were recorded at -70 mV in the presence of 1 μ M tetrodotoxin (TTX) and 100 μ M picrotoxin (PTX). For mEPSC experiments, ACSF contained 2 mM CaCl₂ and 2 mM MgCl₂. Miniature inhibitory post synaptic currents (mIPSCs) were recorded at 0 mV in the presence of 1 μ M TTX, 100 μ M DL-AP5, and 10 μ M CNQX, and ACSF contained 2 mM CaCl₂ and 1 mM MgCl₂. Recording data was obtained using Multiclamp 700B amplifiers (Molecular Devices), and the liquid junction potential was not corrected for. Miniature recording data was collected in gap-free mode in pClamp 10 (Molecular Devices) for 10 minutes at room temperature.

2.2.5 Electrophysiological recording of GABA PPR

Two weeks post-injection, mice were sacrificed and acute slices were prepared as previously described. IPSCs were evoked by activating Chr2+ PV or SST INs by delivering a 1 ms blue light pulse through the 60x objective centered on the PN being recorded. IPSCs onto layer III pyramidal neurons were recorded at 0 mV holding potential in the presence of 10 μ M CNQX and 100 μ M AP-5. Light pulses were delivered at intervals of 50, 100, and 150 ms with \sim 30 individual trials recorded at each interval. Trials were averaged and the paired-pulse ratio calculated as the peak amplitude of the second evoked IPSC divided by the peak amplitude of the first evoked IPSC. In many cases, the first IPSC did not fully decay to baseline before the onset of the second IPSC. In these cases, the baseline of the second IPSC was corrected before the peak was measured. In order to compare the kinetics of the PV vs. SST IN-evoked IPSCs, averaged sweeps collected at the 150 ms interval were normalized, and the decay time constant and half-width were measured using automated procedures in the AxoGraph X 1.5.4 software.

2.2.6 Data analysis and statistics

For pyramidal neuron mEPSC data, 250 events were analyzed per cell and for mIPSC data, 300 events were analyzed per cell using Mini Analysis Program (Synaptosoft). For PV mEPSC data, 500 events were analyzed per cell, and for SST mEPSC data, 350 events were analyzed. Detection parameters for synaptic events, as well as the window across which detected events were reviewed, were maintained across files in order to improve intra-rater reliability. All statistical tests were performed in the Origin9.0 software (OriginLab, Northampton, MA) and GraphPad Prism version 6.0 (GraphPad Software, San Diego, CA). All data were tested for normality using the D'Agostino-Pearson omnibus normality test to guide the selection of parametric or non-parametric statistical tests. For parametric data, a two-tailed t -test or two-way ANOVA was used, and for non-parametric data a two-tailed Mann-Whitney inverted U test or Kruskal-Wallis ANOVA test was used with a post-hoc Mann-Whitney test with Bonferroni correction.

2.3 Results

2.3.1 Changes in spontaneous inhibitory transmission onto pyramidal neurons

As a means to survey whether DISC1 genomic deletion affects synaptic function in the local mPFC circuit, I first recorded action potential-independent excitatory and inhibitory transmission onto layer II/III pyramidal neurons in adult ($>P70$) DISC1 HET and WT mice. Miniature synaptic currents reflect the spontaneous exocytosis of neurotransmitter-filled vesicles. There was no difference in mEPSC frequency or amplitude onto layer II/III pyramidal neurons in DISC1 HET mice compared to WT **Fig2.1A1-4** ($p = .17$, Mann-Whitney; $p = .86$, two-tailed t -test $n = 23, 20$ $N = 4, 5$). While the amplitude of mIPSCs was not different between genotypes ($p = .51$, Mann-Whitney) **Fig2.1B1-2** the frequency of mIPSCs was significantly reduced in the DISC1 HET mice compared to WT **Fig2.1B3-4** ($**p < .01$, Mann-Whitney $n = 27, 29$ $N = 6, 5$) suggesting a presynaptic impairment.

2.3.2 Age-dependent changes in spontaneous inhibitory transmission in DISC1 HET and WT mice

Given that there is evidence that inhibitory transmission matures over the course of postnatal development (Hensch, 2005), I tested whether the reduced mIPSC frequency observed in adult DISC1 HET mice was present in preweanling DISC1 HET mice. I recorded mIPSCs onto layer II/III PNs in P12-P20 DISC1 HET mice and their WT littermates. Kruskal Wallis ANOVA revealed a significant effect of age on amplitude for both genotypes **Fig2.1E** ($\chi(1) = 14$, $***p < 0.001$; $\chi(1) = 15$, $****p < 0.0001$). In addition, WT mice exhibited a significant of age on frequency ($\chi(1) = 4$, $*p < 0.05$, Kruskal-Wallis ANOVA) while DISC1 HET mice did not **Fig2.1 F** ($\chi(1) = 0.29$, $p = 0.59$, Kruskal-Wallis ANOVA). A post-hoc Mann-Whitney test with a Bonferroni correction showed that mIPSC frequency was significantly lower in DISC1 HET compared to WT mice in the juvenile group ($*p < 0.05$). These results suggest that DISC1 HET mice undergo the normal process of strengthening inhibitory synapses during

adolescence, but presynaptic inhibitory neurons fail to exhibit an accompanying age-related increase in release probability or inhibitory synapse number. DISC1 HET mice seem to “start out” with lower spontaneous inhibitory transmission compared to WT mice and do not catch up by adulthood.

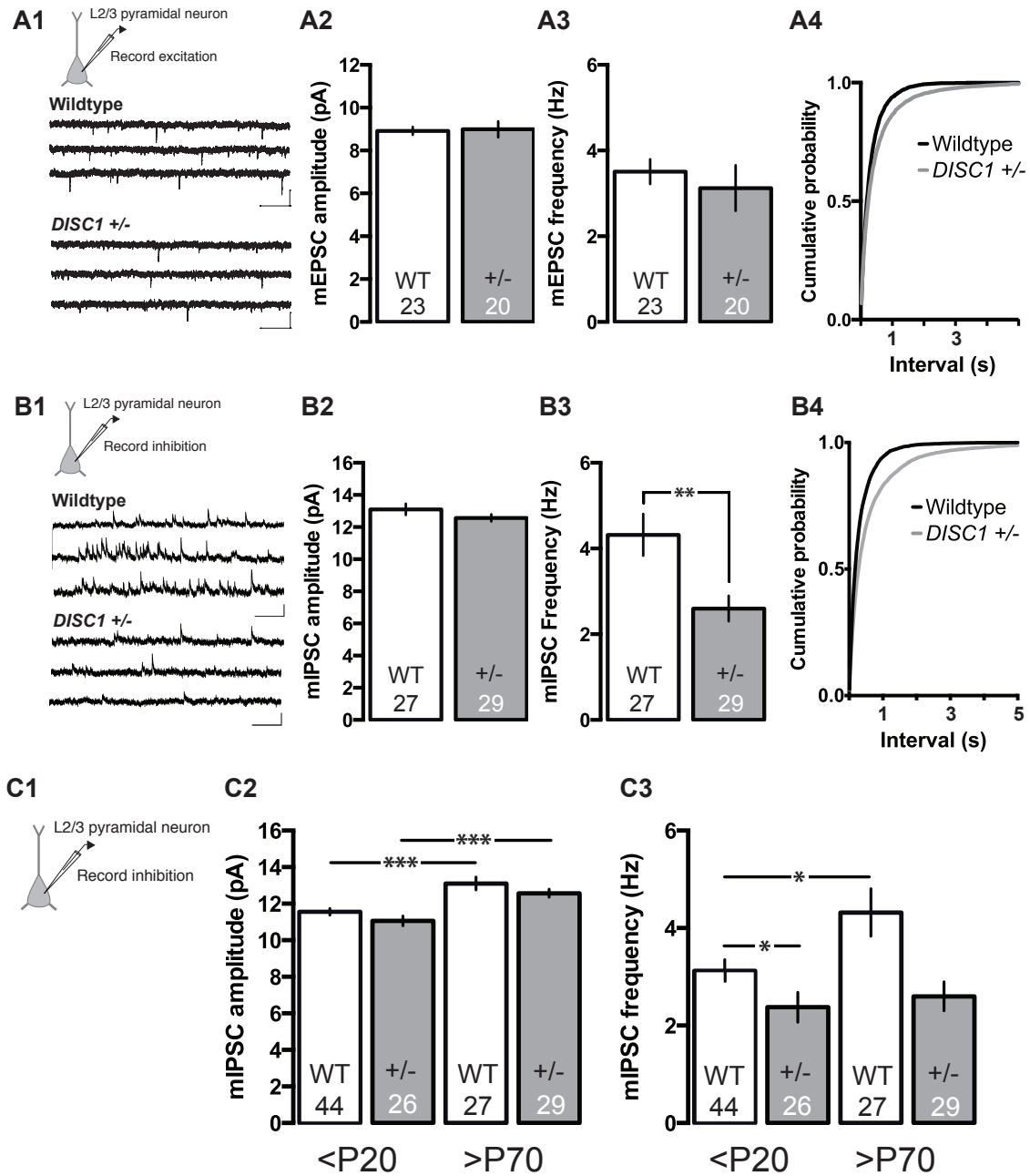


Figure 2.1: **Spontaneous excitatory and inhibitory transmission onto layer II/III PNs in mPFC.** A. Genomic deletion of *DISC1* did not affect mEPSC frequency or amplitude in adult (P70) *DISC1* HET mice compared to wild type littermates. Genomic deletion of *DISC1* significantly reduced the frequency of mIPSCs onto layer III PNs but did not affect mIPSC amplitude. C. Representative traces of mIPSCs recorded in WT and *DISC1* HET mice; scale bar = 500 ms, 20 pA. D. Cumulative probability distributions for mIPSC amplitude and inter-event interval. E. Both WT and HET mice show a significant effect of age on mIPSC amplitude. F. WT mice exhibited a significant interaction between age and mIPSC frequency while *DISC1* HET mice did not. A post-hoc Mann-Whitney test with a Bonferroni correction showed that mIPSC frequency was significantly lower in *DISC1* HET compared to WT mice in the P<20 age group (** $p < 0.001$ ** $p < 0.01$ * $p < 0.05$ Mann-Whitney and Kruskal-Wallis ANOVA test used).

2.3.3 Postnatal DISC1 knockdown

In addition to assessing the effect of genomic DISC1 deletion, I wanted to test the effect of cell-type restricted postnatal knockdown of DISC1. DISC1 mRNA expression peaks during E13.5, consistent with its important role in neuronal differentiation and migration (Brandon & Sawa, 2011; Brandon *et al.*, 2009). Intriguingly, there is a second dramatic increase in DISC1 expression that occurs around the onset of puberty (P35) (Schurov *et al.*, 2004). The significance of this second peak is unknown, but DISC1 has previously been shown to function at the postsynaptic density (Hayashi-Takagi *et al.*, 2010; Wang *et al.*, 2010). It's therefore possible that the later DISC1 expression peak reflects a pool of synaptic DISC1 protein, and could be important for puberty-related synaptic remodeling (Selemon, 2013). To assess the significance of pubertal DISC1 expression, I injected Cre-dependent DISC1 shRNA lentivirus into DISC1 HET and WT *SOM-IRES-Cre* or *PV-IRES-Cre* mice at P40 and recorded 2 weeks later.

2.3.4 Changes in spontaneous transmission onto PV+ interneurons

PV-restricted DISC1 knockdown significantly increased the frequency of mEPSCs onto PV+ interneurons in the mPFC compared to scrambled hairpin ($p > .05$, Mann-Whitney test), while it did not affect mEPSC amplitude **Fig2.2A,B** ($*p < .05$, Mann-Whitney test) ($p = .84$, Mann-Whitney). Meanwhile, there was no significant difference in the frequency or amplitude of mEPSCs onto PV+ INs in adult DISC1 HET vs. DISC1 WT mice **Fig2.2C,D** ($p = .91$, two-tailed t -test, $p = .08$, two-tailed t -test).

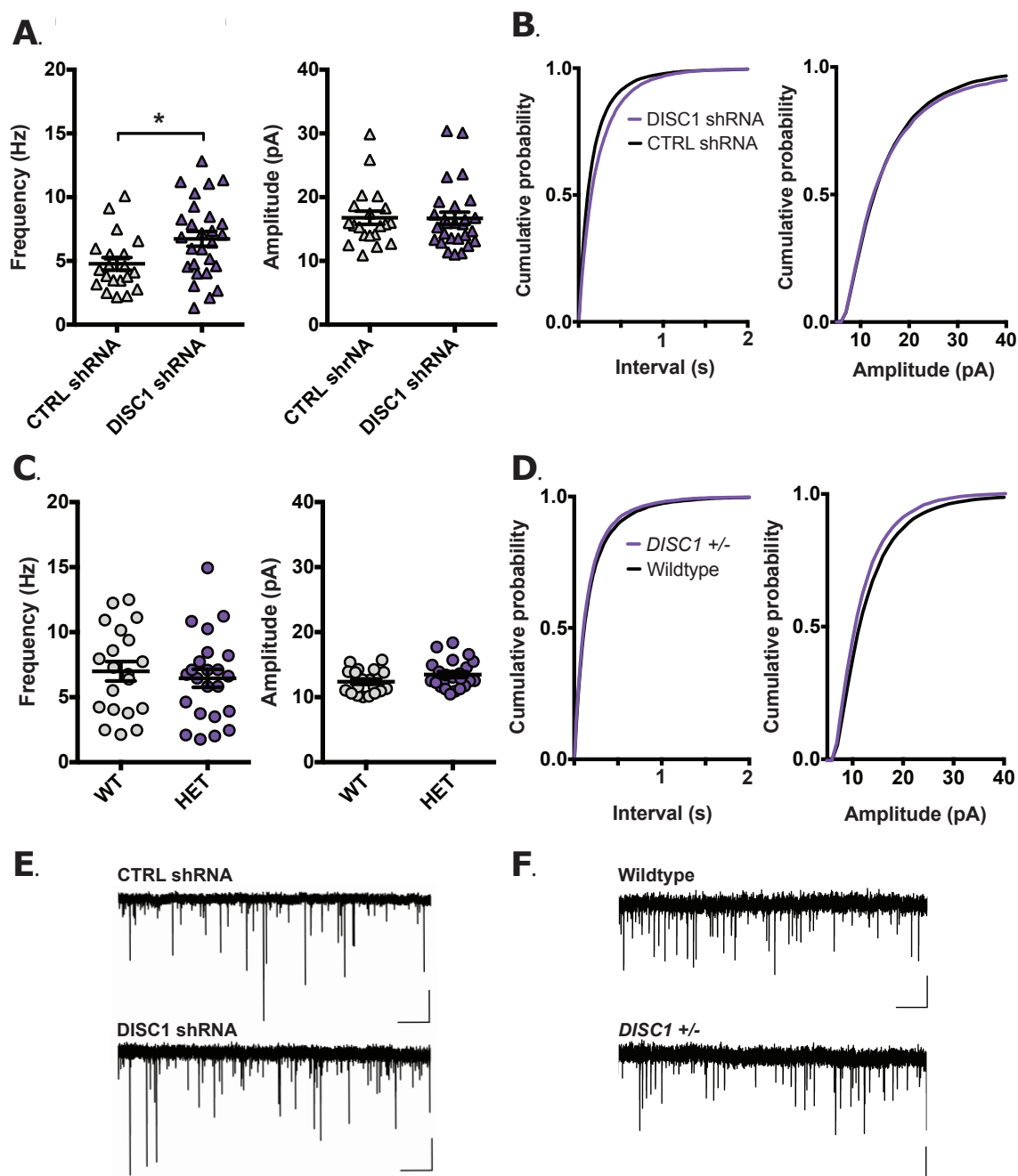


Figure 2.2: **Spontaneous excitatory transmission onto PV+ INs in mPFC.** A. PV+ IN restricted DISC1 knockdown significantly increased mEPSC frequency ($p < .05$, Mann-Whitney) but did not affect mEPSC amplitude compared to scrambled hairpin controls ($n = 27, 20$ N= 5, 4). B. mEPSCs were comparable across WT and DISC1HET genotypes ($n = 20, 23$ N= 4, 4). C.D. Cumulative probability distributions for inter-event interval and amplitude. E.,F. Representative mEPSC traces from knockdown and genomic deletion experiments; scale bar = 500 ms, 10 pA.

2.3.5 Changes in spontaneous transmission onto SST+ interneurons

SST-restricted DISC1 knockdown significantly increased the amplitude of mEPSCs onto SST+ INs in mPFC compared to scrambled control **Fig2.3A,B** (** $p < .01$, two-tailed t -test) while it did not affect mEPSC frequency ($p = .60$, Mann-Whitney). Interestingly, increased mEPSC amplitude onto SST+ INs was also observed when comparing DISC1 HET mice to WT littermates **Fig2.3C,D** (** $p < .01$, Mann-Whitney), with no effect on mEPSC frequency ($p = .125$, Mann-Whitney).

To determine if DISC1 knockdown also altered inhibitory transmission onto SST+ interneurons, I recorded mIPSCs onto SST+ INs infected with DISC1 shRNA or scrambled control shRNA. I found that there was a trend towards increased mIPSC amplitude onto SST+ INs following DISC1 knockdown compared to control but that amplitude was unaffected ($p = .068$ $p = .169$, two-tailed t -test **Fig2.4**).

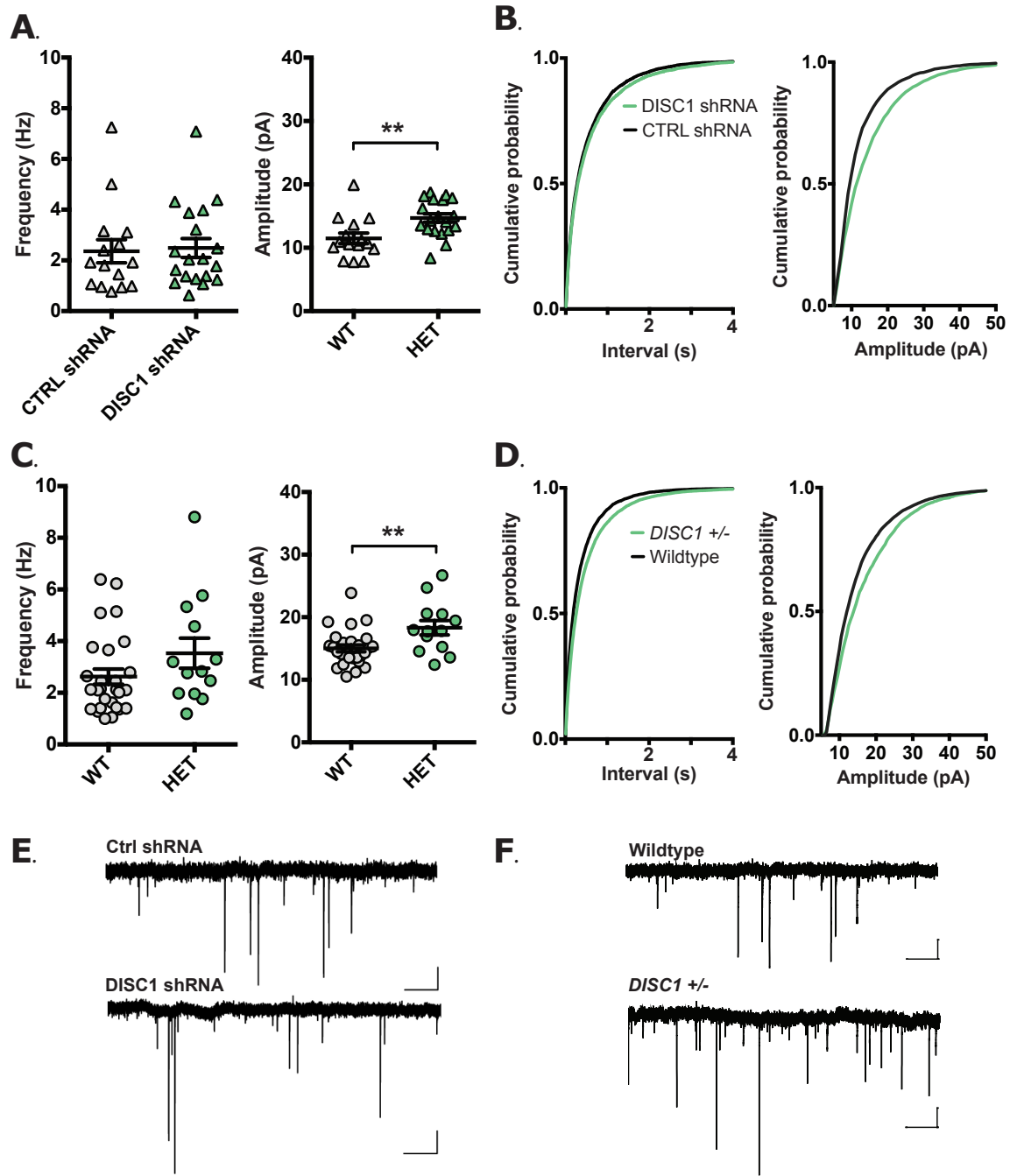


Figure 2.3: **Spontaneous excitatory transmission onto SST+ INs in mPFC.** A. SST+ IN restricted DISC1 knockdown significantly increased mEPSC amplitude (** $p < .01$, Mann-Whitney) but did not affect mEPSC frequency compared to scrambled hairpin controls (p (n= 15, 19 N= 4, 3)). B. mEPSC amplitude was also increased in DISC1 HET mice compared to WT littermates (** $p < .01$, (n= 13, 27 N= 3, 4)). C.D. Cumulative probability distributions for inter-event interval and amplitude. E.F. Representative mEPSC traces from knockdown and genomic deletion experiments; scale bar = 1 s, 10 pA.

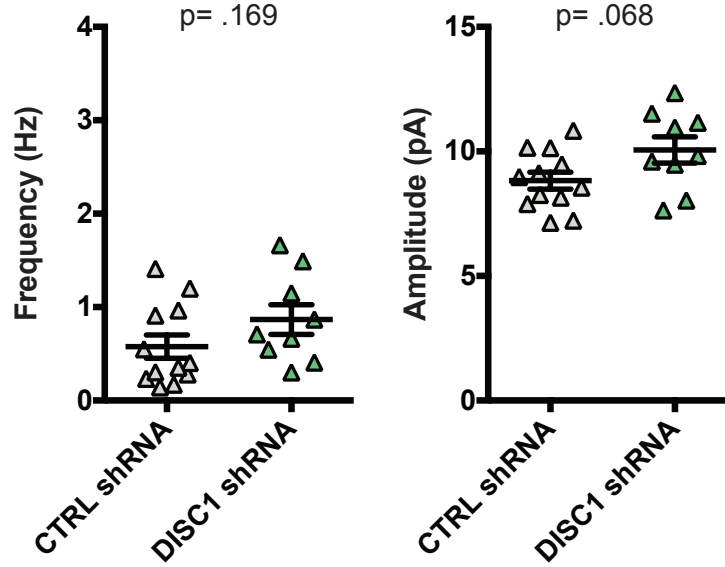


Figure 2.4: Spontaneous inhibitory transmission onto SST+ INs in mPFC. SST+ IN restricted DISC1 knockdown did not significantly alter mIPSC amplitude or frequency onto SST+ INs but there was a trend towards increased amplitude ($p = .068$, two-tailed t -test; $p = .169$ $n = 12$, 9 $N = 3$, 2)

2.3.6 Altered short-term plasticity at PV-PN synapse in DISC1 HET mice.

The observed decrease in mIPSC frequency onto layer II/III PNs in DISC1 HET mice compared to WT mice is compatible with a reduction of inhibitory synapse numbers onto pyramidal neurons, a reduction in presynaptic GABA release probability, or both. Because mPSCs reflect vesicular release from an unidentified mixture of presynaptic neurons, we first sought to test the GABA release properties in two genetically-defined inhibitory interneuron subtypes: PV+ and SST+ inhibitory interneurons. Together, PV and SST interneuron subtypes comprise $\sim 70\%$ of inhibitory interneurons in the (somatosensory) cortex (Rudy *et al.*, 2010).

We first measured the PPR of IPSCs evoked from Chr2+ PV INs onto layer III PNs in mPFC **Fig2.5A,B**. Repeated measures two-way ANOVA was performed for cells that were recorded at the 50, 100, and 150 ms interstimulus intervals (3 HET cells were missing 150 ms data). There was a significant effect of genotype and interval on PPR (genotype, $F(2, 42) = 3.915$ $*p < 0.05$; interval, $F(2, 42) = 6.772$ $**p < 0.01$) and the interaction of the two ($F(21, 42) = 3.915$ $*p < 0.05$). Post hoc Sidak's multiple comparisons test revealed that PPR was significantly higher in DISC1 HET mice than WT mice at the 50 ($***p < 0.001$) and 100 ($*p < 0.05$) inter-

stimulus intervals **Fig2.5B-C**. These results were surprising given that short-term depression is considered to be characteristic of PV-expressing synapses (Caillard *et al.*, 2000; Hefft & Jonas, 2005; Owen *et al.*, 2013). It is likely that the PV-IRES-Cre line captures a heterogenous population of interneurons, and therefore GABA release may be affected in a subset of PV-IRES-Cre cells under conditions of reduced DISC1 expression.

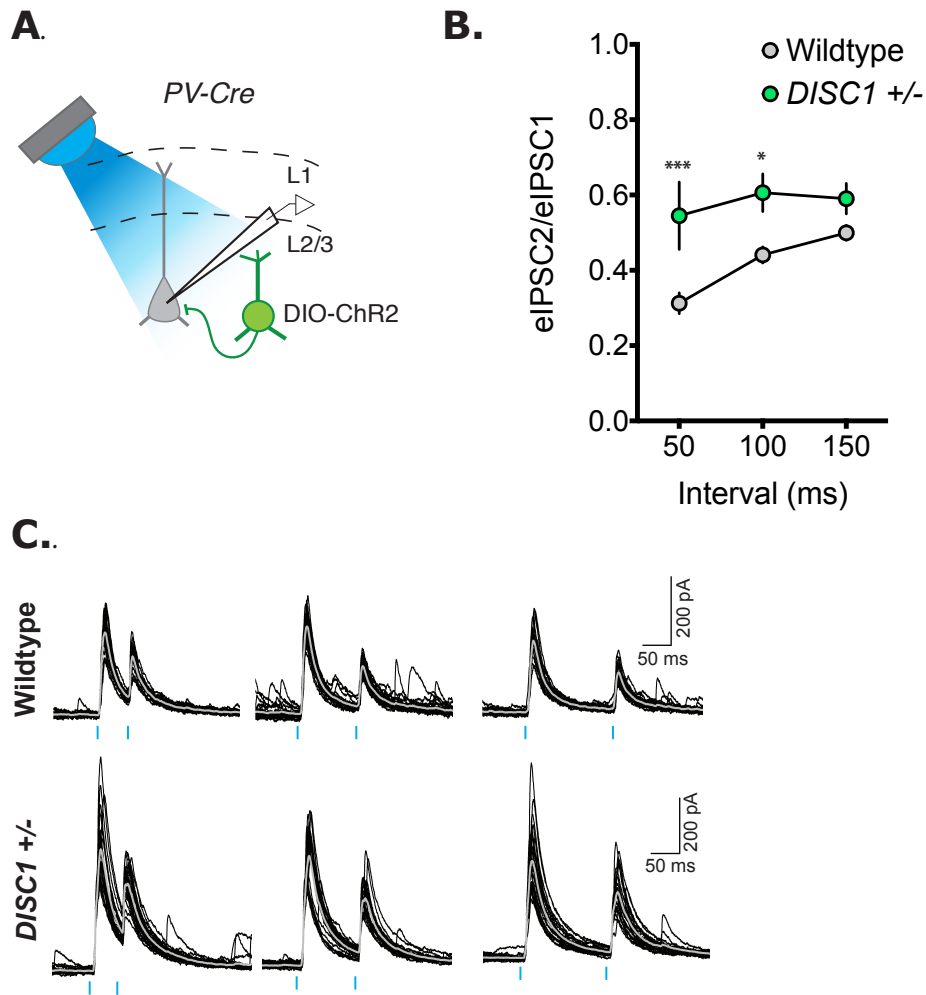


Figure 2.5: PV-evoked IPSC PPR is increased in DISC1 HET mice. A. Recording configuration: 1 ms blue light pulses were delivered at 50, 100, and 150 ms intervals to evoke IPSCs from ChR2+ PV interneurons onto layer II/III PNs in mPFC. C. Representative traces from WT and DISC1 HET mice at 50, 100, and 150 ms intervals. Black lines represent single trials, averaged traces in gray. C. DISC1 HET mice exhibited significantly higher evoked IPSC PPR at 50 ms and 100 ms intervals (** $p < 0.01$; * $p < 0.05$ post-hoc Sidak's multiple comparisons test $n = 15, 12$). $N = 3$ animals per group.

2.3.7 Short-term plasticity at the SST-PN synapse is unaltered in DISC1 HET mice

We next measured the PPR of IPSCs evoked from Chr2+ SST INs onto layer II/III PNs in mPFC **Fig2.6A,B**. A two-way ANOVA showed a significant effect of interval on PPR $F(2, 50) = 24.88$, **** $p < 0.0001$. However, there was no significant effect of genotype on PPR $F(1, 25) = 1.639$, $p = 0.21$, nor was there a significant effect of genotype and interval on PPR $F(2, 50) = 0.47$, $p = 0.63$. SST GABA PPR was consistent between genotypes across all intervals tested ($p > 0.05$ Sidak's multiple comparisons test) **Fig2.6C,D**.

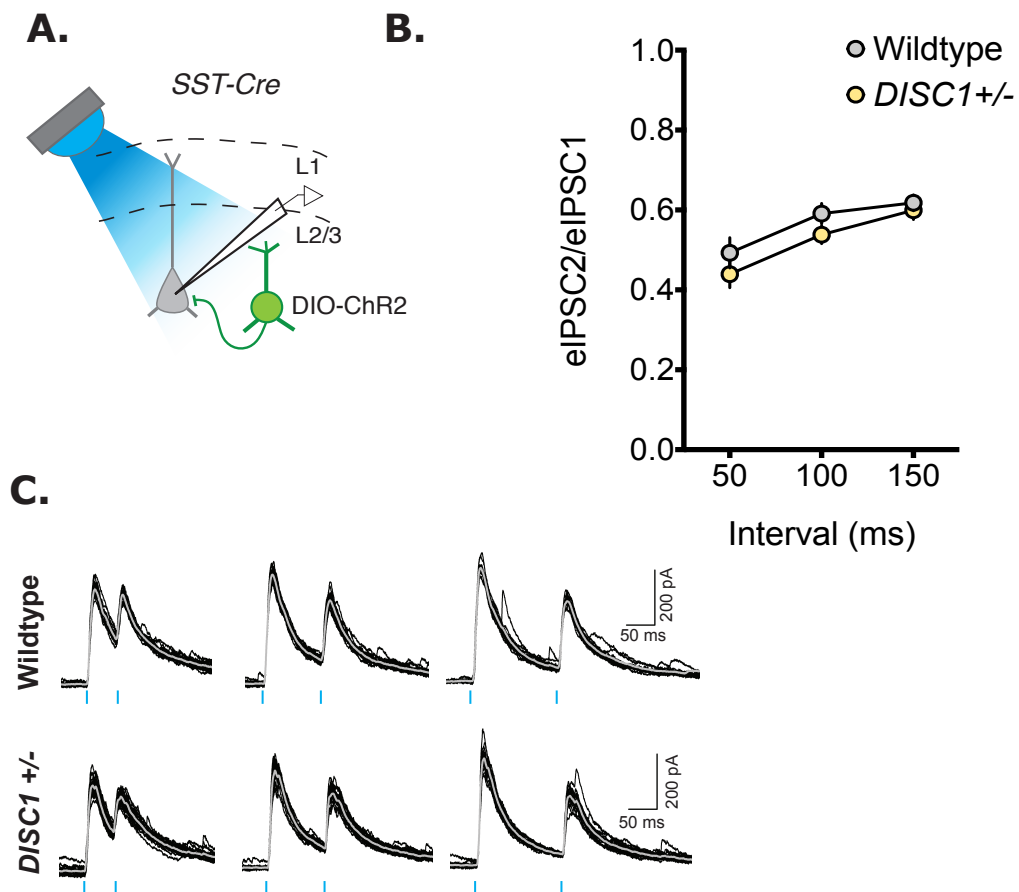


Figure 2.6: SST-evoked IPSC PPR is unchanged in *DISC1* HET mice. A. Recording configuration: 1 ms blue light pulses were delivered at 50, 100, and 150 ms intervals to evoke IPSCs from ChR2+ SST interneurons in mPFC. B. Representative traces from WT and *DISC1* HET mice at 50, 100, and 150 ms intervals. Black lines represent single trials, averaged traces in gray. C. *DISC1* HET mice exhibited the same GABA PPR as WT mice across the intervals tested. D. Boxplots show PPR data was normally distributed and there were no significant differences between genotypes at any interval. N=2 animals per group.

2.3.8 Distinct decay kinetics of GABA transmission from PV vs. SST interneurons

At first glance, IPSCs mediated by SST+ INs appeared to decay more slowly than those mediated by PV+ INs. Therefore, I compared the decay time constants calculated from the normalized average peak IPSC recorded at the 150 ms interval in the GABA PPR experiment **Fig2.7A,B**. Mann-Whitney tests with Bonferroni correction showed that IPSCs mediated by PV INs had smaller half-widths and decay time constants than IPSCs mediated by SST INs in both genotypes (WT: $p=0.03$ n.s., $**p<.01$, HET: $**p<.01$, $****p<0.0001$) **Fig2.7C,D**. This is consistent with reported data regarding uIPSCs from FS/PV and LTS/SST interneurons to pyramidal cells (Kobayashi *et al.*, 2010; Ma *et al.*, 2012) and suggests that IPSC decay kinetics may be a useful measure to identify the source of inhibitory currents. There was no difference between genotypes for IPSC decay time constant (PV: $p=0.83$ SST: $p=0.06$, two-tailed *t*-test with Bonferroni correction) or half-width (PV: $p=0.68$, two-tailed *t*-test with Bonferroni correction SST: $p=0.13$, Mann-Whitney with Bonferroni correction).

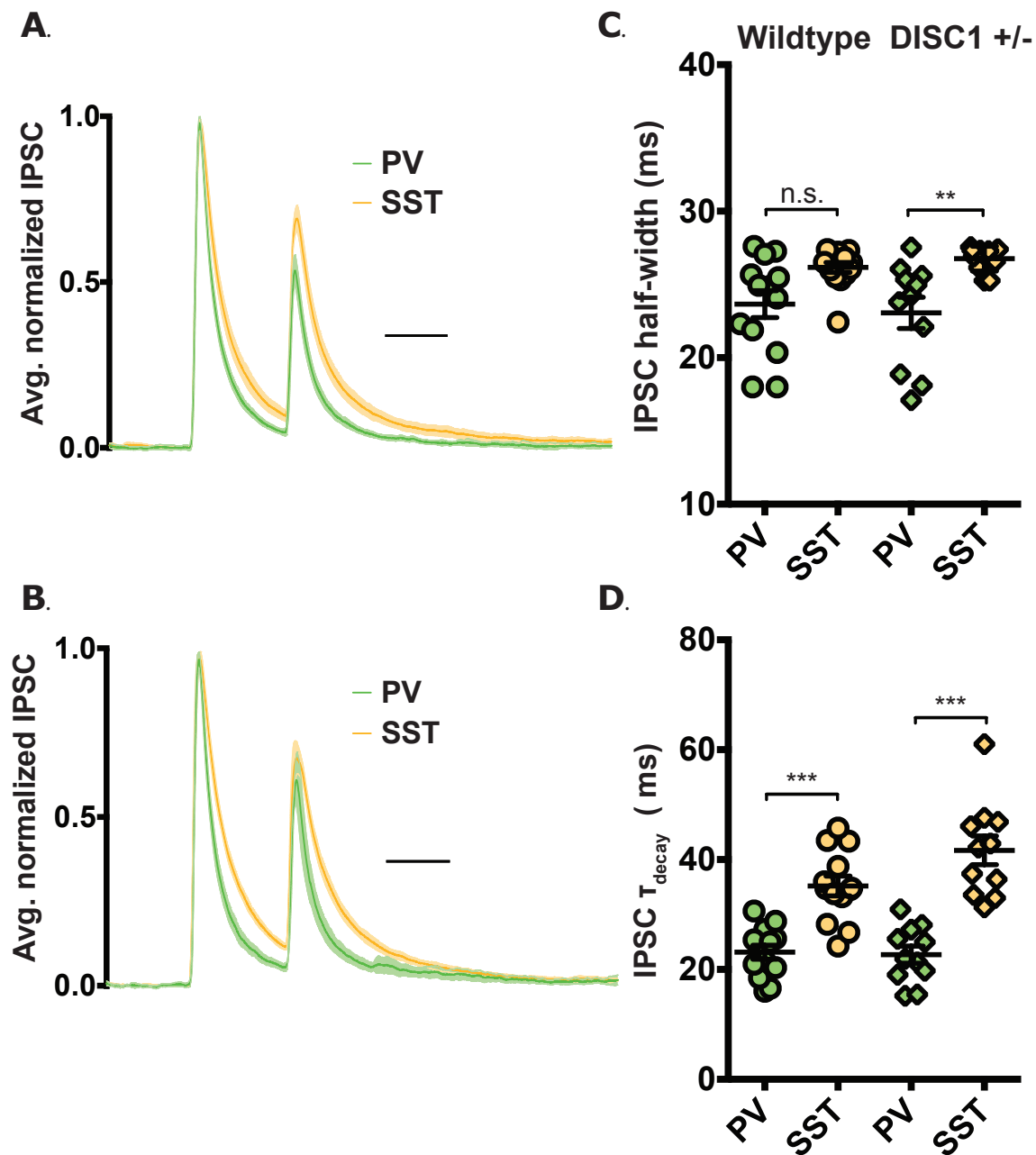


Figure 2.7: **PV and SST INs exhibit distinct IPSC decay kinetics.** A. Average normalized IPSCs evoked by direct Chr2 stimulation of PV or SST INs in WT mice. Line represents mean and shading corresponds to the 95% confidence interval. B. Average normalized IPSCs recorded in DISC1 HET mice. C. IPSC half-width in PV and SST-mediated IPSCs, circles= WT, diamonds= HET. D. IPSC decay time constant of PV and SST-mediated IPSCs. Scale bar= 100 ms.

2.3.9 Conclusions

A set of changes in the mPFC circuitry were observed that suggests that PV interneuron function is altered in the DISC1 HET mouse. Firstly, we found that the frequency but not amplitude of spontaneous inhibitory transmission onto layer III pyramidal neurons was significantly reduced in adult DISC1 HET mice compared to WT littermates that had two copies of the full-length DISC1 gene. Meanwhile, we found no difference in the frequency or amplitude of spontaneous excitatory transmission onto layer III pyramidal neurons in mPFC. A reduction in mIPSC frequency is consistent with reduced GABA release probability, fewer inhibitory synapses onto PNs, or both. In order to investigate whether a presynaptic alteration in GABAergic function contributed to reduced mIPSC frequency, we took advantage of Cre-dependent ChR2 expression in the *PV-IRES-Cre* and *SST-IRES-Cre* mouse lines. By evoking PV or SST-mediated IPSCs onto layer III pyramidal neurons, we were able to assess the short-term dynamics of GABA transmission from these two major interneuron subtypes. We found that the paired-pulse ratio of PV-evoked IPSCs onto pyramidal neurons was significantly increased in DISC1 HET mice compared to WT, while there was no significant difference between genotypes for SST-mediated IPSCs. Interestingly, we found no difference in the decay kinetics of the PV-mediated IPSCs onto pyramidal neurons in DISC1 HET compared to WT. This, along with the evidence that mIPSC amplitude is not affected, suggests that inhibitory synaptic transmission is primarily affected at the presynapse.

In the PV/SST light-activated IPSC recordings, we observed that PV and SST INs exhibited distinct properties in IN-PN transmission. In WT mice, there was a significant effect of cell type on GABA PPR, with SST-evoked IPSCs exhibiting higher PPR than PV-evoked IPSCs at the 50 and 100 ms interstimulus intervals. This pattern was similar to what was observed when comparing FS-PN and SST-PN unitary inhibitory currents in layer IV barrel cortex (Ma *et al.*, 2012). However, because PV-evoked IPSC PPR was significantly increased in the DISC1 HET mice, they did not exhibit a significant effect of cell-type on GABA PPR. This is intriguing because normally, there is reciprocal relationship between the kinetics and short-term plasticity properties of input and output synapses of PV and SST INs (Beierlein *et al.*, 2003; Ma *et al.*, 2012). That is, EPSPs onto PV/FS INs are fast rising as are uIPSCs from

PV/FS INs. In addition, PV-PN synapses depress during ongoing activity, making feedback and feedforward inhibition through PV INs optimized to transmit transient information as opposed to sustained information about ongoing behavior (Ma *et al.*, 2012). Conversely, PN-SST synapses exhibit slower kinetics in both directions, and SST-PN IPSCs facilitate. In the PN-SST-PN circuit, SST-PN IPSCs are less temporally precise, but they are able to sustain inhibition onto PN dendrites and potentially gate plasticity. If PV-mediated IPSCs in the DISC1 HET mice do not rapidly depress, this may impair the ability of PV INs to precisely transmit signals regarding transient stimuli.

This data suggests that genomic deletion of DISC1 primarily affects inhibitory as opposed to excitatory synaptic transmission onto pyramidal neurons in the prefrontal cortex. We have not measured mIPSCs in other cortical areas, so we do not know whether this is a brain region-specific effect. To date, studies assessing the neurophysiological effects of DISC1 deficiency are surprisingly sparse (Duan *et al.*, 2007; Hayashi-Takagi *et al.*, 2010; Holley *et al.*, 2013; Kvajo *et al.*, 2011; Maher & Loturco, 2012; Niwa *et al.*, 2010). However, our finding is consistent with another report of decreased spontaneous inhibitory transmission onto layer II/III pyramidal neurons in mPFC of male mice expressing a truncated form of DISC1 (Holley *et al.*, 2013). DISC1 expression has been shown to be particularly high at the postsynaptic density (Carlisle *et al.*, 2011; Hayashi-Takagi *et al.*, 2010; Kirkpatrick *et al.*, 2006; Paspalas *et al.*, 2013; Wang *et al.*, 2010) and consequently most investigations of DISC1's effect on synaptic transmission have focused on postsynaptic function. However, DISC1 is also expressed in axons and presynaptic terminals (Kirkpatrick *et al.*, 2006; Wang *et al.*, 2010) and interacts with proteins that are involved in axon cargo transport, vesicle docking, and exocytosis (Camargo *et al.*, 2007). The role of DISC1 in presynaptic function has been highlighted by two recent studies: frequency facilitation, a form of short-term plasticity, was reduced in the mossy fiber/CA3 circuit of truncated DISC1 mice (Kvajo *et al.*, 2011) and glutamate release probability from pyramidal neurons was shown to be reduced following *in utero* DISC1 knockdown in pyramidal neurons (Maher & Loturco, 2012). Currently, the potential mechanisms of DISC1's effect on presynaptic release are unknown, although DISC1 knockdown was reported to slow the transport of synaptic vesicles along the neuronal processes of cultured primary neurons (Flores *et al.*,

2011).

While our study is the first to specifically assess the presynaptic function of inhibitory interneurons in a DISC1 mouse model, other studies have made observations that hint at PV dysfunction: reduced sIPSC frequency was seen in the frontal cortex of male mice expressing a truncated form of human DISC1 (hDISC1) (Holley *et al.*, 2013), reduced PV expression has been observed in the PFC of many DISC1 models (Ayhan *et al.*, 2010; Hikida *et al.*, 2007; Ibi *et al.*, 2010; Lee *et al.*, 2013a; Niwa *et al.*, 2010; Shen *et al.*, 2008), and tangential migration of MGE-derived neurons is impaired (Lee *et al.*, 2013b; Steinecke *et al.*, 2012). While it's been shown that DISC1 is expressed in MGE-derived neurons, which include PV and SST INs, the expression profiles of DISC1 (such as splice isoform expression, and subcellular localization) in these INs are not known. Therefore differences in synaptic phenotypes in PV vs. SST in the DISC1 HET background may be due to cell type differences in DISC1 expression profiles and function. Single-cell RNA-seq studies that focus on genetically-defined populations of PV or SST INs could shed light on the expression patterns of DISC1 in these two IN types.

One of the goals of this work was to evaluate whether DISC1 genomic deletion, which decreases DISC1 expression by half brain-wide and presumably in all cell-types (Jaaro-Peled *et al. submitted*), affects synaptic transmission differently than cell-type restricted postnatal knockdown of DISC1. In order to assess synaptic function in defined populations of neurons, we crossed the DISC1 heterozygous mice into the *PV-IRES-Cre; Ai14* and *SST-IRES-Cre; Ai14* reporter lines. This approach allows us to assay the effect of DISC1 deletion in defined cell types within a haploinsufficiency model that is believed to mimic the effects DISC1 translocation. We were interested to compare the mini recording results collected from HET mice to recordings collected from cell-type restricted knockdown. In the SST INs, we observed a significant increase in the mEPSC amplitude onto SST INs in heterozygous and SST-specific DISC1 knockdown experiments. This suggests that DISC1 expression alters SST postsynaptic function in a manner that is “cell-autonomous.”

Meanwhile, we found that mEPSCs were not different onto PV INs of DISC1 HET mice, but PV-restricted DISC1 knockdown increased mEPSC frequency onto PV INs. This finding is a little surprising given that a change in frequency suggests an effect at the presynapse, where

DISC1 expression was not altered. However, one possibility is that the increased mEPSC frequency seen in the PV DISC1 knockdown was a homeostatic response to increased network activity (possibly caused by reduced PV IN function following DISC1 knockdown) (Chang *et al.*, 2010). The fact that we did not observe this effect in the DISC1 heterozygous mice suggests that either the timing of DISC1 loss, or the cumulative impact of DISC1 loss within all neurons of the network differentially influence excitatory input on PV INs. Compared to SST INs, this suggests that the impact of DISC1 loss in PV INs may be more affected by the function of the network. This may be consistent with the observation that PV expression is reduced when DISC1 expression is disrupted in pyramidal neurons (Brandon & Sawa, 2011). An open question is whether the DISC1 heterozygous effects such as the reduced mIPSC frequency or increased PPR from PV INs can be recapitulated by PV-restricted DISC1 knockdown. The fact that we observed reduced mIPSC frequency in preweanling DISC1 HET mice suggests that this impairment is a result of early developmental mechanisms, and not necessarily related to the “second wave” of DISC1 expression during adolescence (Schurov *et al.*, 2004).

	Pyramidal		Somatostatin		Parvalbumin	
	HET	KD	HET	KD	HET	KD
miniEPSC freq	↔	↔	↔	↔	↔	↑
miniEPSC amp	↔	-	↑	↑	↔	↔
miniIPSC freq	↓	-	-	↔	-	-
miniIPSC amp	↔	-	-	↔	-	-
GABA PPR	-	-	↔	-	↑	-
IPSC decay	-	-	↔	-	↔	-

Table 2.1: **Summary of synaptic effects in DISC1 heterozygous and DISC1 knockdown experiments**

Chapter 3

Feedforward inhibition in the MD-mPFC projection

3.1 Introduction

In this chapter, we probed the function of the thalamocortical projection from the mediodorsal thalamus (MD) to the dorsal anterior cingulate cortex (dACC). In the second chapter of this thesis, we found that the frequency of mIPSC transmission onto layer III PNs in the mPFC was reduced and that the PPR of PV IN-mediated IPSCs onto layer III PNs was increased in the DISC1 HET mice. These findings point to an impairment in mPFC PV-PN GABA transmission in the context of DISC1 loss-of-function. It has been proposed that reduced GABA signaling from PV INs in the DLPFC could contribute to the pathophysiology of working memory impairments in SZ (Lewis, 2009), in keeping with evidence that GABA transmission is important for working memory (Enomoto *et al.*, 2011; Sawaguchi *et al.*, 1989). One mechanism by which PFC GABA transmission could be impaired is reduced feedforward inhibition from the mediodorsal thalamus which sends direct projections to layer III and V pyramidal and inhibitory neurons in the PFC (Kuroda *et al.*, 2004; Rotaru *et al.*, 2005). Lesion of the mediodorsal thalamus produces cognitive impairments that in many ways resemble those caused by PFC lesion (Mitchell & Chakraborty, 2013) suggesting that communication between the MD and mPFC is crucial

for behavioral flexibility and working memory processes. Feedforward inhibition is important for narrowing the window of excitatory integration and thus sharpening spike timing (Pouille & Scanziani, 2001), and is thus predicted to be an important mechanism for filtering out weak responses and synchronizing the firing of neuronal assemblies that are potentially involved in the same task (Engel & Singer, 2001).

To date, the role of PV IN function in the normal activity coupling between the MD and mPFC is unexplored, although intriguingly, functional connectivity between the MD and PFC is reduced in individuals with SZ (Mitelman *et al.*, 2005; Schlosser *et al.*, 2008; Seidman *et al.*, 1994; Zhou *et al.*, 2007). PV INs have an established role in generating gamma oscillations (Cardin *et al.*, 2009; Sohal *et al.*, 2009), which increase in the DLPFC with working memory load (Howard *et al.*, 2003) and are weaker in people with SZ (Cho *et al.*, 2006; Minzenberg *et al.*, 2010). Therefore, impaired regulation of PN excitatory integration by PV INs could lead to impairments in gamma oscillations and, therefore, working memory (Lewis, 2009). While the schizophrenia literature has focused much of its attention of gamma oscillations, more subtle elevations in E/I balance are also predicted to perturb working memory (Marín, 2012).

The seminal work of Patricia Goldman-Rakic revealed that persistent firing of spatially-tuned PFC pyramidal neurons during delay periods predicted performance on a delayed oculomotor WM task (Funahashi *et al.*, 1989), and that increasing E/I balance via GABA_A antagonism destroys spatial tuning of delay period neurons in primate DLPFC (Rao *et al.*, 2000). In a computational model of working memory that includes 2 key network properties – strong recurrent excitation to sustain persistent activity and lateral inhibition to shape selectivity of representation – introducing disinhibition leads to higher baseline firing rates and broadened working memory activity patterns (Murray *et al.*, 2014). At the behavioral level, disinhibition accelerates the deterioration of the precision of information held in WM. Such deterioration would be predicted to impair working memory performance on shorter delay trials than when E/I is balanced. In DISC1 mouse models, the most commonly observed changes seen across models are reduced PV expression in the PFC and impaired working memory performance (Ayhan *et al.*, 2010; Brandon & Sawa, 2011; Clapcote *et al.*, 2007; Hikida *et al.*, 2007; Koike *et al.*, 2006; Kvaajo *et al.*, 2008; Niwa *et al.*, 2010; Shen *et al.*, 2008), raising the question of

whether E/I balance is altered in DISC1 HET mice. Although the data suggests that DISC1 expression may be required for normal PV expression, the surprising thing is that it is required in a non-cell-autonomous way. That is, expressing a truncated form of DISC1 downstream of the CaMK promoter (Hikida *et al.*, 2007), or the transient knockdown of DISC1 in migrating pyramidal neurons (Niwa *et al.*, 2010), both produce reductions in PV expression. Regardless, the co-occurring changes in mPFC PV expression and working memory performance suggests that PV pathophysiology might be the link between altered DISC1 expression and working memory impairment.

3.1.1 The role of PV+ INs in thalamocortical projections

To aid in the understanding of the potential role of feedforward inhibition in the mPFC, there is a rich body of literature from TC circuits in the sensory cortices. Intracortical glutamatergic synapses predominate over thalamocortical glutamatergic synapses in the cortex, with an estimated 10-23% of synapses onto cortical neurons in the thalamorecipient layer being of thalamic origin (Benshalom & White, 1986). A recent study that isolated thalamic excitatory contribution to V1 by optogenetically activating PV+ INs to silence intracortical communication, found that thalamic excitation contributes roughly a third of the total excitation in V1 (Lien & Scanziani, 2013). Lien *et al.* observed that isolated thalamic and total excitation were similarly tuned to orientation and direction, suggesting that the primary function of cortical circuits is to amplify tuned thalamic input. The pattern and magnitude of this TC amplification should depend largely on the function of inhibitory interneurons that are either recruited directly by the thalamus (feed-forward) or by local cortical pyramidal neurons (feed-back). Feed-forward inhibition, the faster of the two, is capable of truncating ongoing TC responses, thus suppressing spikes in neurons that receive weak TC input and imposing temporal precision on neurons that reach threshold.

In order for inhibitory interneurons to shape the receptive fields of neighboring pyramidal neurons, they must be more effectively recruited by TC inputs. TC recruitment of feed-forward primarily through fast-spiking PV interneurons is well-studied in the VPM-barrel cortex circuit (Agmon & Connors, 1992; Cruikshank *et al.*, 2007; Daw *et al.*, 2007; Gabernet

et al., 2005; Gil & Amitai, 1996; Porter *et al.*, 2001; Sun *et al.*, 2006; Swadlow, 2002). Single unit recordings *in vivo* have also shown that fast-spiking inhibitory INs demonstrate robust responses to thalamocortical (TC) activation. The basis for robust recruitment of FS INs appears to be due to larger excitatory conductances rather than intrinsic mechanisms (Cruikshank *et al.*, 2007). Furthermore, the threshold for IPSP recruitment in the TC pathway is significantly lower than the threshold within intracortical circuits (Gil & Amitai, 1996). As FS IN-mediated feed-forward inhibition has been observed in a wide range of cortical areas (Miller *et al.*, 2001; Pouille & Scanziani, 2001; Wehr & Zador, 2003), it is believed to be a fundamental property of the TC microcircuit. Therefore, we hypothesized that the same mechanisms should be in place within prefrontal cortex, whose long-range afferents it has only recently become possible to study with the advent of optogenetics (Cruikshank *et al.*, 2012).

In this section, we took advantage of the ability to directly excite ChR2-expressing axons and terminals in order to trigger neurotransmitter release in the prefrontal cortex. This method of viral transduction in one brain region and illumination of downstream axons makes it possible to interrogate long-range projections between the thalamus and prefrontal cortex that would be severed in most practical slice preparations (Yizhar *et al.*, 2011) and has successfully been used to study TC projections in other cortical areas (Cruikshank *et al.*, 2010; Hooks *et al.*, 2013; Petreanu *et al.*, 2007). We sought to functionally validate the reported projection from MD to PV INs and determine if PV INs mediate thalamocortical feedforward inhibition onto layer III PNs. We then compared the ratio of GABA : AMPA currents recruited onto layer III PNs by MD afferent stimulation in DISC1 WT and HET mice with the hypothesis that GABA : AMPA ratio would be reduced in DISC1 HET mice. Finally, we performed a set of inhibitory optogenetic experiments to test whether PV silencing abolishes MD-evoked IPSCs. Below I outline the background of the mediodorsal thalamus, its pathology in schizophrenia, and its proposed function in recruiting feedforward inhibition in the mPFC.

3.1.2 General anatomy/connectivity of MD

The mediodorsal thalamus is classified as a higher order relay nucleus as it's been reported to receive “driver” inputs from layer V of prefrontal cortex (Sherman & Guillery, 2002) and in contrast to primary relay nuclei that receive sensory information directly from the periphery, the mediodorsal thalamus receives little to no sensory input. The MD exhibits extensive reciprocal connections with the prefrontal cortex, and in fact, the prefrontal cortex is generally defined as the frontal region of the brain that receives input from the MD. Thalamocortical projections generally terminate in cortical layer IV, and neurons in layer VI – and to a lesser extent V – project back to the thalamus. In well-studied thalamocortical loops such as the VB to the barrel cortex, coupled thalamic and cortical regions exhibit functional similarities. Ultrastructural studies have shown that layer VI axons have small terminals that contact peripheral dendritic segments, layer V axons are large and contact the dendritic segments. This has led to the idea that layer V inputs act as “drivers” whereas layer VI inputs modulate thalamic neuron activity (Guillery, 2003). The fact that MD exhibits specific and reciprocal connections with the prefrontal cortex suggests that it participates in limbic and cognitive processes that the prefrontal cortex participates in, and there are reported to be a small number of layer V corticothalamic neurons that receive direct input from MD and send their axons to MD (Kuroda *et al.*, 1993). Evidence of the importance of cortical activity for second-order thalamic activity comes from inactivation studies that found while primary thalamic nuclei are minimally affected by cortical inactivation, second-order thalamic nuclei become unresponsive to peripheral input, highlighting the driving influence of cortical input for second-order relays (Diamond *et al.*, 1992). Cooling of the PFC was demonstrated to decrease firing rates in the MD, suggesting that MD likewise receives substantial cortical drive (Alexander & Fuster, 1973).

In rats, extensive electron microscopic studies have shown that MD efferents terminate primarily in layer III – and to a lesser extent I and V – forming asymmetric synapses onto the apical dendrites of pyramidal cells whose somata lie in layers III and V in the mPFC (Kuroda *et al.*, 1995b, 1996; Rotaru *et al.*, 2005; Vogt *et al.*, 1981). Due to differences in dendritic branching within layer III, it is believed that pyramidal neurons whose somata lie in layer III are more greatly influenced by MD inputs than layer V pyramidal neurons (Kuroda *et al.*,

1996). At least some of these layer III thalamorecipient neurons project callosally (Kuroda *et al.*, 1995a). However, another study that looked at callosal and thalamic afferents to cingulate cortex together found that the terminal fields were largely non-overlapping, suggesting that MD mainly targets the output neurons of the cortex (Vogt *et al.*, 1981). In addition, MD afferents also form synapses onto the dendritic shafts of GABAergic INs in layer III and V of mPFC (Kuroda *et al.*, 2004, 1996), particularly those that express parvalbumin (Rotaru *et al.*, 2005). Ultrastructural findings are summarized in **Fig3.1**.

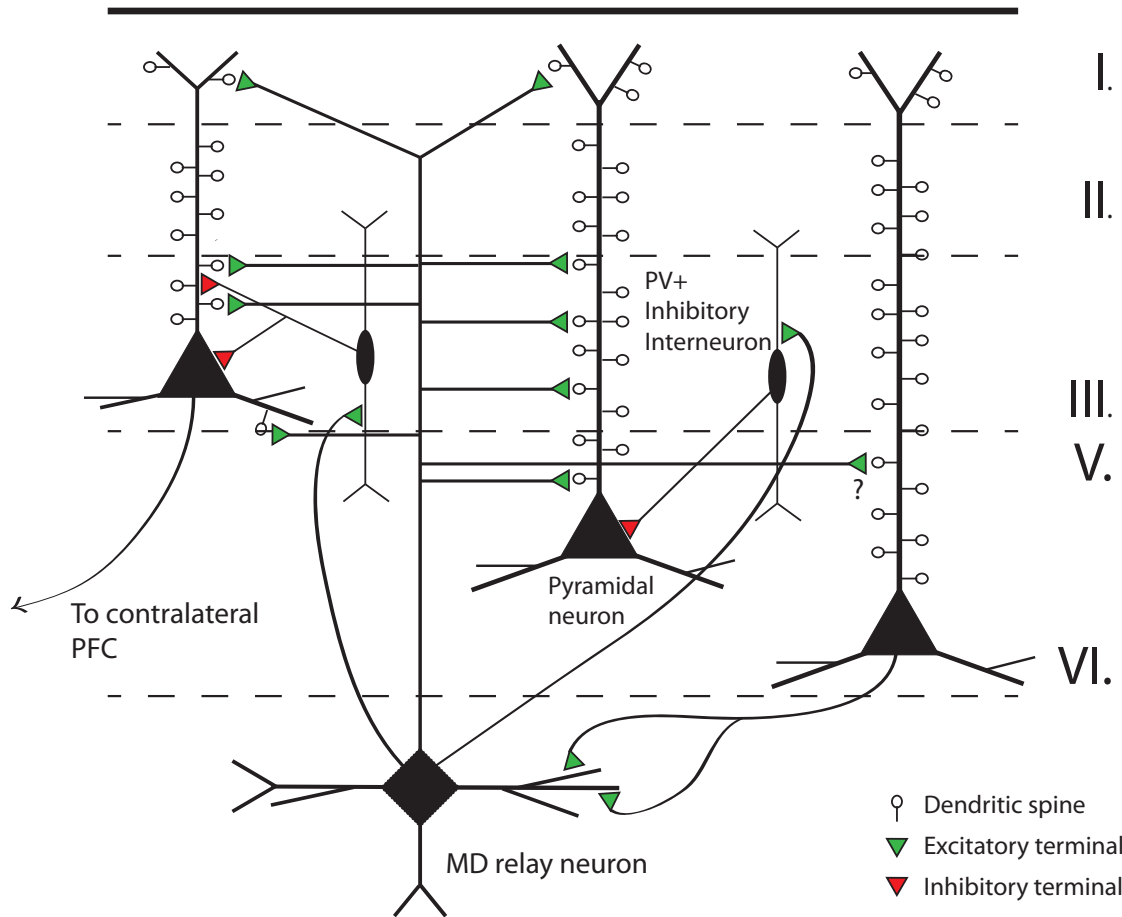


Figure 3.1: **Summary of existing anatomical data for MD-PFC projection** MD axons primarily form asymmetric synapses onto the dendritic spines of pyramidal neurons whose somata lie in layer III and V in dACC. It's believed that due to the position of their basilar dendrites, layer III PNs receive the most input from MD. Axon terminals also make asymmetric synapses onto the dendritic shafts on inhibitory interneurons, particularly those that label for parvalbumin.

The boundaries of the thalamic and prefrontal regions are poorly defined, and there has been extensive debate over what the equivalent prefrontal cortical regions are across species and where the divisions should be drawn (Heidbreder & Groenewegen, 2003; Öngür & Price, 2000; Van De Werd *et al.*, 2010; Vogt & Vogt, 2004). This had led to some confusion in the literature as to whether the MD primarily projects to the cingulate cortex or the prelimbic cortex. The mediodorsal thalamus (MD) can be parcellated into roughly three subnuclei: the medial (magnocellular), central, and lateral (parvocellular) MD that exhibit different topographies of afferent and efferent projections (Groenewegen, 1988). Importantly, the pattern of thalamocortical and corticothalamic terminations are topographically similar. The medial portion of the MD is believed to be most reciprocally connected the ventral portion of the mPFC (PrL/IL); the central portion mainly has reciprocal connectivity with the ventral granular insula and lateral orbital areas; the lateral portion of the MD meanwhile is reciprocally connected with the dorsal anterior cingulate cortex (Groenewegen, 1988).

A recent tracing paper reassessed the MD-PFC pathway in mouse and made several observations that are in disagreement with the previous literature in rats (Matyas *et al.*, 2014). First, they found that small injections of the retrograded tracer CTB into MD consistently labeled neurons in M2 and dACC, with only a few scattered cells found in PrL and IL. CTB injections into dACC labeled the lateral MD, similar to earlier anatomical studies that observed a topographical relationship with dorsal PFC receiving input from the lateral MD **Fig3.2A** (Groenewegen, 1988; Ray & Price, 1992). Conversely, CTB injection into PrL labeled neurons in the medial “transition zone” of the MD/midline thalamic nuclei (Matyas *et al.*, 2014). This pattern was also consistent with retrograde labeling from the PrL primarily labeled neurons in the medial portion of the MD **Fig3.2B**. The topography of PFC-MD inputs may have been missed by earlier studies that concluded the MD projects principally to the PrL because injection sites were often large spread into the midline thalamic nuclei **Fig3.2C**. Consistent with the Matyas *et al.* findings, another tracing study also concluded that axons from the MD primarily project to layer III of the dACC (Wang & Shyu, 2004). Secondly, Matyas *et al.* observed that the dorsal/ventral border of dACC and PrL could be defined by a sudden drop off in parvalbumin staining in the superficial layers of PrL (Matyas *et al.*, 2014). This paper highlights

the importance of independently validating brain region connectivity before attempting circuit-based physiology studies, and presents interesting chemoarchitectonic parameters to distinguish dACC from PrL.

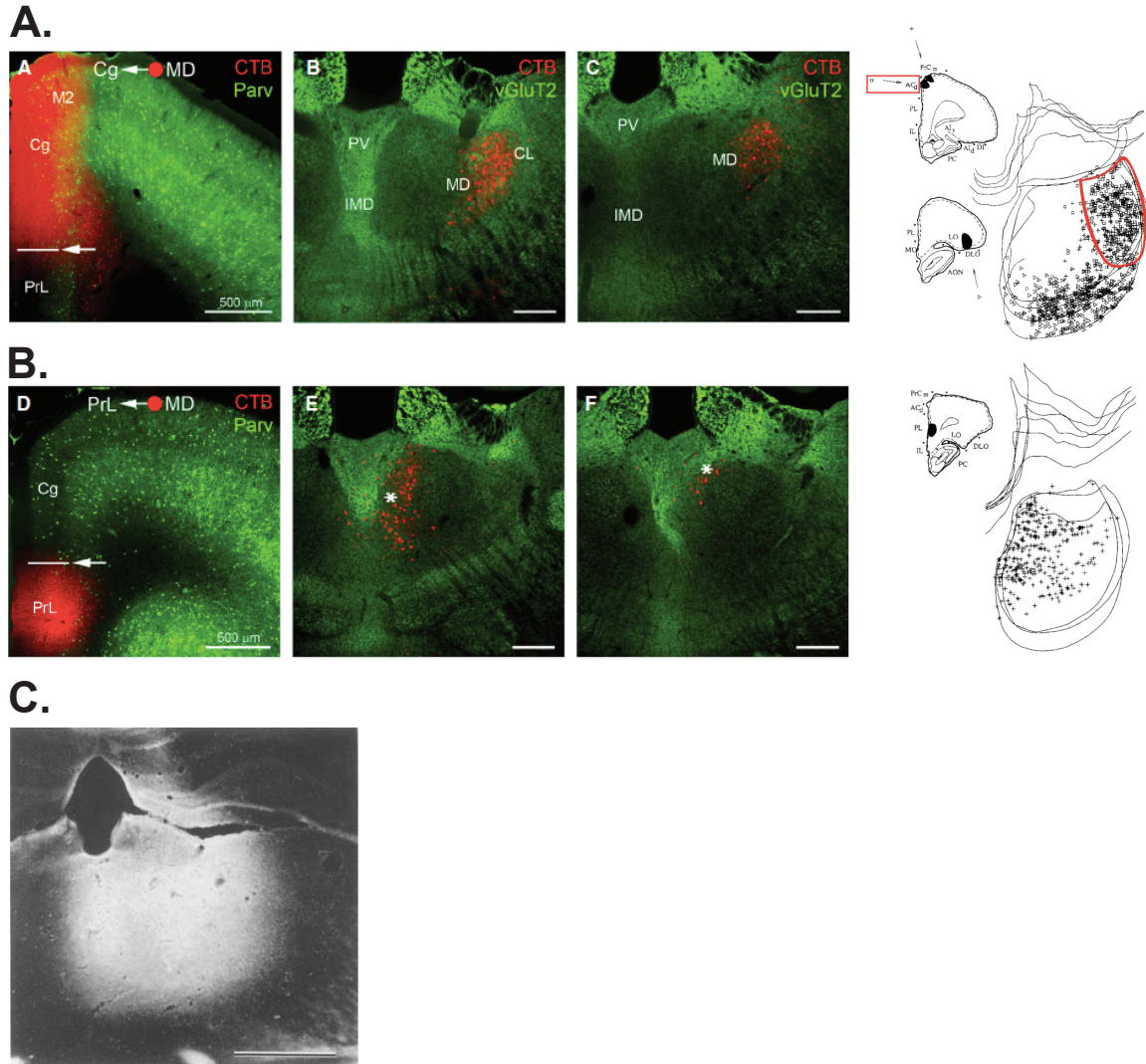


Figure 3.2: Retrograde tracing from dACC and PrL reveals topographical separation of thalamic projection. A. CTB injections into dACC labels projection neurons in the central/lateral portion of the MD (from Matyas *et al.* 2014). Right panel, red outline shows retrogradely labeled neurons in MD after cingulate injection (from Ray *et al.* 1992). B. Conversely, CTB injection into PrL label projection neurons in the most anteromedial portion of the MD, which Matyas *et al.* refer to as a transition zone with the midline thalamic nuclei. Right panel shows pattern of retrogradely neurons along medial MD following injection into PrL (Ray *et al.* 1992). C. Injection location from Kuroda *et al.* 1995 that was used to evaluate the projection patterns of MD axons to the mPFC. Note the spread of wheat germ-agglutinin-horseradish peroxidase (WGA-HRP) into the neighboring midline and intralaminar thalamic nuclei. VGlut2 staining was used as a marker for the rostral MD/midline transition zone, as midline nuclei receive stronger glutamatergic afferents from the brainstem than MD does. Scale bar = 1 mm.

The major input sources to the MD include the PFC, piriform cortex, olfactory tubercle, the basal amygdala (recently contested, see (Matyas *et al.*, 2014), the ventral pallidum, the thalamic reticular nucleus (TRN), the superior colliculus, the substantia nigra pars reticulata, and the dorsal tegmental area (Kuroda *et al.*, 1998; Ray & Price, 1992). Notably, the MD receives inputs from dopamine-rich regions of the limbic system, such as the nucleus accumbens, ventral tegmental area, and ventral pallidum. It has been shown *in vitro* that dopamine increases the intrinsic excitability of relay neurons in the MD (Lavin & Grace, 1998). The MD receives GABAergic input from two main sources; the ventral pallidum and the substantia nigra pars reticulata, with minor GABAergic projections from the substantial innominata, the zone incerta, the vertical limb of the diagonal band, and the ventral pallidal parts of the olfactory tubercle (Bartho *et al.*, 2002; Churchill *et al.*, 1996; Kuroda & Price, 1991a,b; Mitchell & Chakraborty, 2013).

3.1.3 MD dysfunction in schizophrenia

While most attention has focused on structural and molecular changes in the prefrontal cortex, other areas such as thalamus, hippocampus, and basal ganglia demonstrate volume reduction in patients with SZ. The MD has been reported to have fewer cells in patients with SZ compared to healthy controls (Heckers, 1997; Popken *et al.*, 2000; Young *et al.*, 2000). While several studies report robust reductions, such that there is virtually no overlap in cell numbers between control and SZ groups (Young *et al.*, 2000), another study reported a modest reduction in MD volume but no difference in cell density (Danos *et al.*, 2005). Interestingly, one of the earliest reported and most stable findings of brain structure abnormalities in schizophrenia is an enlargement of the lateral ventricles (Andreasen, 1997). Ventricle enlargement may be explained, in part, by reduced volume in the thalamus, which lies adjacent to the lateral ventricle: in fact, a group found that thalamic volume— particularly the MD— inversely correlated with ventricle volume (Gaser *et al.*, 2004).

Functional imaging studies have also shown a reduction in the resting state and working memory task-dependent functional connectivity between the MD and the PFC in chronic and first episode SZ patients (Mitelman *et al.*, 2005; Schlosser *et al.*, 2008; Seidman *et al.*, 1994;

Zhou *et al.*, 2007). A meta-analysis of 41 neuroimaging studies of executive function in patients with SZ and healthy controls reported a consistent pattern of reduced activation in bilateral DLPFC, ACC, and MD (Minzenberg *et al.*, 2009). Several other studies have found evidence for reduced gray matter density in both MD and the PFC (Ananth *et al.*, 2002; Brickman *et al.*, 2004; James *et al.*, 2004; Marengo *et al.*, 2012; McIntosh *et al.*, 2004; Rose *et al.*, 2006). A recent study reported that a significantly reduced connectivity between the MD and the ACC was detected in patients compared to controls, and connectivity was inversely correlated with Stroop task performance (Wagner *et al.*, 2013). This provides further support for dysregulation of the thalamofrontal network in schizophrenia.

3.1.4 MD function

More than a mere relay, the MD appears to integrate information from PFC, limbic structures, and basal ganglia to flexibly adapt behavior. A recent study by Parnaudeau *et al.* showed that chemogenetic inhibition of MD neurons disrupts acquisition and performance in a T-maze working memory task (Parnaudeau *et al.*, 2013). A similar impairment in delayed non-match to sample (DNMS) performance was shown by pharmacologically inactivation of MD (Floresco *et al.*, 1999; Romanides *et al.*, 1999). The subtle reduction in MD firing rate caused by CNO administration was accompanied by a disruption of choice phase associated MD-mPFC beta (13-30 Hz) frequency synchrony. Interestingly, the power spectra in MD and mPFC were not affected, suggesting that reducing MD activity didn't weaken beta oscillation power *per se* but rather disrupted the connectivity between the two regions. Furthermore, lag analysis suggested a predominant MD to mPFC directionality in the beta frequency range, consistent with prospective choice information in the T-maze flowing from the MD to the mPFC.

This finding is reminiscent of recordings by Watanabe *et al.* in nonhuman primates during a saccade task that showed that a greater number of MD neurons exhibit pre-saccadic activity than in the DLPFC, where neuronal responses were mainly post-saccadic. Most interestingly, they observed that during an anti-saccade task, in which a visual cue prompts the subject to saccade away from the visual stimulus after a delay, the direction of population vectors in MD rotated away from the cued direction towards the saccade direction early in

the delay period (Funahashi *et al.*, 2004; Watanabe & Funahashi, 2012; Watanabe & Takeda, 2009). This shift of neural population activity towards the saccade target direction preference began earlier in the MD than in the DLPFC, suggesting that the MD conveys information to the PFC regarding future actions. Impaired performance of mice in the DNMS task could therefore reflect the inability of the MD to convey or maintain “on-line” the choice motor plan to the mPFC during the delay period between arm selection and outcome. The inability to maintain a prospective choice representation could impair the mouse’s ability to evaluate its choice and update its strategy based on feedback for the subsequent trial. While the Par-naudeau study suggests that MD conveys prospective choice information to mPFC, another recent study reported that single unit activity patterns during the delay period of a working memory task more strongly represented a mouse’s previously chosen goal than the upcoming goal (Han *et al.*, 2013). In addition, another rodent study found that during an instrumental learning task, most task-related firing in MD occurred after reward delivery, suggesting that the MD-mPFC circuit may be more involved in evaluating feedback than encoding choice (Yu *et al.*, 2012). However, one earlier study did observe conditioned behavior-related neurons that increased their activity just prior to licking to avoid a shock or receive a reward. Notably, the small number of units they found that fit this profile were located in the lateral portion of the MD (Oyoshi *et al.*, 1996). Therefore, the activity of MD units may depend on the topographical projections of the MD subregion. For example, the lateral portion of the MD projects to the motor-planning related areas of the the mPFC (M2 and dACC). Therefore, it may be predicted that MD neurons in the lateral portion of the MD may exhibit more prospective motor-related activity.

The MD is not only implicated in working memory performance; inactivation and lesion studies in rat showed that lesioning the MD didn’t impair single object recognition but impaired object-in-place and recency recognition memory (Cross *et al.*, 2013; Mitchell & Dalrymple-Alford, 2005). These impairments were nearly identical to what was seen when mPFC alone is lesioned, suggesting that MD and mPFC are important for recognizing objects and cues (and perhaps selecting an appropriate behavioral response) within a given context (Cross *et al.*, 2013; Hannesson *et al.*, 2004). Interestingly, MD lesion studies in primates have revealed that there is

some distinction between the impairments caused by MD lesion vs. mPFC lesion; namely, MD lesion impaired memory of a new set of objects-in-scene while it spared the monkey’s ability to implement the task strategy it had previously learned (Baxter, 2013). Reminiscent of the recency findings in rats, it seems that MD is involved in binding contextual information (in this case the background scene) to a perceived object (in this case the rewarded/non-rewarded embedded cue) in order to facilitate later retrieval and behavioral response.

Likewise, it’s predicted that the MD could function to reverse such cue/context associations in order to flexibly adapt in the face of updating reward contingencies. This hypothesis is consistent with a recent study in mice that found that chemogenetically inhibiting MD impaired the ability to adapt to changing contingencies between actions and outcomes (Par-naudeau *et al.*, 2014). Namely, the authors found an impairment in reversal learning and outcome-specific Pavlovian-to-instrumental transfer (PIT). Interestingly, MD inhibition during the Pavlovian training, but not the PIT testing itself reduced the tendency of mice to make an instrumental response to the congruent side that the CS had been paired with during the Pavlovian training. This suggests that inhibiting MD during learning impaired the mouse’s ability to later retrieve the stimulus-outcome association in order to guide action selection during the PIT test. In keeping with the result that MD inhibition doesn’t impair simple Pavlovian conditioning, ablating mPFC neurons that project to MD with tetanus toxin did not alter contextual or cued fear conditioning (Xu & Südhof, 2013).

The MD has also been studied for its role in conveying nociceptive information to the dACC to regulate the affective and autonomic response to pain. A number of studies have observed nociceptive responses in the MD and neighboring centrolateral nucleus (CL) (Sikes & Vogt, 1992; Wang *et al.*, 2003; Whitt *et al.*, 2013). Interestingly, MD and dACC responses appear at the very onset of a cue that leads to painful stimulation, suggesting that they encode an anticipatory (or motivational) response to pain-related environmental changes (Wang *et al.*, 2003). One study found that lidocaine infusion into the medial thalamic area (not specifically MD) blocked unit responses in the dACC to noxious electrical stimulation (Sikes & Vogt, 1992). Interestingly, the researchers noted that the majority of responsive units were found in layer III, consistent with the MD-dACC projection pattern we’ve observed. They

also noted that there was an initial period of inhibition in response to nociceptive stimulation and suggested that it was caused by inhibitory INs that are directly recruited by the MD. A more recent study found that spinal cord injury increased the spontaneous firing rates of MD units and increased the magnitude and duration of responses to noxious stimuli (Whitt *et al.*, 2013). Similar changes were observed by pharmacologically inactivating the zone incerta (ZI) (which leads to immediate hyperalgesia), suggesting that spinal cord injury alters MD response properties via disinhibition through the ZI. Intriguingly, chronic pain is often associated with working memory impairments (Moriarty *et al.*, 2011), and in mice, inflammatory pain impaired spatial working memory performance and caused a global decrease in MD-mPFC connectivity (Cardoso-cruz *et al.*, 2013). This pain-induced change MD-mPFC connectivity and working memory impairment has striking parallels to reduced activation of the DLPFC, AAC, MD network seen in individuals with SZ (Minzenberg *et al.*, 2009).

In a study by Floresco *et al.*, repetitive burst stimulation in MD produced robust, short-term potentiation of hippocampal-evoked firing in mPFC neurons (Floresco & Grace, 2003). The ability of MD to gate PFC neuronal responses to hippocampal input raises the intriguing possibility that MD is involved in strategy selection by either supporting or blocking associational plasticity at hippocampal-PFC synapses. Two studies suggest that synaptic potentiation in the MD-mPFC pathway is an important component in acquisition and retention of fear extinction memory. Low frequency stimulation (LFS) of the MD prior to extinction training was shown to induce LTD in the MD-mPFC pathway and impair the maintenance of extinction memory (Herry & Garcia, 2002). Interestingly, LFS of the ventral hippocampus immediately after extinction training also induced LTD in the MD-mPFC pathway and impaired extinction recall (Hugues & Garcia, 2007). Because MD is not directly connected to vHipp, vHipp LFS-induced synaptic depression in the MD-mPFC pathway could occur downstream as associative LTD in neurons that receive convergent input from vHipp and MD. The Hugues study found that LTP in the vHipp-mPFC and MD-mPFC projections were a normal part of extinction learning. Potentiation first occurred in the vHipp-mPFC during early extinction training, whereas MD-mPFC potentiation peaked 7 days post extinction training, when vHipp-mPFC field potentials had returned to baseline. This suggests that during the course

of extinction learning the extinction memory is transferred from the vHipp-mPFC pathway to the MD-mPFC pathway.

3.1.5 Evidence for MD recruitment of PV interneurons

In addition to synapses onto dendritic spines of PNs, MD afferents form synapses onto the dendritic shafts of GABAergic INs (Kuroda *et al.*, 2004, 1996), particularly those that express parvalbumin (Rotaru *et al.*, 2005). It has also been shown that pharmacological disinhibition of MD results in c-fos expression of mPFC neurons that colabel for parvalbumin, as well as calbindin and VIP (Bubser *et al.*, 1998). Of course, it could not be determined from this study if interneurons are activated via direct recruitment from the thalamus or indirectly via local pyramidal neurons. The projection pattern of MD axons delineates a circuit whereby MD afferents excite both layer III and V pyramidal neurons that project to contralateral mPFC or to subcortical areas such as the ventral striatum. PV+ INs that receive monosynaptic excitatory input from MD are then poised to inhibit callosal or subcortically-projecting neurons via feedforward inhibition. A still unresolved issue is to what extent projection neurons in dACC that project to MD receive direct input from the thalamus, that is, is there a closed loop? An earlier tracing study reported that MD afferents synapse onto layer V CT PNs that project back to MD (Kuroda *et al.*, 1993), and a recent paper reported recording from a layer V neuron that was labeled by retrobeads injection into MD (Lee *et al.*, 2014). CTB tracing labels dACC neurons primarily in layer VI, although it's proposed that MD receives "driver" input from layer V projection neurons. Evidence for cortical driver inputs to MD comes from PFC cooling experiments (Alexander & Fuster, 1973). MD ChR2-evoked recordings from MD CTB or retrobead labeled neurons in dACC should clarify this issue. It would be of interest to assess whether neurons that project to the MD receive stronger feedforward inhibition, as is suggested by a recent study (Lee *et al.*, 2014).

In vivo electrophysiology results support the idea that MD recruits feedforward inhibitory circuits within the mPFC. Floresco *et al.* observed that the main effect of stimulating MD was to inhibit PFC neuronal firing in response to hippocampal efferent stimulation (Floresco & Grace, 2003). The temporal window during which MD stimulation gated hippocampal-evoked

firing was 25-100 ms, consistent with its potential role in shaping the response properties of PFC pyramidal neurons to coincident input. Other studies have detected convergent input from MD and hippocampus onto single PFC pyramidal neurons and observed that MD stimulation produces an EPSP-IPSP sequence (Gigg *et al.*, 1994). While it has been proposed that MD axons activate fast-spiking interneurons (Floresco & Grace, 2003), to date this has not been demonstrated. There are several predicted differences in the MD-mPFC pathway compared to the VB-barrel cortex pathway: 1) there is no layer IV in mPFC, therefore the major thalamorecipient layer is layer III 2) the mPFC compared to sensory cortices exhibits a high degree of recurrent connectivity (Mason *et al.* 1991; Thomson *et al.* 1993; Wang *et al.* 2006) which may promote the recruitment of feedback inhibition to a greater degree.

3.2 Methods

3.2.1 Animals

For rabies tracing experiments, *PV-Cre;Rosa26-stopfloxed-tTA* mice were used. For feedforward inhibition experiments, I crossed DISC1 HET *PV-IRES-Cre; Ai14* mice to *PV-IRES-Cre; Ai14* WT mice. Because the parents were heterozygous for *Cre* and *Ai14* the offspring were either WT or DISC1 HET and were either positive for *both* Cre and Ai14 – and thus labeled PV+ INs red – or only carried Cre *or* Ai14 and thus did not label PV+ INs. *PV-IRES-Cre; Ai14* “reporter” mice were used in experiments that required targeted recordings of PV+ INs, whereas “reporter” and “non-reporter” mice were used in experiments that only involved pyramidal neuron recordings. For DREADD and halorhodopsin experiments *PV-IRES-Cre* and *SST-IRES-Cre* mice were used that were not crossed onto the DISC1 background or *Ai14* background. Male and female mice were used for all recordings.

3.2.2 Stereotaxic surgery, viral constructs, and perfusion

Mice were stereotaxically injected unilaterally with adeno-associated virus (AAV) vector coding ChR2(H134R)-YFP under control of the CAG promoter into mediodorsal thalamus between

P40-P45. Surgical procedures were carried out as previously described. The stereotaxic coordinates used for MD were as follows: A/P -1.58 mm; M/L -0.44 mm; D/V -3.20 mm. Surgical procedures were standardized to minimize the variability of AAV injections, using the same stereotaxic coordinates for MD and the same amount of AAV injected for all mice. To ensure minimal leak into surrounding brain areas, injection pipettes remained in the brain for approximately 5 minutes post-injection before they were slowly withdrawn. Therefore, due to capillary action, the final injected volume of CAG-ChR2 AAV was between 0.3 and 0.35 μ l (10^{12} virus molecules per ml). Recording experiments were performed 3-4 weeks later, when coronal mPFC slices were cut at 300 μ m thickness. For each mouse, MD containing slices were cut at 350 μ m and imaged to examine the location and extent of ChR2 expression in the MD. Mice were excluded if the extent of infection was either too large and leaked into surrounding brain regions (e.g. hippocampus) or if expression was too low. Rodent MD lacks interneurons; therefore all ChR2 infected neurons are expected to be relay projection neurons (Kuroda *et al.*, 1998).

For CTB tracing I injected 0.2 μ l (2% in phosphate-buffered saline) mixed with 0.3 μ l of AAV-CAG-ChR2-YFP virus in order to label MD axons and mPFC CT neurons. 1 week later, mice were perfused intracardially with cold phosphate buffered saline (PBS) for 1 min and 4% paraformaldehyde (PFA) in PBS for 5 min. Brains were removed immediately from the skull and placed in PFA for 12 hours and then in 30% sucrose in PBS solution for 24 hours. 50- μ m thick slices were cut using freezing microtome (Leica SM 2010R, Leica). After washing sections with PBS (3x 5 mins), sections were mounted onto slides with Fluoromount-G mounting medium (Beckman Coulter).

For combined MD ChR2 and mPFC PV or SST halorhodopsin experiments, in addition to the MD injection procedure previously described, *PV-IRES-Cre* or *SST-IRES-Cre* mice were stereotaxically injected with 0.5 μ l of DIO-eNpHR3.0 virus into the dorsal mPFC: A/P 1.94 mm; M/L -3.34 mm; D/V. Mice were injected at approximately P45 and recorded 3-4 weeks later.

3.2.3 Electrophysiology

Slice preparation was performed as described in Chapter 2 methods. The internal solution for voltage-clamp experiments recording MD-axon evoked IPSCs and EPSCs contained 140 mM K Gluconate, 10 mM HEPES, 2 mM MgCl₂, 0.05 mM CaCl₂, 4 mM MgATP, 0.4 mM NaGTP, 10 mM Na₂-Phosphocreatine, 10 mM BAPTA, and 6 mM QX-314, with pH adjusted to 7.25 and diluted to 290 mOsm. IPSC reversal (E_{IPSC}) was first determined by recording IPSCs in the presence of AMPA (5 μ M CNQX) and NMDA blockers (100 μ M AP-5) at varying holding potentials (20 mV steps) and measuring the IPSC amplitude. A linear regression was used to calculate the best fit line, and the x-intercept was used as the E_{IPSC} . Under our recording conditions, the E_{IPSC} was \sim -60 mV. IPSCs were recorded at 0 mV, and the only drug applied to the bath for EI experiments was 100 μ M AP-5. For cell-attached spike and current-clamp experiments, the internal solution consisted of 130 mM potassium gluconate, 5 mM KCl, 10 mM HEPES, 2.5 mM MgCl₂, 4 mM Na₂ATP, 0.4 mM Na₃GTP, 10 mM sodium phosphocreatine and 0.6 mM EGTA (pH 7.2).

To evoke synaptic transmission using Chr2, we used a single-wavelength LED system ($\lambda = 470$ nm, CoolLED.com) connected to the epifluorescence port of the Olympus BX51 microscope. To restrict the size of the light beam for focal stimulation, a built-in shutter along the light path in the BX51 microscope was used. Light pulses of 0.5 ms triggered by a TTL (transistor-transistor logic) signal from the Clampex software (Molecular Devices), were used to evoke synaptic transmission from Chr2+ MD axon terminals onto layer III neurons in mPFC. To activate halorhodopsin neuronal inhibition, two Red LED ($\lambda = 625$ nm, Luminus, CBT-40 series) were used. The LEDs were secured at an angle oblique to the surface of the bath solution (\sim 20 degrees) and were simultaneously triggered by a TTL signal from the Clampex software (Molecular Devices). The intensity at the sample was \sim 0.8 mW/mm². For PV both and SST halorhodopsin experiments, the Red LEDs were triggered 5 ms prior to Chr2 stimulation (0.5 ms pulse) for a total continuous light pulse duration of 20 ms.

In order to measure NMDA vs. AMPA mediated currents in response to MD stimulation, I recorded responses at -70 mV and +40 mV in the presence of PTX (100 μ M). The internal

solution for this recording included 115 mM cesium methanesulphonate, 20 mM CsCl, 10 mM HEPES, 2.5 mM MgCl₂, 4 mM Na₂-ATP, 0.4 mM Na₃GTP, 10 mM sodium phosphocreatine and 0.6 mM EGTA (pH 7.2). NMDAR-mediated responses were quantified as the mean current between 110 ms and 160 ms after stimulation.

3.2.4 PV monosynaptic rabies tracing from mPFC

Cre-dependent monosynaptic rabies tracing was performed from PV+ starter cells. Briefly, PV-LSL-tTA mice were injected into mPFC with 100-300 nL of helper virus (AAV2/9-TRE-HTG). Two weeks later, .5 uL of rabies virus (EnvA-SAD-ΔG-mcherry) was injected under conditions in the mPFC. 5-7 days post-rabies infection mice were sacrificed and perfused for histological examination. 50 uM sections were cut and imaged with a Zeiss 780 LSM confocal microscope and images were viewed using ImageJ.

3.2.5 Data analysis

EPSC latency, 20-80% rise-time, half-width, and decay time constant (calculated over 20-80% of the decay phase) were calculated from either the averaged trace or individual sweeps for each cell using automated procedures in the AxoGraph X 1.5.4 software. EPSC latency was detected when the initial slope exceeded a threshold of -2 pA/ms, and IPSC latency was calculated from the peak of the inward current that preceded the IPSC. For rise-time, half-width, and decay time constant measurements, IPSCs were detected in the AxoGraph software using a threshold of 10 pA/ms initial slope. Action potential latencies were detected as the time to peak.

3.3 Results

3.3.1 PV monosynaptic rabies tracing from mPFC

The results of our Cre-dependent Chr2 evoked IPSC PPR experiments in *PV-IRES-Cre* and *SST-IRES-Cre* mice suggested that GABA release from PV INs is impaired in DISC1 HET mice. In other cortical regions, PV INs are recruited by the thalamus to mediate feedforward inhibition and shape the receptive fields and temporal response properties of pyramidal neurons. GABAergic transmission in PFC has been shown to be important for cognitive tasks like working memory. Furthermore, in schizophrenia, for which cognitive impairment is a core feature, GABAergic markers are reduced in PFC. Therefore we were interested in studying a projection directly recruits PV INs in the mPFC and is relevant to cognition. It was previously reported that the MD thalamus directly projects to PV INs in the mPFC (Rotaru *et al.*, 2005). The role of the MD-mPFC circuit in working memory was recently highlighted (Parnaudeau *et al.*, 2013), suggesting that this could be a particularly interesting circuit with which to probe the function of mPFC PV INs in the DISC1 HET mice. Therefore we performed Cre-dependent rabies tracing from PV-Cre starter cells in the mPFC and looked for retrograde labeling in the MD.

To determine whether PV INs could also mediate feedforward inhibition in the MD-dACC circuit, we first examined whether MD neurons directly innervate PV INs in the dACC. To this end, we used a modified rabies virus system that can trace the monosynaptic inputs onto genetically identified neurons based on (Wall *et al.*, 2010) strategy. Because helper virus infection depends on expression of the tetracycline trans-activator (tTA; see Methods) in this system, we used the *PV-Cre;Rosa26-stopfloxed-tTA* mice, in which tTA is specifically expressed in PV neurons. We injected dACC unilaterally in these mice with the helper virus AAV-TRE-hGFP-TVA-G and two weeks later injected the same location with the rabies-EnvA-SAD-ΔG-mCherry **Fig3.3A**, for which seven days were allowed to achieve trans-synaptic labeling. In the mPFC, hGFP+ PV cells, mCherry+ rabies-EnvA-SAD-ΔG-infected cells, and cells colabeled for both hGFP and mCherry were observed **Fig3.3B**. These hGFP/mCherry double-positive cells represent the PV starter cells for rabies input tracing. This approach revealed that a sub-

stantial population of neurons in the central and lateral aspects of the MD, with a few scattered neurons in the intermediodorsal thalamic nucleus and centrolateral thalamic nucleus, directly project onto the PV INs of dACC **Fig3.3C**. Based on the location of the retrogradely labeled neurons, I targeted my AAV-CAG-ChR2-GFP injections into the corresponding coordinates of MD: A/P -1.58 mm; M/L -0.44 mm; D/V -3.20 mm. Using these coordinates, I hoped to infect MD neurons that would likely project to mPFC PV INs.

3.3.2 Anatomical organization of the MD-PFC circuit

I was curious to compare the results of anterograde and retrograde tracing obtained using our MD stereotaxic coordinates – (modified from (Parnaudeau *et al.*, 2013) – with those of Matyas *et al.*. My retrograde CTB results were remarkably consistent with the pattern of CTB labeling observed in Matyas *et al.* **Fig3.4A-C**. CTB-labelled neurons were located primarily in dACC and ventral orbital (VO) and lateral orbital (LO) cortices in rostral mPFC and almost exclusively dACC and M2 in caudal mPFC sections **Fig3.4C**. In contrast, when the midline thalamic nuclei were injected with CTB, fewer neurons were seen in the VO/LO and labeled neurons appeared to extend more ventrally along the rostral mPFC. In caudal mPFC sections, CTB-labelled neurons were located in IL as opposed to dACC **Fig3.4D**. These results suggest that, consistent with the results of Matyas *et al.*, focal injections into MD primarily label neurons in the dorsal portion of mPFC. From CTB injections we also noted that while MD sends ipsilateral projections to the dACC, there is some degree of crossover in the dACC-MD pathway **Fig3.4C**.

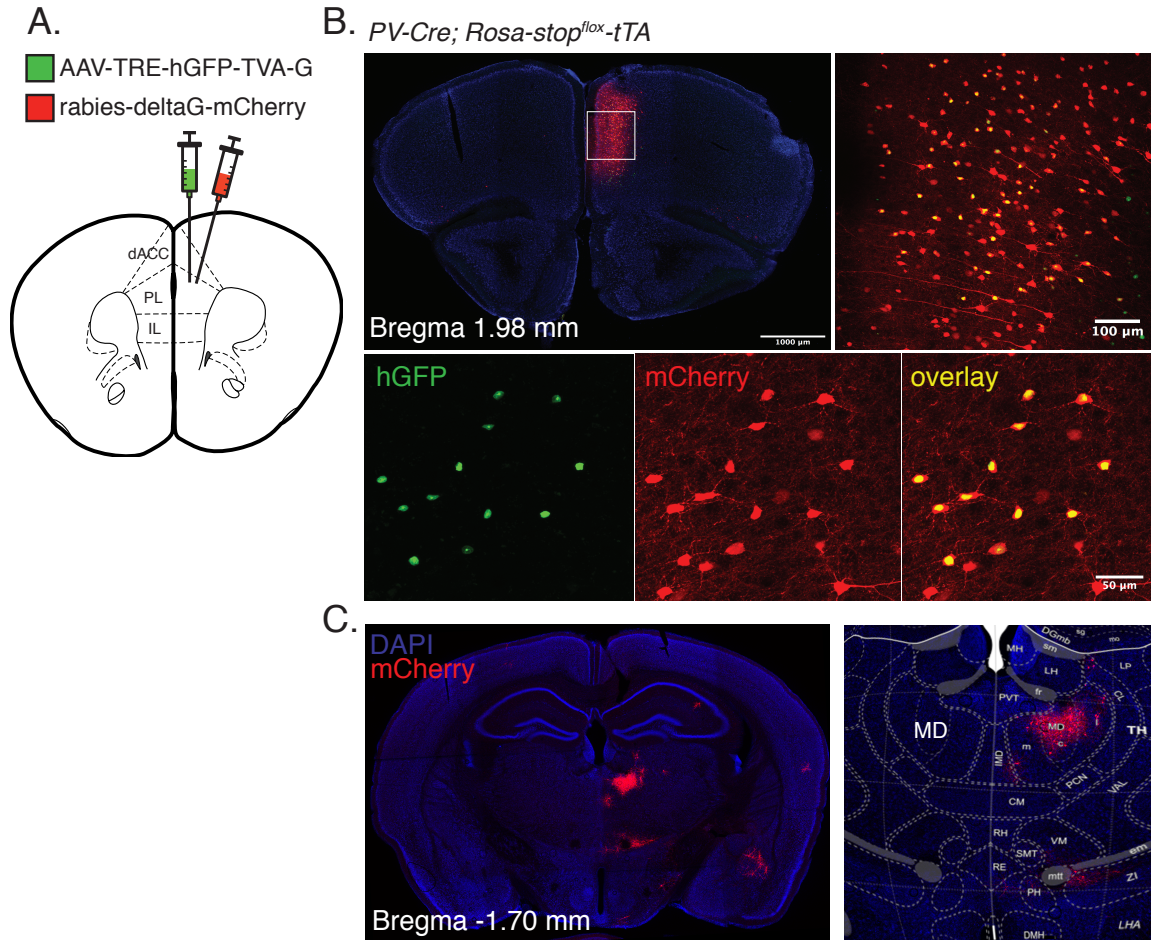


Figure 3.3: mPFC PV rabies tracing reveals dense input from MD. A. EnvA-SAD-ΔG-mCherry was delivered unilaterally into the mPFC of *PV-Cre; Rosa-stop^{flax}-tTA* mice two weeks post injection of helper virus (AAV2/9-TRE-HTG) into the same location. B. Top panel: rabies starter virus injection location, 5 days after rabies virus injection. Boxed region imaged at 20x to right. Middle panel: PV starter cells colabeled for hGFP and mCherry, indicating that they were infected with both rabies helper virus and rabies virus, thus rendering rabies competent to transport. C. Retrograde spread of rabies virus revealed a dense cluster of projection neurons in the central and lateral aspects of the mediodorsal thalamus (MD).

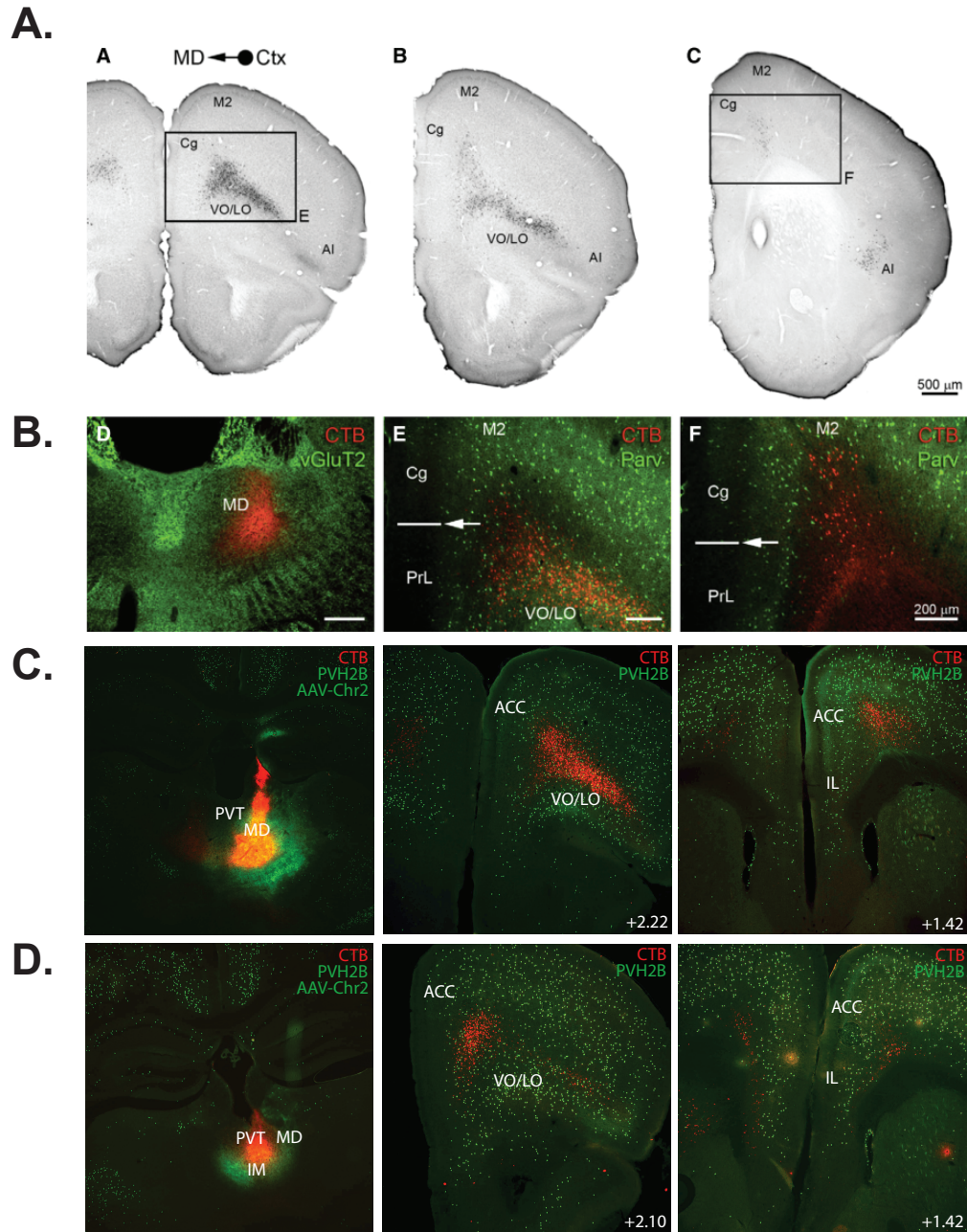


Figure 3.4: **dACC neurons project to the MD.** A. CTB+ projection neurons in cingulate, ventral orbital and lateral orbital frontal cortex from Matyas *et al.* 2014. Most posterior section, far right, shows almost exclusive labeling in cingulate. B. MD CTB injection location that corresponds to panel A. From left: MD CTB injection in red, vGluT2 in green delineates boundaries between MD and other midline thalamic nuclei; dmPFC section with parvalbumin (PV) staining in green. Line indicates drop out of PV labeling in superficial layers. C. From left to right; MD CTB injection in red, ChR2-AAV in green; CTB+ projection neurons in frontal cortex, note pattern is similar to far left section in panel A; more posterior section with CTB+ pattern that corresponds with far right section in A. D. Midline thalamic nuclei (paraventricular nucleus and intermediodorsal nucleus) CTB injection in red, ChR2-AAV in green; CTB+ neurons in frontal cortex, note CTB doesn't label VO/LO heavily and extends more ventrally in mPFC; more posterior section with CTB+ neurons that are localized ventral to cingulate corresponding to infralimbic cortex.

Next, I injected AAV-ChR2-YFP virus into the MD of *PV-IRES-Cre; Ai14* mice to compare the axonal arborizations of MD projection neurons to the dACC/PrL boundary identified by the drop off of superficial PV+ INs reported in (Matyas *et al.*, 2014). I observed that ChR2+ MD axons overlapped almost perfectly with the portion of mPFC that displays superficial PV+ INs **Fig3.5**. Taken together with the PV rabies and MD CTB tracing, these results suggest that MD is poised to recruit layer III PV INs to mediate feedforward inhibition in dACC. The relative lack of superficial PV INs in PrL is intriguing and raises questions about the role of superficial PV INs in shaping the response properties of dACC as opposed to PrL. In the future, these chemoarchitectonic markers can serve as a useful tool to differentiate between the dACC and PrL, which be crucial to understanding their distinct functions.

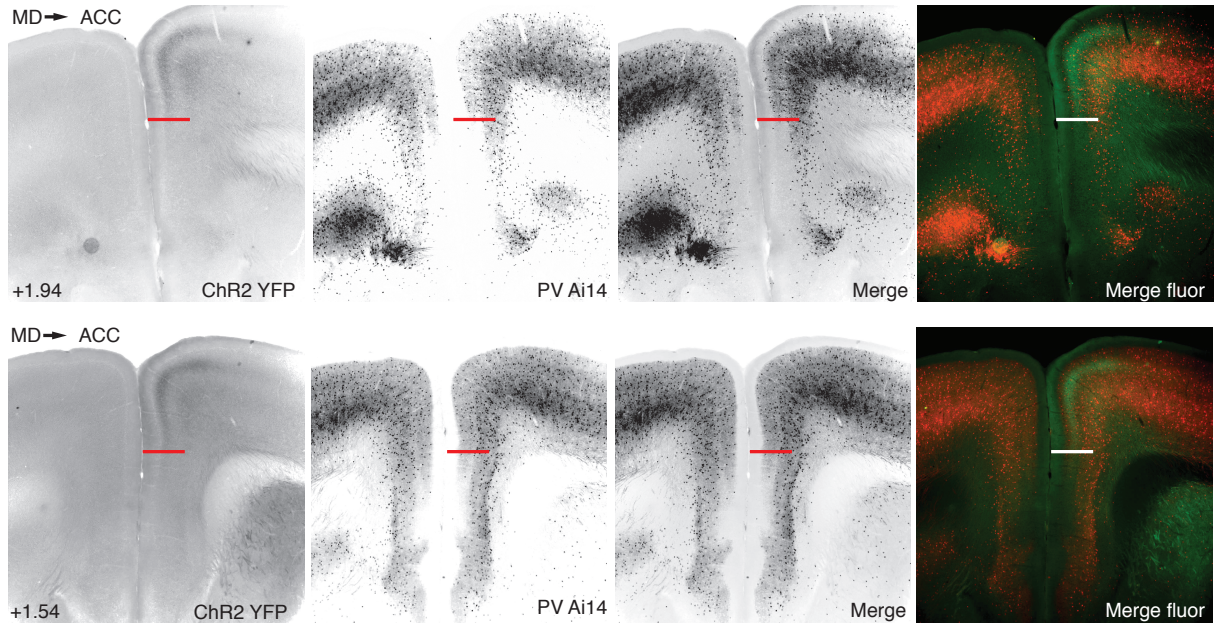


Figure 3.5: MD axons colocalize with superficial PV+ INs in dACC Injection scheme: ChR2 virus was injected unilaterally into MD of *PV-IRES-Cre; Ai14* mice. Top and bottom panels, left to right: ChR2+ MD axons terminate in dorsal mPFC. Red line indicates ventral boundary of MD axon labeling; PV Ai14 reporter- note the sudden drop in the number of superficial layer PV+ INs corresponding to the ventral border of MD axon labeling; merged subtraction image of MD axons with PV reporter; merged fluorescent image. MD ChR2+ axons green; *PV-IRES-Cre; Ai14* reporter red.

3.3.3 Optogenetic activation of MD-dACC circuit

To delineate the functional connectivity between the MD and the dACC, we injected the MD with the AAV-CAG-ChR2(H134R)-YFP, which expresses the light-sensitive cation channel channelrhodopsin-2 (ChR2) (Zhang *et al.*, 2006) tagged with the yellow fluorescent protein (YFP) **Fig3.6A,B**. We first confirmed that MD axons make functional synapses onto principal neurons in layer III of mPFC. Layer III neurons in the vicinity of YFP+ puncta were targeted for recording. We next used blue light pulses (0.5 ms) to stimulate ChR2-expressing axons originating from MD neurons in acute slices while recording, using whole cell patch-clamp technique, excitatory and inhibitory postsynaptic currents (EPSCs and IPSCs, respectively) from layer III pyramidal neurons (PNs) in the dACC **Fig3.6C**. Photostimulation of MD axons reliably elicited both EPSCs and IPSCs in all layer III PNs recorded **Fig3.6D**, with the onset latency of the IPSCs being longer than that of the EPSCs (the latency to onset of the MD-driven EPSCs and IPSCs was 5.48 ± 0.12 ms and 10.24 ± 0.26 ms, respectively) **Fig3.6E**. IPSCs were blocked by application of either GABAA receptor antagonist picrotoxin (PTX) or AMPA/kainate receptor antagonist CNQX **Fig3.6F-H**, indicating that they are polysynaptic inhibitory currents.

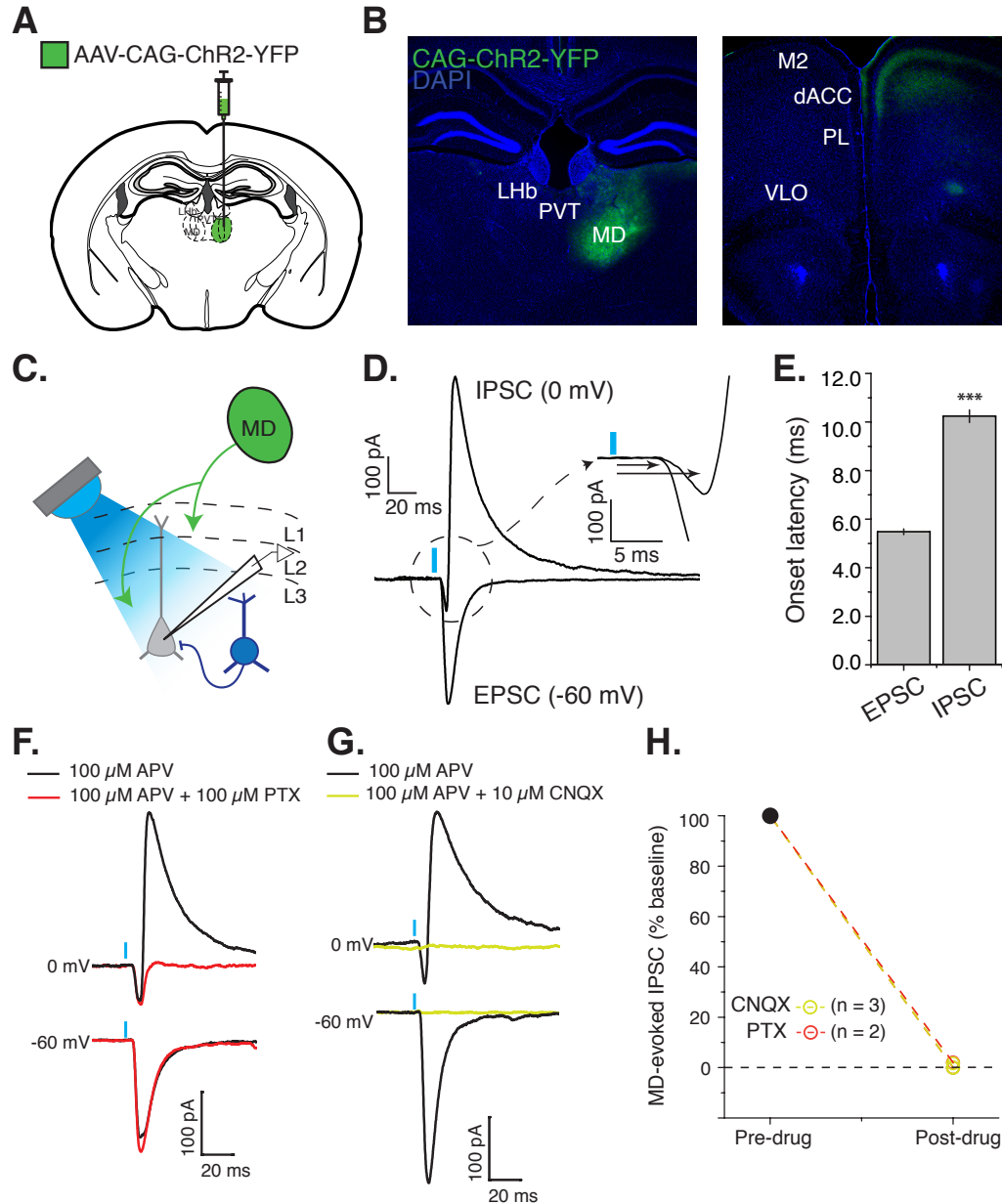


Figure 3.6: Optogenetic stimulation of MD axons drives monosynaptic EPSCs and delayed IPSCs onto layer III pyramidal neurons in dACC. A. AAV-CAG-ChR2(H134R)-YFP was injected unilaterally into MD. B. 3-4 weeks later, robust YFP signal was observed within the MD and in layers I, III, and V of the dorsal portion of the mPFC, corresponding to dorsal anterior cingulate cortex (dACC). C. Layer III pyramidal neurons (PNs) were recorded in whole-cell voltage clamp mode while MD axons were activated by a brief 0.5 ms 470 nm λ light pulse delivered through a 60x objective. D. PNs were recorded at E_{IPSC} (-60 mV) and 0 mV. MD axon stimulation elicited a short-latency monosynaptic inward current followed by a delayed outward current. E. Onset latency of light-evoked IPSCs was significantly more delayed than that of light-evoked EPSCs (10.25 ± 0.26 ms vs. 5.48 ± 0.12 ms, $***p < 0.00001$ two sample t -test). F. MD-evoked outward currents, recorded at 0 mV in the presence of the NMDA receptor antagonist AP-5 were blocked by picrotoxin (PTX), confirming that they are GABAA mediated. G. AMPA/kainate antagonist CNQX abolished both inward and outward currents, indicating that MD-evoked IPSCs are polysynaptic in nature. H. Combined quantification of IPSC suppression following drug application (total of 5 neurons recorded from 5 animals).

3.3.4 MD-evoked IPSCs are likely disynaptic, mediated by PV INs

In complex circuits, each synapse that contributes to a response increases the latency and jitter of the response onset. To determine if the inhibition recruited by MD axon stimulation was mainly disynaptic or polysynaptic, we compared the onset latency of IPSCs (10% rise time) evoked at either low probability (>50% failure rate) or high probability (0% failure rate) within the same neurons **Fig3.7A**. Using “minimal” stimulation, we sought to isolate thalamically-driven IPSCs by avoiding polysynaptic excitation. We found that the latency to onset for reliably-evoked IPSCs was significantly shorter than for minimally-evoked IPSCs (reliable, 11.0 ± 0.45 ; minimal, 13.25 ± 0.46 ; $^{**}p < 0.005$ $F(1, 8) = 19.03$ one-way repeated measures ANOVA $n=9$) **Fig3.7B**. The fact that the latency of MD-evoked IPSCs decreased as IPSC amplitude increased argues against the idea that increasingly recruited polysynaptic activity drove the IPSC. The IPSC latencies are rather long compared to what has recently been reported using optogenetic stimulation (Cho *et al.*, 2013), but several main factors likely contribute to this: 1) recordings were performed at room temperature and 2) short duration, low intensity light stimulation was used 3) IPSCs were not recorded at E_{EPSC} . Recordings were performed at 0 mV, where we observed an inward current that preceded the outward current, and it is possible that the inward current masked the true onset of the IPSC. However, while the onset jitter of the EPSCs was significantly smaller than that of MD-driven IPSCs onto PNs (EPSC, 0.24 ± 0.03 , IPSC 0.38 ± 0.04 ; $Z = 3.33$, $^{***}p < 0.001$, Wilcoxon signed ranks test) **Fig3.7C**, as would be expected for monosynaptic versus disynaptic responses, the jitter of the MD-driven IPSCs in PNs is similar to what has been previously reported for disynaptic inhibition (Kanichay & Silver, 2008). This result suggests that inputs from MD drive disynaptic feedforward inhibition onto layer III PNs in the dACC.

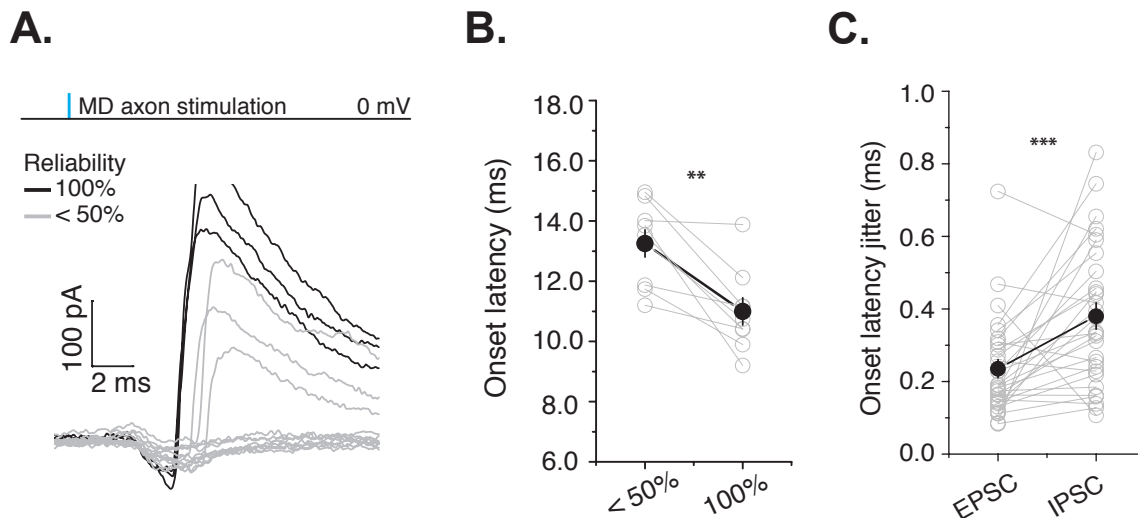


Figure 3.7: **MD-evoked IPSCs are likely disynaptic.** A. Sample trace from layer 3 PN in which low stimulation was used to evoke MD-driven IPSCs with low probability (<50%, in gray). Stimulation intensity was then increased until IPSCs exhibited 100% reliable responses (black). B. Reliably-evoked IPSCs exhibited significantly shorter onset latencies compared to minimal IPSCs, measured from the onset of light stimulation to 10% rise time (** $p < 0.005$ one-way repeated measures ANOVA). C. MD-evoked IPSCs exhibit sub-millisecond onset jitter that is significantly higher than the jitter of MD-evoked EPSCs (** $p < 0.001$, Wilcoxon signed ranks test).

Given that we had previously observed that PV- and SST-evoked IPSCs exhibit distinct decay kinetics (Chapter 1), we compared the kinetics of MD-evoked IPSCs to direct light-evoked IPSCs from PV INs, using the same stimulation and recording parameters **Fig3.8A**. We found that the kinetics of the MD-driven feedforward IPSCs in dACC PNs were similar to that of IPSCs in these neurons evoked by direct photostimulation of local PV INs **Fig3.8B-C** (rise time: feedforward IPSCs, 2.17 ± 0.18 , $n = 14$; PV-evoked, 1.76 ± 0.31 ms, $n = 5$; $p > 0.05$, t -test; decay time: feedforward IPSCs, 29.09 ± 1.27 ms, $n = 14$; PV-evoked, 31.22 ± 2.12 ms, $n = 5$; $t(7.08) = 0.86$, $p > 0.05$, t -test).

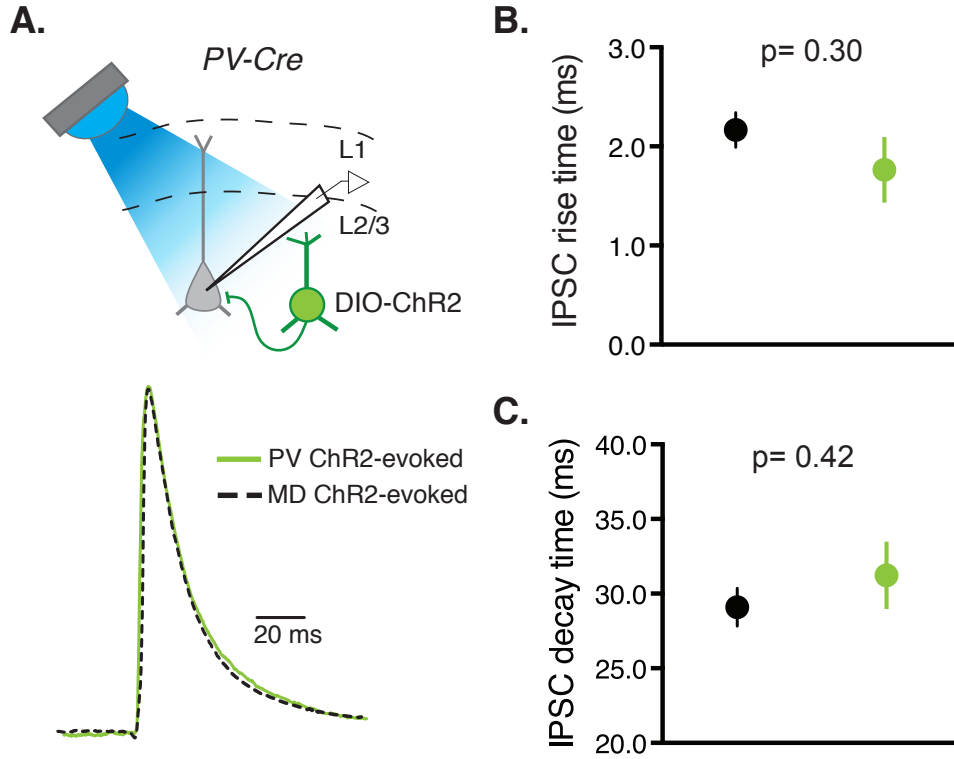


Figure 3.8: Feedforward IPSCs resemble IPSCs directly mediated by PV INs A. Left: AAV-DIO-ChR2-YFP was expressed in PV INs in dACC, and layer 3 PNs were recorded at 0 mV in whole-cell voltage-clamp mode while PV axons were activated using the same stimulation protocol as in MD activation experiments. Right: time-aligned, normalized sample traces of IPSCs recorded in response to MD axon stimulation (black dashed line) or direct PV ChR2 activation (in green). B. Feedforward IPSCs exhibited similar rise time as PV-evoked IPSCs (rise time: feedforward IPSCs, 2.17 ± 0.18 ms, $n = 14$; PV-evoked, 1.76 ± 0.31 ms, $n = 5$; $p > 0.05$, two sample t -test). C. Feedforward and local PV-evoked IPSCs exhibited very similar 80-20% decay times (feedforward IPSCs, 29.09 ± 1.27 ms, $n = 14$; PV-evoked, 31.22 ± 2.12 ms, $n = 5$; $t(7.08) = 0.86$, $p > 0.05$, two sample t -test).

3.3.5 Thalamocortical transmission onto PV INs and PNs

To determine the functional connectivity between MD neurons and PV INs in the dACC, we injected MD with the AAV-CAG-ChR2(H134R)-YFP at the location determined by rabies tracing that project to dACC PV INs **Fig3.9A**. We used the PV-Cre;Ai14 mice, in which PV INs in the mPFC are readily identified on the basis of their red fluorescence. In order to confirm that L3 PV INs in dACC receive direct excitatory input from the MD, we recorded EPSCs in PV INs, as well as neighboring PNs in dACC ($<50\text{ }\mu\text{m}$ apart), in response to photostimulation of MD axon fibers expressing ChR2 **Fig3.9B-C**. Robust EPSCs were readily recorded from both PV INs and PNs, with the EPSC rise-time of PV INs being significantly faster than that of PNs (PV, $1.22 \pm 0.14\text{ ms}$; PN, $2.21 \pm 0.15\text{ ms}$; $**p<0.005$ $t= 3.89$ $DF= 8$ paired sample t -test) **Fig3.9D-E**. The faster EPSC rise-time of PV INs resulted in these neurons reaching peak EPSC amplitude earlier than neighboring PNs (PV INs, $7.7 \pm 0.4\text{ ms}$; PNs, $11.1 \pm 0.4\text{ ms}$; $***p<0.0005$ paired t -test $t= 8.03$ $DF= 8$), suggesting that MD inputs are capable of evoking action potentials in PV INs within a time frame during which they can shape network activity driven by thalamocortical excitation. These results demonstrate that layer III PV INs in the dACC receive direct excitatory inputs from the MD, and raise the possibility that these PV INs mediate MD-driven feedforward inhibition in the dACC.

Next, we compared the synaptic and cellular properties of layer III PV INs with those of PNs in the dACC using the WT *PV-Cre; Ai14* mice. Surprisingly, we found that the amplitude of EPSCs onto PV INs was not significantly larger than that onto neighboring PNs in the dACC in response to photostimulation of axons originating from the MD (PV INs, $167.2 \pm 30.0\text{ pA}$; PNs, $113.7 \pm 48.8\text{ pA}$; $p= 0.10$ $t= -1.84$ $DF= 8$ paired sample t -test) **Fig3.9F**. In addition, the MD-driven EPSCs onto both cell-types showed strong pair-pulse depression (100 ms inter-pulse interval), indicating high presynaptic release probability (PN, 0.54 ± 0.05 ; PV, 0.52 ± 0.04 $p>0.05$ $t=0.32$ $DF= 25.82$ two sample t -test) **Fig3.9G**. These results differ from findings in the sensory cortices, where thalamic drive onto fast-spiking INs (presumptive PV INs) is much stronger and shows a higher degree of pair-pulse depression than synapses onto layer IV principle neurons (Beierlein *et al.*, 2003; Cruikshank *et al.*, 2007; Gabernet *et al.*, 2005).

Both PV INs and PNs in the dACC received MD-driven feedforward inhibition, which showed strong pair-pulse depression (100 ms inter-pulse interval) (PNs, 0.07 ± 0.02 , $n = 13$; PV INs, 0.15 ± 0.07 , $n = 6$, $p > 0.05$ $t = -1.16$ $DF = 5.67$) **Fig3.9H**. These results are consistent with sensory thalamocortical transmission, whereby feedforward inhibition decreases dramatically during repeated stimulation, thus increasing the integration window in thalamorecipient neurons in the cortex (Gabernet *et al.*, 2005).

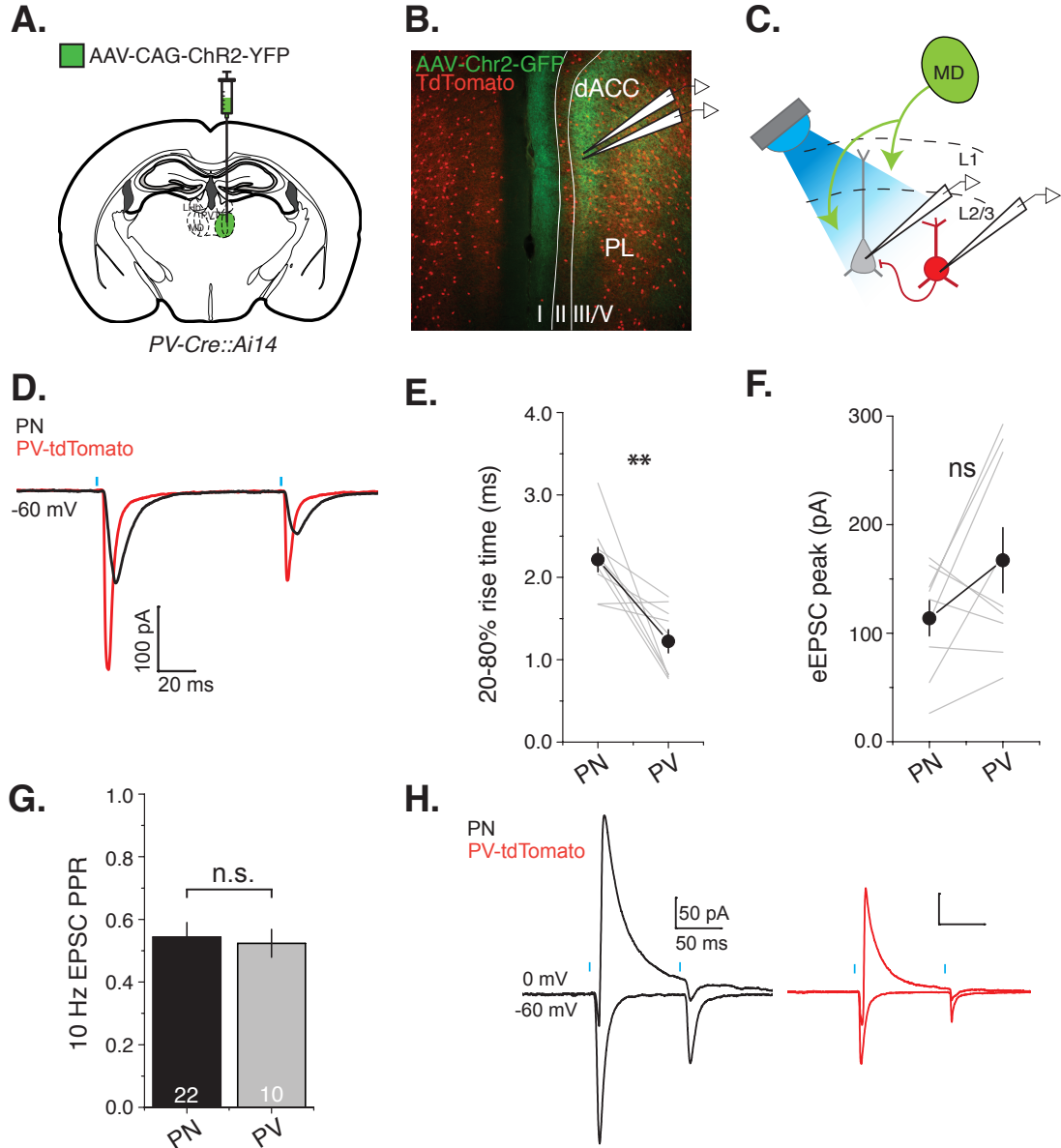


Figure 3.9: MD directly activates PV interneurons in layer 3 dACC A. *PV-Cre;Ai14* mice were injected into MD with 0.3 μ L AAV-CAG-ChR2-YFP. B. 3 weeks later high expression was observed in MD axons terminating in layers I, III, and V in dACC. PV and PNs in the vicinity of GFP+ puncta within layer 3 were targeted for recording. Note the marked drop off in superficial TdTomato+ PV INs ventral to the region of mPFC labeled by YFP+ MD axons. C,D. MD light-evoked responses were sequentially recorded in neighboring PV and PNs in dACC ($<50 \mu$ m apart). E. EPSC rise times were significantly faster in PV INs compared to the EPSC rise times in PNs (** $p < 0.005$ paired sample t -test). F. There was no significant difference in MD-evoked EPSC amplitude onto neighboring PV vs. pyramidal neurons ($p = 0.10$ paired sample t -test). G. PPR of MD-evoked EPSCs onto PV INs and PNs was equal across a 100 ms interval ($p > 0.05$ two sample t -test). H. PV INs that receive monosynaptic excitatory input from MD also receive feedforward inhibition. MD-evoked IPSCs onto PV INs and PNs are strongly depressing at 100 ms stimulation interval (PN, 0.07 ± 0.02 ; PV, 0.15 ± 0.07 $p > 0.05$ $t = -1.16$ DF = 5.67 two sample t -test).

In order to compare the level of inhibition produced by PV INs in the MD-dACC pathway in WT vs. DISC1 HET mice, we first tested whether glutamatergic transmission onto PV INs from the MD was similar across DISC1 HET and WT mice. Otherwise, within the disynaptic circuit, it is difficult to interpret whether a reduction in feedforward inhibition is due to altered GABA release or reduced thalamic drive onto PV INs. Preliminary data were collected using Cs-internal solution, and later recordings were made using K-gluconate internal + QX-314. Here, I've combined preliminary Cs- and later K-gluconate internal data for paired PV/PN recordings. I first performed sequential recordings of neighboring PV INs (identified by tdTomato) and PNs. A property of thalamocortical circuits in sensory systems is the robust activation of fast-spiking PV INs that mediate feedforward inhibition (Cruikshank *et al.*, 2007). PV INs respond more strongly to TC excitatory input than local pyramidal neurons due to the strength of TC synaptic inputs and not due to differences in intrinsic membrane properties (Cruikshank *et al.*, 2007). In order to compare the ratio of direct MD thalamocortical excitation onto PV INs vs. PNs I calculated the following:

$$\frac{peak\ PV\ AMPA - peak\ PN\ AMPA}{peak\ PV\ AMPA + peak\ PN\ AMPA}$$

I found that the MD-evoked AMPA current was greater onto PV INs compared to PNs in both WT and DISC1 HET mice (WT, 0.33 ± 0.09 HET, 0.26 ± 0.08 $p = 0.61$ two-tailed t -test) **Fig3.10A-B**. While this data suggests that the ratio of excitation onto PV INs vs. PNs is consistent across genotypes, we cannot determine if the absolute amount of MD-mPFC excitatory transmission is the same. I next recorded MD-evoked AMPA and NMDA currents in the presence of PTX (100 μ M) onto PV+ INs and PNs within the same PFC slices. In the presence of PTX, brief (0.5 ms), low intensity light stimulation recruited substantial recurrent excitatory input onto the recorded cells, particularly the PV INs. Consequently, very low intensity light stimulation was used to avoid the generation of epileptiform activity. The mPFC is known to exhibit high reciprocal connectivity among neurons in comparison to sensory cortex (Mason *et al.*, 1991; Schwindel *et al.*, 2014; Wang *et al.*, 2006). This may explain why it was difficult to isolate light-evoked monosynaptic excitatory currents in the presence of PTX; it appears that intact feedforward inhibition suppresses recurrent excitation in response to incoming thalamocortical input. A two-way ANOVA revealed that there was a main effect of cell type but no significant effect of genotype or the interaction of genotype with cell type on the % AMPA transmission (cell type $F(1, 33) = 23.78$, **** $p < 0.0001$ genotype $F(1, 33) = 0.95$, $p = .34$, interaction $F(1, 33) = 1.09$, $p = 0.30$). AMPA% was significantly higher in PV INs vs. PNs for both genotypes (WT and HET ** $p < 0.01$, Tukey's multiple comparisons) **Fig3.10C-D**.

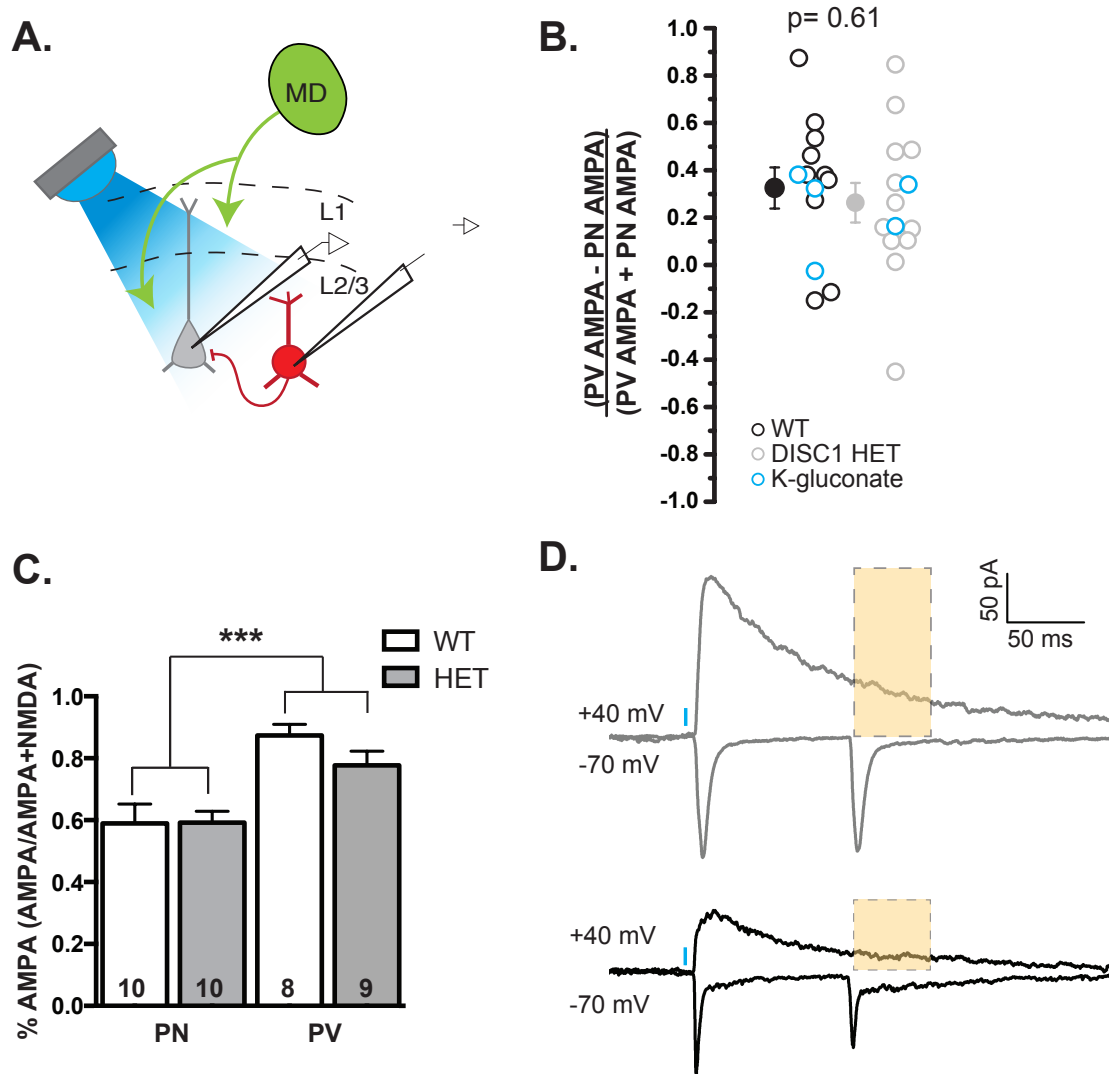


Figure 3.10: **Unaltered response properties of PN/PV neurons in DISC1 compared to WT mice.** A. Recording configuration. B. PV INs on average responded more strongly to MD input than neighboring PNs. WT and DISC1 HET mice do not show a significant difference in relative PV response strength. Blue circles indicate K-gluconate internal recordings as opposed to Cs. C-D. PNs exhibit significantly higher NMDA component at the MD-dACC synapse compared to PV INs *** $p < 0.001$ two-tailed t -test

3.3.6 Relative timing of MD-evoked EPSCs and IPSCs

I next compared MD-evoked IPSC and EPSC rise-times between DISC1 HET and WT mice. The 20-80% rise-times for light-evoked IPSCs were (WT, $2.46 \pm .12$ HET, $2.33 \pm .17$ p= 0.59, two-tailed *t*-test). The 20-80% rise-times for MD-evoked EPSCs were slightly faster (WT, 2.15 ± 0.09 HET, 2.19 ± 0.12 p= 0.77, two-tailed *t*-test). In polysynaptic circuits, each additional synapse that contributes to a response increases the latency and jitter of the onset. We therefore compared the jitter (SD across trials) of latency to the 10% rise time for IPSCs and EPSCs recorded at the same stimulation intensity. As predicted, the jitter for EPSC onset was low in WT and DISC1 HET mice (WT, 0.24 ± 0.03 HET, 0.24 ± 0.02 ms p= 0.88, Mann-Whitney) **Fig3.11A**. While the jitter was larger for MD-evoked IPSCs, all cells exhibited jitter <1 ms with a mean jitter of $0.39 \pm .03$ ms in WT mice and 0.47 ± 0.05 ms in HET mice (p= 0.22, two-tailed *t*-test). In both genotypes, IPSC onset had a significantly higher jitter than EPSC onset (WT, **p<0.01 Wilcoxon signed ranks test HET, ***p<0.001, paired two-tailed *t*-test) **Fig3.11A**. This is to be expected, as the disynaptic IPSC jitter is additionally affected by IN spike jitter and the jitter of IN-PN transmission. The low IPSC onset jitter we observed suggests that trial to trial, IPSCs are time-locked to the stimulus, consistent with disynaptic as opposed to polysynaptic inhibition **Fig3.11B** (Kanichay & Silver, 2008; Torborg *et al.*, 2011).

We next looked at the relative timing of the EPSCs and IPSCs evoked by MD light stimulation in DISC1 WT and HET mice. We compared the respective 10% rise time points to determine the EPSC-IPSC delay (based on (Mittmann *et al.*, 2005)). Comparing the 10% rise time point more accurately reflects the overlap of EPSC and IPSC currents than peak offset, as peak times are affected by varying EPSC and IPSC rise times. We found that mean delay between EPSC and IPSC onset was 4.7 ± 0.26 in WT and 5.5 ± 0.26 in HET mice **Fig3.11C**. This delay is longer than what has been reported in other studies of feedforward inhibition (Cho *et al.*, 2013; Cruikshank *et al.*, 2007; Mittmann *et al.*, 2005) but it may be that the IPSC onset is delayed by the inward current. In fact, we noted that one neuron that exhibited a more typical delay of 1.7 ms also didn't display any inward current at 0 mV. This hypothesis can easily be tested by recording IPSCs at 0 mV and the experimentally-determined EPSC reversal potential to compare the onset latency. Comparison of WT and HET mice showed that there

was a small but significant increase in the EPSC-IPSC delay in DISC1 HET mice (* $p < 0.05$, two-tailed t -test).

Photostimulation of MD afferents occasionally resulted in IPSCs onto layer III pyramidal neurons that exhibited two distinct peaks **Fig3.11D**. This second peak could come from polysynaptic input or from PV INs firing more than one action potential in response to light stimulation (which we have observed). Pooling double-peak traces from 21 neurons in 13 mice, the mean latency to the first peak was calculated to be $14.78 \pm .50$ ms while the latency to the second peak was $20.47 \pm .83$ ms **Fig3.11D**. From this data we restricted our assessment of feedforward inhibition to averaged IPSC traces whose peaks occurred within 19 ms after stimulation onset. This data was then used to compare GABA: AMPA ratios of MD-evoked synaptic transmission onto layer III PNs in DISC1 WT and HET mice. Because we compared peak current amplitudes as opposed to charge transfer, I did not sort data based on other measures such as the IPSC decay time constant. However, we observed that the IPSC decay time constant remained consistent across increasing stimulation intensity, arguing against the substantial recruitment of feedback inhibition.

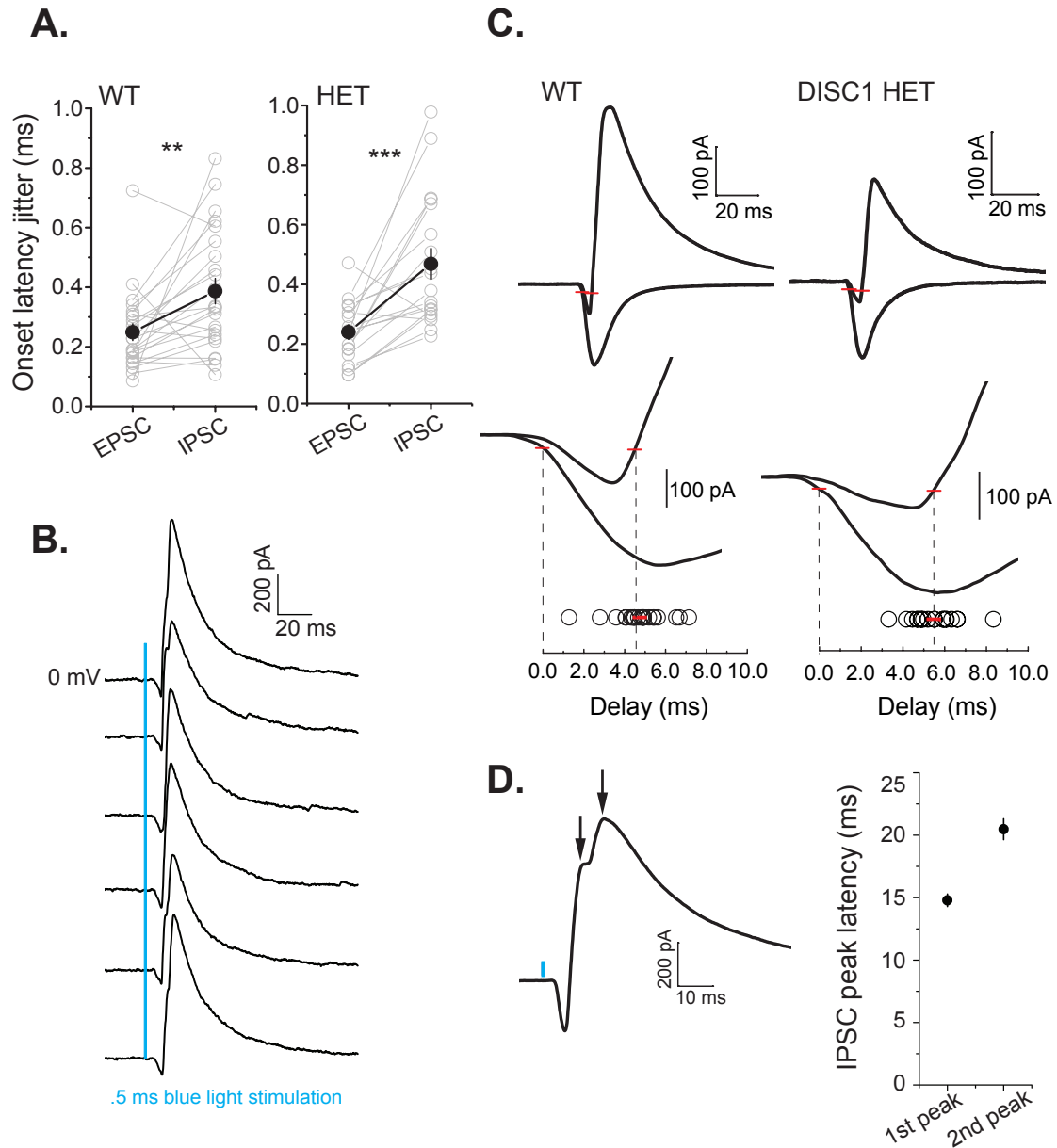


Figure 3.11: MD-evoked IPSCs onset consistent with disinaptic inhibition. A. Light-evoked IPSCs display onset latency jitter (S.D. of onset to 10% rise time) that is significantly higher than EPSC jitter but still time-locked to the stimulus in both WT and HET mice ($n = 23, 19$). B. Sample traces of sequentially recorded IPSC sweeps in WT; onset jitter = 0.40. C. Inhibitory and excitatory MD-evoked synaptic currents were separated by voltage clamping at E_{IPSC} (-60 mV) and 0 mV (not equal to the AMPA reversal potential). The peak amplitudes were measured and the 10% rise time point calculated for EPSCs and IPSCs in DISC1 WT and HET mice (sample neurons, marked by red bar). For each recorded neuron, the EPSC 10% rise time point was subtracted from the IPSC 10% rise time point to calculate the delay (WT, 4.7 ± 0.26 HET, 5.5 ± 0.26 $p < 0.05$ two-tailed t -test. Note that 10% rise time points slightly precede or coincide with the peak of the EPSC. D. While IPSC onset jitter and rise time had low variability, sometimes clear double peaks were observed in the trace. The mean latency of the first compared to second peak was $14.78 \pm .50$ ms vs. $20.47 \pm .83$ ms ($n = 21$ neurons, pooled from 13 animals WT and HET). Based on this delayed peak, we restricted our feedforward IPSC comparison to averaged traces with a peak latency < 19 ms. ** $p < 0.01$, *** $p < 0.001$

In my MD-evoked IPSC recordings, I took special care to distinguish whether I was recording disynaptic IPSCs that were mediated by INs directly activated by MD axons, or polysynaptic IPSCs that were mediated by INs that were activated by local PNs **Fig3.12A**. I considered the relevant steps required to initiate the IPSC, from photostimulation, to EPSC onset, PV AP peak, and IPSC onset. Given that the mean IPSC latency to onset was 9.46 ms (calculated from inflection point from inward to outward current) and the mean PV AP peak time was 7.8 ms, the estimated PV-PN synaptic latency would be ~ 1.6 ms. This value is consistent with the 1-2 ms range for PV-PN synaptic latencies observed in the hippocampus (Hefft & Jonas, 2005) and mPFC **Fig3.12B** (Cardin *et al.*, 2009; Gao *et al.*, 2003; González-burgos *et al.*, 2005). This observation alone does not support the idea that PV INs mediate disynaptic inhibition, but it demonstrates that PV INs spike with a latency that is consistent with the onset of the MD-evoked IPSC. Rarely, neurons were recorded that did not exhibit any clear feedforward inhibitory currents **Fig3.12C**. By comparing these traces to those of typical MD-evoked IPSCs, one can see that these late IPSCs have variable onset times, exhibit multiple peaks, and have slower decay kinetics, suggesting that they may correspond to feedback inhibition recruited by another IN subtype. While this data alone does not support the model that MD-evoked IPSCs are disynaptic, low IPSC onset jitter lends support.

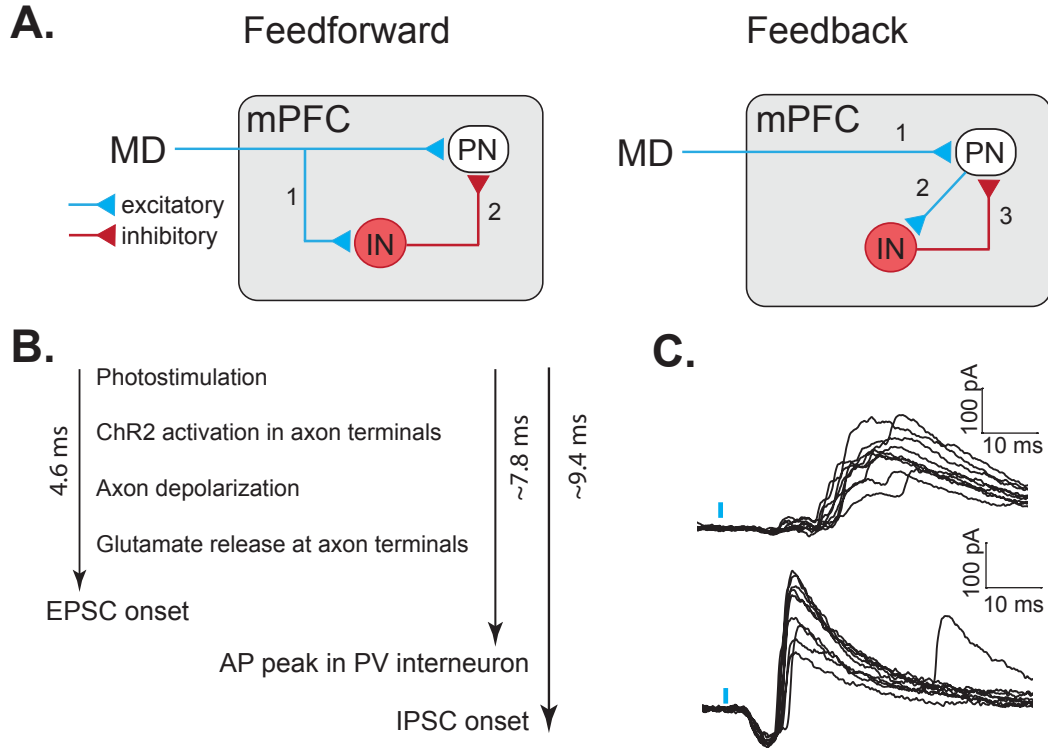


Figure 3.12: MD-evoked IPSC latency is consistent with disynaptic feedforward inhibition. A. Circuit diagrams describe the disynaptic route of feedforward inhibition versus the tri- or polysynaptic route of feedback inhibition. PN, layer III pyramidal neuron and IN, presumptive PV interneurons. B. Sequence of events required to generate disynaptic IPSCs in the MD-dACC pathway, latencies derived from electrophysiological recordings. C. Top trace: clearly delayed feedback inhibition in the absence of feedforward inhibition. Note the variable onset and slow decay of the IPSCs. Bottom: neuron recorded in the same mouse that exhibits typical disynaptic inhibitory currents. Note low jitter of onset and rapid decay kinetics. Figures A. and B. adapted from supplementary figures in (Cho *et al.*, 2013)

3.3.7 Chemicogenetic inhibition of PV+ interneurons during MD axon stimulation

In order to confirm that PV interneurons are in fact the main mediators of feedforward inhibition from the MD, I carried out a series of experiments to selectively suppress PV+ interneuron response to MD axon stimulation while recording evoked inhibitory currents onto layer III PNs. The first approach utilized the DREADD (designer receptor exclusively activated by designer drug) system (Rogan & Roth, 2011). The inhibitory DREADD is a modified G-protein coupled receptor that decreases neuronal activity by inducing an inward rectifying potassium current response when bound by the exogenous ligand clozapine-N-oxide (CNO) (Armbruster *et al.*, 2007). I took advantage of Cre-dependent inhibitory DREADD virus AAV-DIO-hM4Di-mCherry to selectively express the DREADD receptor in PV INs of PV-IRES-Cre mice. I injected 1 uL of AAV-DIO-hM4Di-mCherry bilaterally into mPFC and injected the MD bilaterally with 0.3 uL of AAV-CAG-ChR2-YFP per hemisphere.

Layer III mPFC pyramidal neurons were patched and MD-evoked IPSCs recorded for 2-6 minutes to establish a baseline response prior to washing on 10 uM of CNO **Fig3.13A**. “After CNO” IPSCs were measured 8-10 minutes after CNO was applied. I observed that up to 30 minutes of CNO washout did not cause appreciable recovery of the IPSC, and therefore one cell was recorded per section. Of the 6 neurons recorded from two animals, 5 exhibited CNO suppression of MD-evoked IPSCs **Fig3.13B**. Among the neurons that were affected by CNO bath application, the percent IPSC suppression was $89.1 \pm .05$. When all 6 cells were considered, CNO still significantly reduced the amplitude of the MD-evoked IPSC (* $p < .05$, Wilcoxon signed ranks test). It is possible that the pyramidal neuron that was unaffected by CNO application was not targeted by hM4Di-infected PV INs. To that end, I noticed that the densest hM4Di infection was in the ventral portion of the mPFC that did not overlap with the MD ChR2 YFP+ axons in both animals **Fig3.13C**. I injected a large volume (1 uL) in order to infect the maximum number of PV INs possible, and the virus likely spread. Regardless, the effect CNO had on MD-evoked IPSCs in PrL/dACC layer III PNs was striking considering the small number of local infected PV INs.

It bears mentioning that the IPSC peaks compared before and after CNO were the first peak in occasionally complex IPSCs. Interestingly, CNO had different effects on the early and late components of the IPSC. **Fig3.13D** is a sample trace of a pyramidal neuron that exhibited a short latency single IPSC peak (latency $14.8 \pm .53$ ms (SD)) and exhibited rapid suppression of the evoked IPSC following CNO application **Fig3.13E**. CNO also induced a significant shift in the time of peak **Fig3.13F** ($F(1, 16) = 49.0$, **** $p < 0.0001$, one-way ANOVA). **Fig3.13G** is an example cell that exhibited two IPSC peaks separated by ~ 14 ms. Intriguingly, CNO rapidly suppressed the short latency (~ 16 ms) IPSC peak and enhanced the late (~ 30 ms) IPSC peak but did not affect MD-evoked EPSCs **Fig3.13G,H**. The early IPSC peak latency was not altered by CNO, while the late peak latency was significantly shifted forward in time (early: $F(1, 33) = 1.33$, $p = 0.26$; late: $F(1, 33) = 62.1$, **** $p < 0.0001$ one-way ANOVA) **Fig3.13I**.

Given the small number of cells and mixture of responses, the PV DREADD results are more exploratory than conclusive. However, this experiment did uncover a potential link between the latency of the MD-evoked IPSC peak and the inhibitory cell-type of origin. The PV DREADD suppression results suggest that short latency (< 19 ms) IPSCs are mediated by PV+ INs, while longer delay IPSCs (≥ 30 ms) are mediated by a different population of inhibitory INs. The opposite effect of CNO on the early and late IPSC components in **Fig3.13G** suggests that the late IPSC represents feedback inhibition. It's tempting to speculate that feedback inhibition gets increasingly recruited as feedforward inhibition is reduced, allowing pyramidal neurons to reach threshold and spike in response to MD stimulation. This experiment suggests that the recruitment of feedforward vs. feedback inhibition is sensitive to stimulation intensity, therefore I set my stimulation to the maximum intensity that evoked a single, short-latency IPSC peak in subsequent E/I experiments. Two major limitations of the DREADD approach were 1) it is low-throughput: only one cell could be recorded per slice, and total recording time including wash on and off was nearly 45 minutes 2) the CNO effect was relatively slow and not reversible over the time course I recorded. Therefore, given its temporal precision and reversibility, optogenetic silencing of PV interneurons was a more attractive option moving forward.

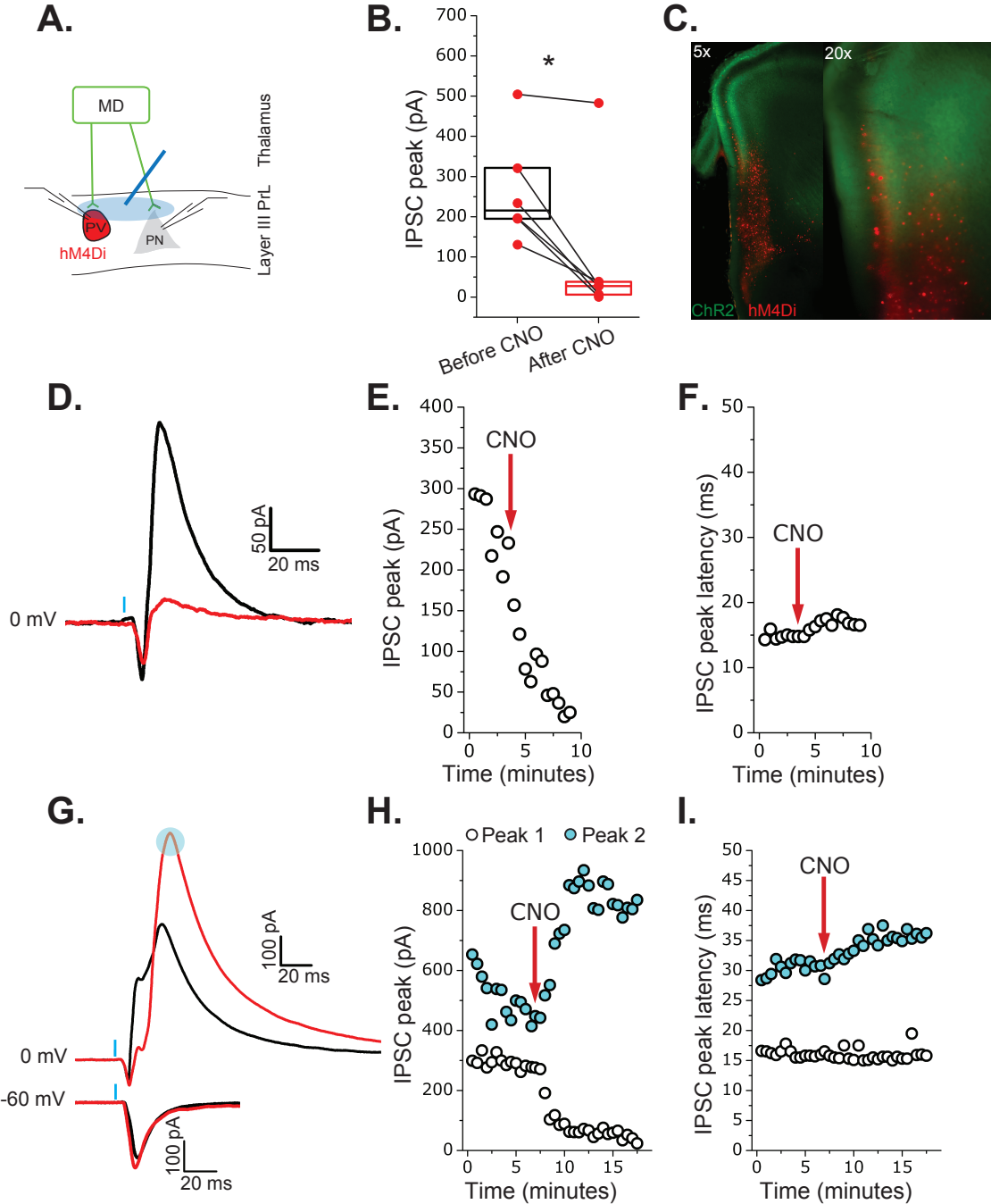


Figure 3.13: Chemicogenetic inhibition of PV+ interneurons during MD axon stimulation. A. Recording configuration. B. CNO significantly reduced MD-evoked IPSC amplitude ($p < 0.05$, Wilcoxon signed ranks test $n = 6, 2$). Data points represent 30 traces averaged immediately prior to CNO application and 8-10 minutes after application (box plots 25, 75 percentile). C. mPFC section imaged after recording shows ChR2+ axon labeling and distribution of hM4Di expression at 5x and 20x magnification. D. Sample cell with single IPSC peak; black before CNO, red after CNO. E. CNO induced rapid suppression of IPSC. Each data point is the average of 10 trials. F. CNO caused a slight but significant shift in the IPSC peak latency (**** $p < .0001$, one-way ANOVA). G. Sample cell with complex, double IPSC peak. H. CNO induced rapid suppression of first peak and enhanced the second peak. I. CNO significantly increased the latency to peak of the second IPSC peak but not the first (**** $p < .0001$, one-way ANOVA).

3.3.8 Optogenetic silencing of PV+ interneurons during MD axon stimulation

To directly test the hypothesis that these PV INs mediate the MD-driven feedforward inhibition, we sought to inhibit these neurons while monitoring the MD-driven synaptic responses in dACC PNs. To achieve this goal, we first injected the MD of the PV-Cre mice with AAV-CAG-ChR2(H134R)-YFP, and subsequently injected the dACC in the same mice with pAAV-Ef1a-DIO-eNpHR3.0-mCherry that expresses the light-gated chloride pump halorhodopsin (eNpHR3.0) in a Cre-dependent manner and can suppress neuronal firing in response to red light (Gradinaru *et al.*, 2010) **Fig3.14A**. We verified that activation of eNpHR3.0 reversibly inhibited PV IN firing **Fig3.14B** via its potent hyperpolarization (41.9 ± 4.8 mV hyperpolarization, $n=5$) **Fig3.14C**. Inhibition of PV INs dramatically reduced, and in some cases abolished, the MD-driven feedforward inhibitory currents in layer III PNs, measured at either 0 mV or -30 mV holding potential (0 mV *** $p<0.001$ $W=-66.00$ Wilcoxon matched-pairs signed-rank test) **Fig3.14D-E**) and this effect was reversible upon the cessation of the red light illumination ($F(1.232, 4.93) = 29.88$, ** $p<0.01$, one-way repeated measures ANOVA; Tukey's post-hoc test, * $p<0.05$; ** $p<0.01$) **Fig3.14F**. Interestingly, inhibition of PV INs prolonged the MD-driven EPSCs in PNs recorded at -30 mV holding potential, as measured by the EPSC half-width (*** $p<0.001$, paired t -test) **Fig3.14G**. In contrast, the peak amplitude of the MD-driven EPSC at -30 mV was not altered by PV IN inhibition (red LED off, -129.40 ± 26.12 pA; red LED on, -122.25 ± 30.04 pA, $W=-17.0$, $p>0.05$, Wilcoxon matched-pairs signed rank test) **Fig3.14H**.

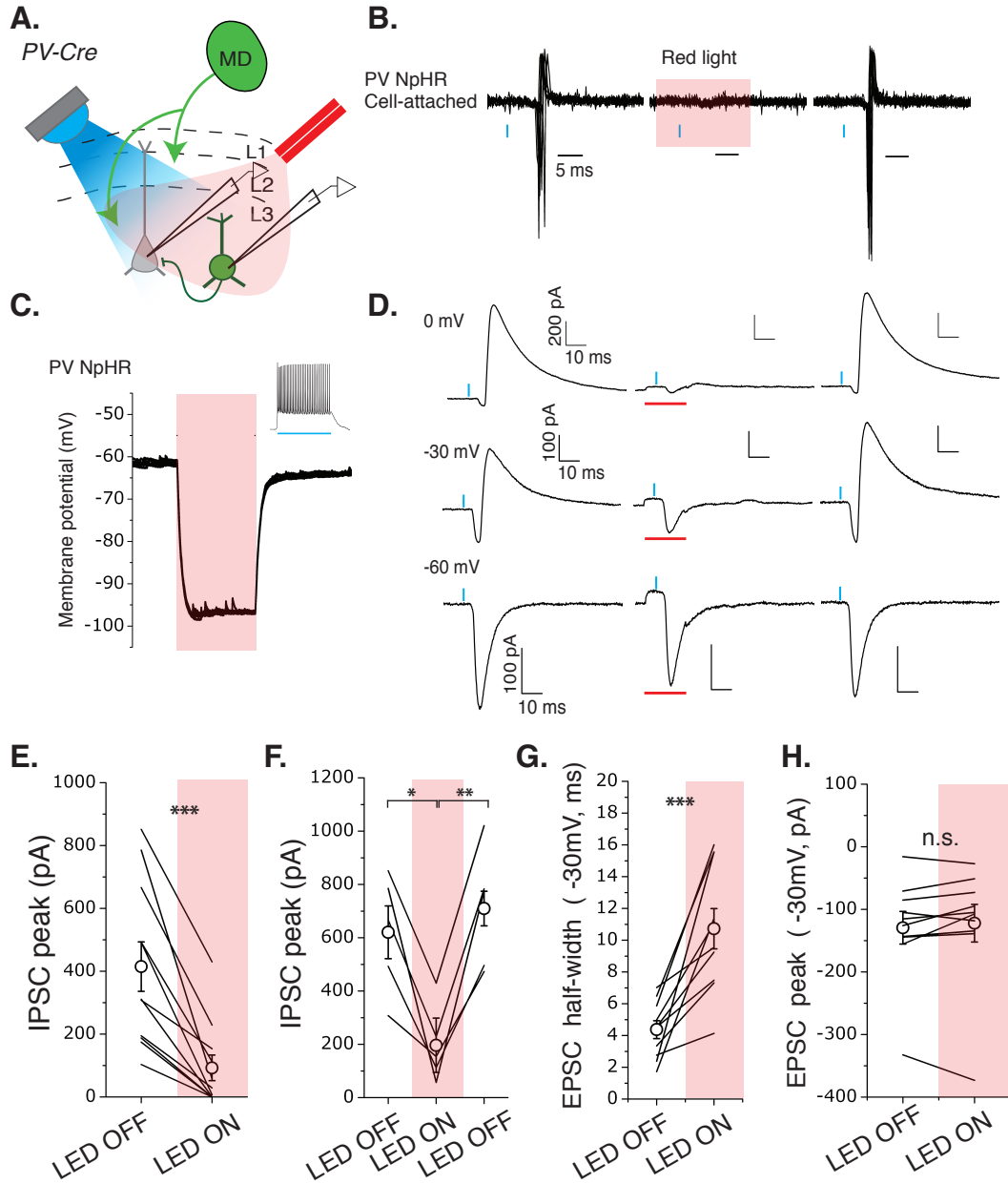


Figure 3.14: Optogenetic silencing of PV+ INs during MD axon stimulation. A. 470 nm λ light was used to excite MD axons while simultaneously 625 nm λ light was used to activate NpHR3.0 and silence PV INs. Red LEDs were triggered 5 ms prior to the onset of the 0.5 ms blue light pulse and illuminated for a total of 20 ms. B. Cell-attached recordings from GFP+ eNpHR3.0-infected PV INs revealed short-latency spikes with low jitter following ChR2 activation (latency to peak = 5.46 ± 0.13 ms, jitter (S.D.) = 0.36 ± 0.09 n=3) that were reversibly blocked by concurrent red LED stimulation (indicated by red shading). C. Red LED stim. hyperpolarized GFP+ PV INs. Inset: 500 ms blue light pulse drove fast spiking in eNpHR3.0+ PV IN. D. Sample trace: red LED stim. reversibly suppressed ChR2-evoked IPSCs onto layer III PN recorded at 0 mV or -30 mV. E. Peak IPSC amplitude recorded at 0 mV was significantly reduced by red LED stim. F. Silencing PV+ INs reversibly reduced MD-evoked IPSC amplitude. G. eNpHR3.0 activation prolonged ChR2+ evoked inward excitatory currents recorded at -30 mV, as measured by the EPSC half-width. H. red LED stim. did not affect EPSC peak amplitude recorded at -30 mV ($p > 0.05$, Wilcoxon matched-pairs signed rank test). * $p < 0.05$, ** $p < 0.01$, *** $p < 0.001$. N=5

3.3.9 Suppressing SST interneurons while stimulating MD terminals

To determine whether the somatostatin (SST) neurons, another major class of inhibitory interneurons, also contribute to the MD-driven feedforward inhibition in the dACC, we repeated the above halorhodopsin inactivation experiment with the exception that SST INs, not PV INs, were inhibited. For this purpose we used the SST-Cre mice, in which Cre is expressed under the endogenous SST promoter (Taniguchi *et al.*, 2011) **Fig3.15A**. Although activation of eNpHR3.0 effectively suppressed SST INs in the dACC **Fig3.15B** and induced potent hyperpolarization (67.25 ± 12.36 mV hyperpolarization, $n=5$) **Fig3.15C**, it did not reduce the MD-driven feedforward inhibition onto L3 PNs **Fig3.15D**; rather, feedforward inhibition was enhanced ($F(21.554, 12.43) = 32.23$, $***p<0.0001$, one-way repeated measures ANOVA; Tukey's post-hoc test, $***p<0.001$) **Fig3.15E**. Surprisingly, IPSC amplitude remained higher than baseline even after the red LEDs were turned off ($***p<0.001$ Tukey's post-hoc comparison) **Fig3.15F**. Unlike during PV IN inactivation, we found no change in the EPSC half-width when SST INs were silenced (red LED off, 2.87 ± 0.27 ms; red LED on, 2.72 ± 0.25 ms, $t(5) = 1.79$, $p>0.05$, paired *t*-test) **Fig3.15F**.

The MD-driven spiking of PV INs had significantly shorter latencies than that of SST INs and exhibited a trend towards lower spike jitter (latency to peak: PV, 5.46 ± 0.13 ms, $n = 3$, SST, 18.99 ± 1.77 ms, $n = 4$, $t = 7.64$, $df = 3.03$, $**p<0.01$, *t*-test; jitter: PV, 0.36 ± 0.09 , $n=3$, SST, 2.29 ± 0.72 ms, $n = 4$, $t = 2.67$, $df = 3.09$, $p = 0.07$, *t*-test) **Fig3.15G**. These results suggest that the MD-driven, SST IN-mediated inhibition in the dACC is polysynaptic in nature.

Together, these results indicate that the majority of MD-driven disynaptic feedforward inhibition in dACC layer III PNs is mediated by PV INs. Removal of PV-mediated inhibition increased the duration of EPSCs in layer III PNs, presumably increasing the window of time during which PNs are capable of integrating excitatory inputs. Interestingly, we did not observe an increase in the peak amplitude of MD-driven EPSCs in the PNs when PV INs were inhibited (**Fig3.14H**), consistent with a model in which MD-driven feedforward inhibition limits the time-course rather than amplitude of excitatory thalamocortical transmission.

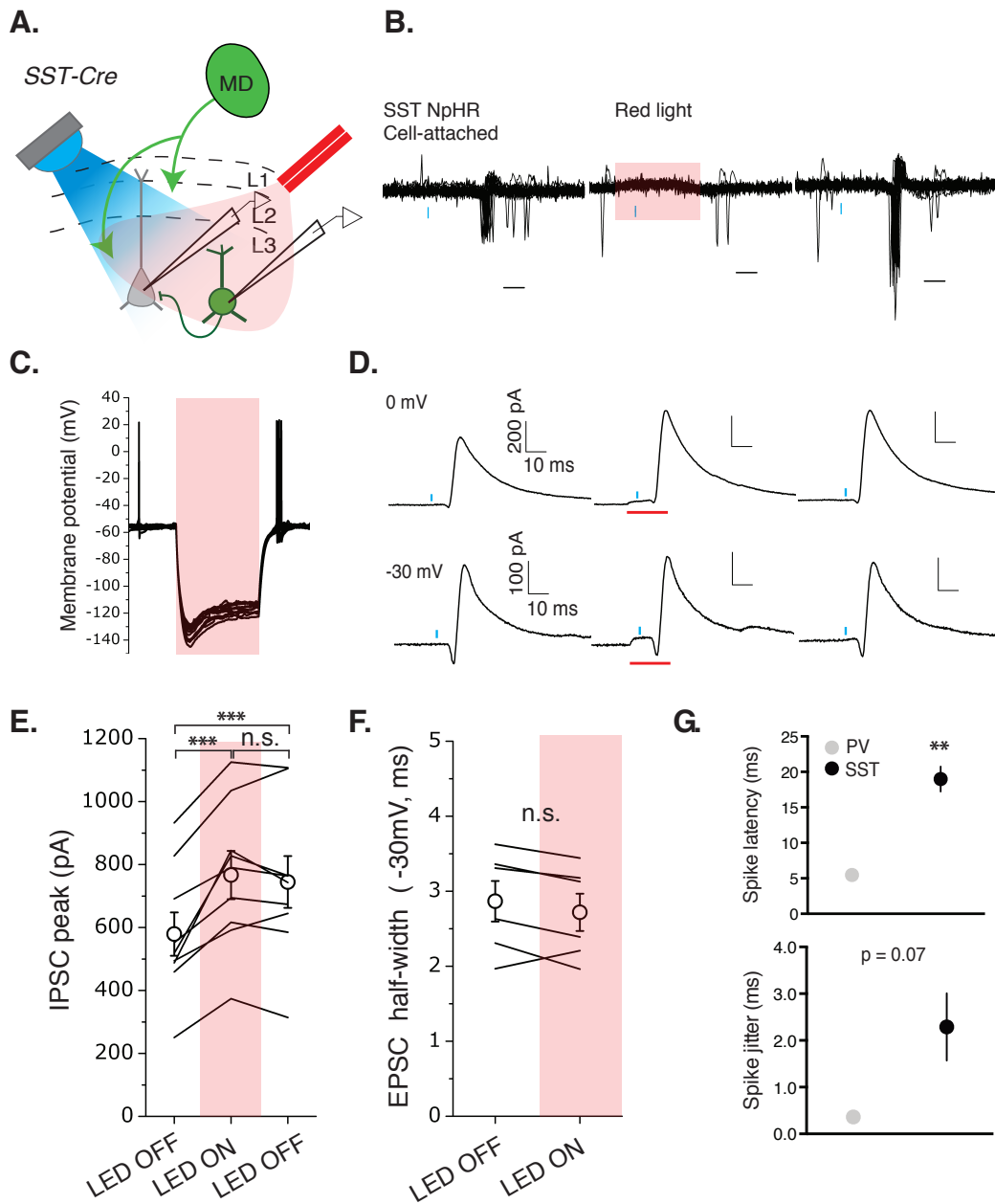


Figure 3.15: **Optogenetic silencing of SST+ INs during MD axon stimulation** A. DIO-eNpHR3.0 virus was injected into mPFC of SST-Cre mice to inactivate SST INs during MD axon stimulation. B. Chr2 activation drove spiking in 4/6 GFP+ SST INs recorded: latency to spike peak = 18.99 ± 1.77 ms, jitter (S.D.) = 2.29 ± 0.72 ms ($n=4$) and was inhibited by red LED stimulation. C. Red LED stimulation caused on average 67.25 ± 12.36 mV hyperpolarization in GFP+ SOM INs recorded ($n=5$). D. Sample trace showing the effect of SST IN silencing on MD-evoked IPSCs. E. Red LED stim. significantly altered the magnitude of MD-evoked IPSCs onto layer III PN, increasing MD-evoked IPSC amplitude. IPSC amplitude remained higher than baseline even after LEDs were turned off. F. SST IN inactivation did not affect EPSC half-width recorded at -30 mV. G. Top: MD-evoked spiking in PV INs exhibited much shorter latency than spikes in SST INs (latency to peak: 5.46 ± 0.13 ms, $n=3$, SST, 18.99 ± 1.77 ms, $n=4$). Bottom: PV spikes exhibited slightly lower jitter than SST spikes but this did not reach significance (jitter: PV, 0.36 ± 0.09 , $n=3$, SST, 2.29 ± 0.72 ms, $n=4$, $p=0.07$, t-test). ** $p<0.01$ *** $p<0.001$

3.3.10 PV halorhodopsin effect on PN PSPs

DIO-eNpHR3.0 viral injections into *PV-IRES-Cre* and *SST-IRES-Cre* mice **Fig. 3.16A,B** both resulted in high levels of eNpHR3.0 expression in PV+ or SST+ INs, respectively **Fig. 3.16C-F**. In addition, at least one DIO-eNpHR3.0-GFP+ INs was recorded per slice to ensure sufficient red LED-induced hyperpolarization prior to recording MD-evoked IPSCs. Therefore, it's unlikely the dramatically different effects of PV+ vs. SST+ IN silencing can be attributed to differences in halorhodopsin expression. Feedforward inhibition would serve to sharpen responses to thalamic input; it has been shown that GABAA blockers prolongs evoked EPSPs, as measured by increased decay time constant and PSP half-width (Chittajallu & Isaac, 2010; Lee *et al.*, 2014; Mittmann *et al.*, 2005). Therefore, we performed preliminary recordings to assess the role of PV INs in controlling PSP half-width of pyramidal neurons. In three neurons that could be held in current clamp at a stable resting potential across trials of “halo off” “halo on” “halo off” we observed that red LED stimulation reversibly increased the decay time constant of the MD-evoked PSP **Fig. 3.17A,B**. In 1 of the 3 neurons, we saw the neuron reached threshold when the red LED was turned on 5 ms prior to blue light stimulation and remained on for 20 ms total. When the red LED was turned off again, the neuron's responses returned to subthreshold.

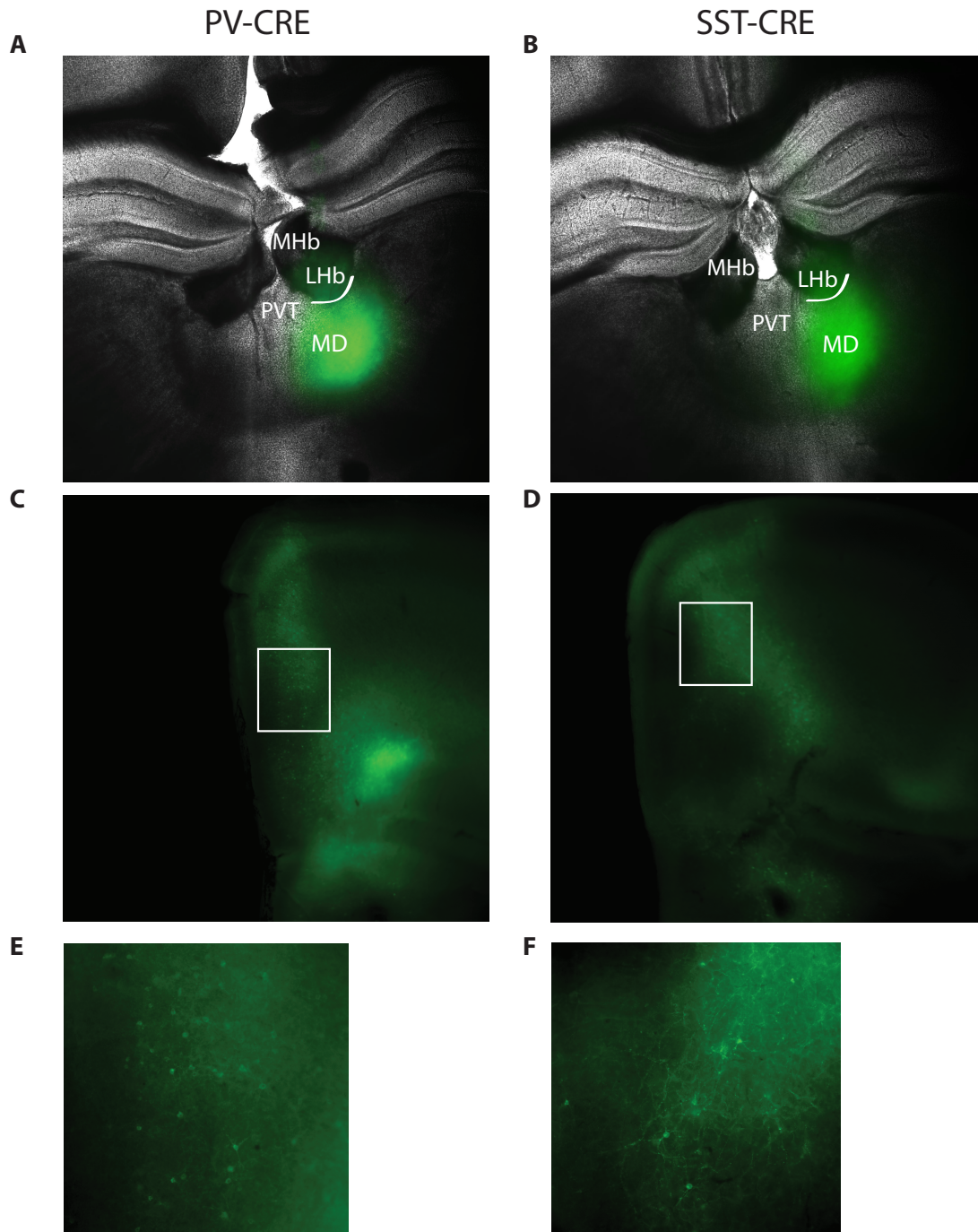


Figure 3.16: Halorhodopsin expression. A, B. Sample images of ChR2 injection location in a *PV-IRES-Cre* and a *SST-IRES-Cre* mouse, respectively. C. 5x image of an acute slice from a *PV-IRES-Cre* mouse after recording; DIO-eNpHR3.0-GFP+ neurons in green. D. 20x magnification of white box from C. D. 5x image of acute slice from a *SST-IRES-Cre* mouse after recording; note that there was substantial photobleaching. F. 20x magnification of white box from D.

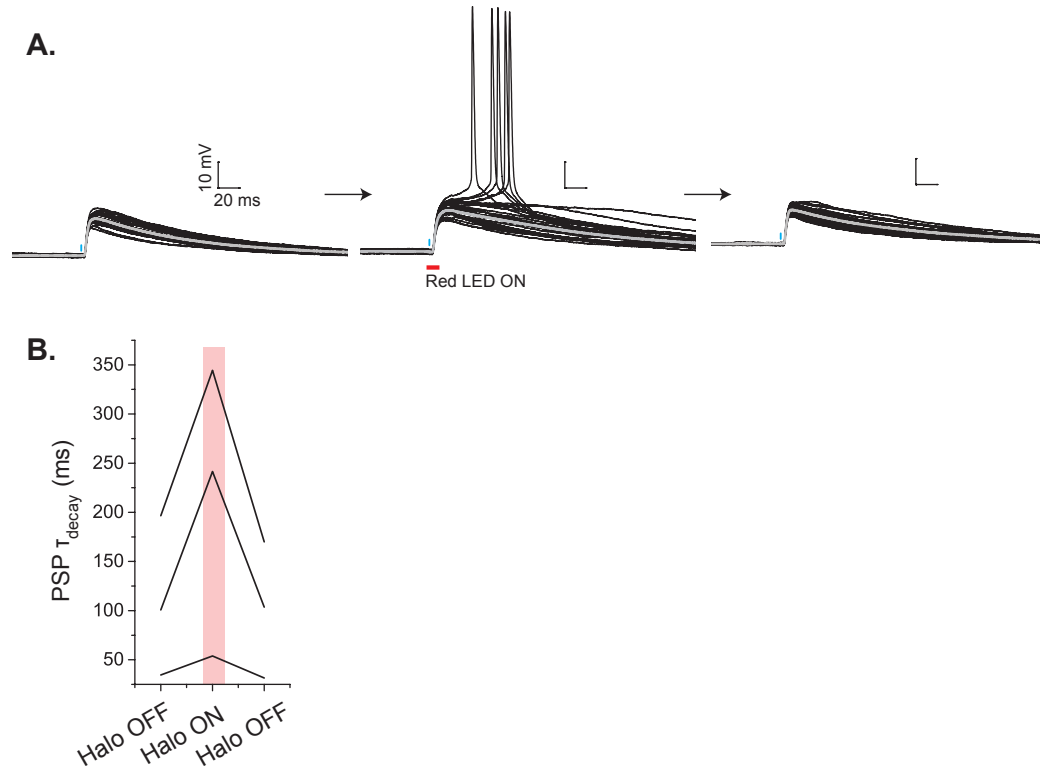


Figure 3.17: Optogenetic silencing of PV+ INs increases MD-evoked PSP duration. A. Sample traces from neuron sequentially recorded “halo off” “halo on” and “halo off”. Gray traces represent the averaged PSP, for the middle panel red LED was turned on 5 ms prior to blue light for a total duration of 20 ms. For middle panel subthreshold PSPs were averaged. Right panel: same neuron recorded at same stimulation intensity as middle panel in the absence of red light. B. PSP decay time constant increases with PV IN silencing. Preliminary data (n=3).

3.3.11 E/I balance in the MD-mPFC pathway

Excitation to inhibition (E/I) balance is believed to be important for the fidelity of information transfer in the cortex. Elevating EI balance by either optogenetically stimulating principal neurons or silencing PV INs in the mPFC impaired conditioned fear learning and caused social behavior deficits in mice (Yizhar *et al.*, 2011). Notably, Yizhar *et al.* reported that modulating the activity of even a sparse population of PV+ INs had a profound effect on unit activity in mPFC. This suggests that a small number of PV INs can largely influence mPFC circuit function. Recent work also supports the idea that PV INs are the main determinant of E/I balance in the cortex (Xue *et al.*, 2014).

Given that we observed that PV INs receive monosynaptic excitatory input from the MD and exhibit larger magnitude responses than neighboring PNs, we hypothesized that short latency IPSCs evoked by MD axon stimulation are mediated by PV INs. In addition, we previously observed increased PPR of PV-mediated IPSCs in the DISC1 HET mice. Therefore, we predicted that if PV INs are the main mediators of feedforward inhibition from the MD, in the DISC1 HET mice we would see an increase in the excitation/inhibition ratio of synaptic input driven by the MD-mPFC pathway. Therefore, we measured the ratio of excitatory current to inhibitory current onto pyramidal neurons evoked by MD axon stimulation in the mPFC.

We found that while the total current (GABA+AMPA) evoked by MD stimulation onto dACC PNs was consistent between DISC1 HET and WT mice ($p = .41$, two-tailed t -test), the GABA contribution was significantly reduced in the DISC1 HET mice (** $p < 0.01$ two-tailed t -test) **Fig3.18A,B**. The mean GABA:AMPA ratio in WT mice was $2.65 \pm .30$ vs. 1.56 ± 0.26 in DISC1 het mice (** $p < 0.01$ two-tailed t -test) **Fig3.18C,D**. The cumulative probability distributions for DISC1 HET and WT mice were significantly different for IPSC peak amplitudes but not ESPC amplitudes (* $p < 0.05$, Kolmogorov-Smirnov test) **Fig3.18E**, indicating that reduced GABA:AMPA ratio in DISC1 HET mice is due to smaller feedforward inhibitory currents.

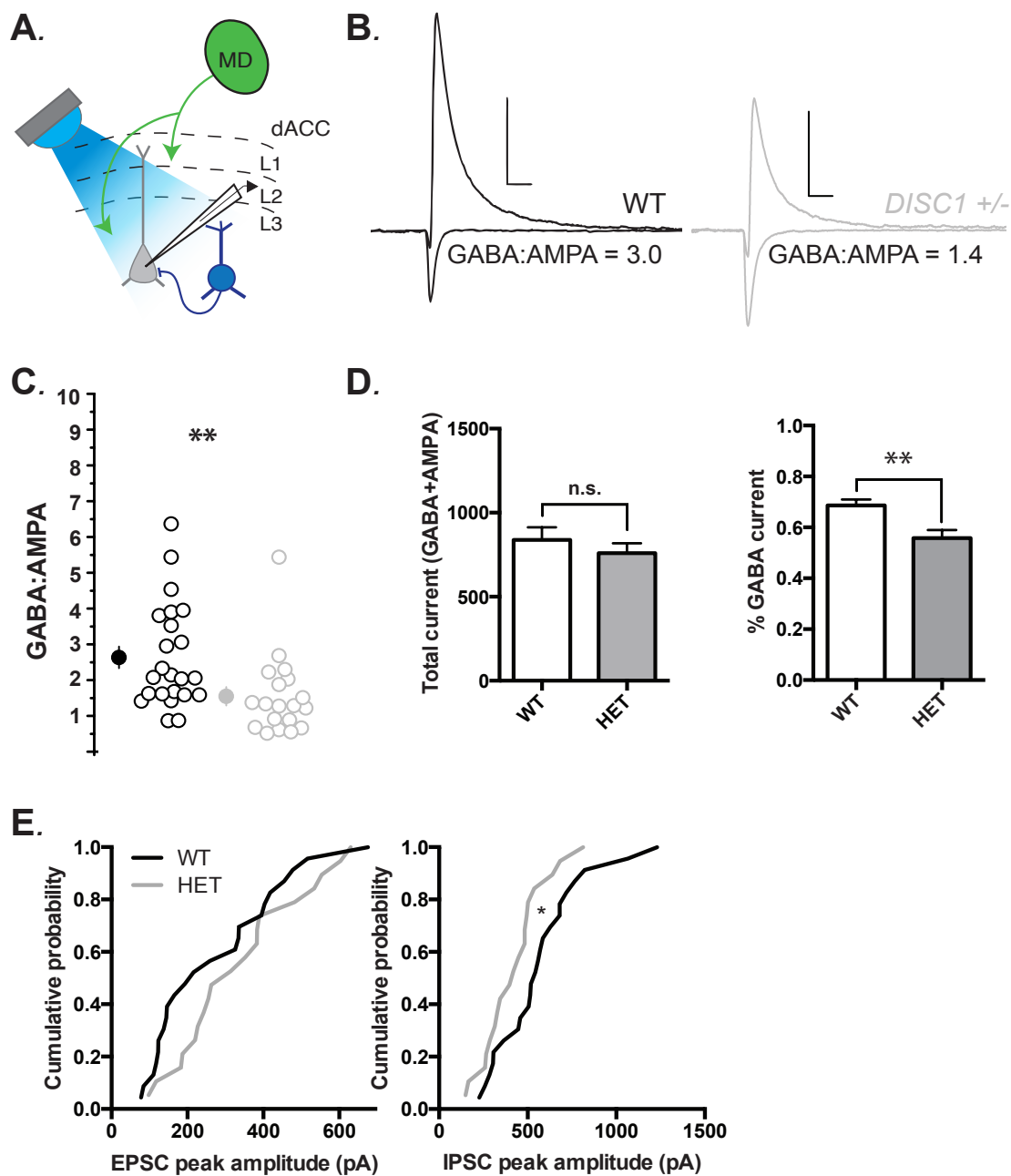


Figure 3.18: Reduced feedforward inhibition onto layer III pyramidal neurons in *DISC1*^{+/-} mice. A. Recording scheme: whole-cell patch recordings were performed in layer III PNs in ACC and monosynaptic AMPA and disynaptic GABA currents recorded following 0.5 ms blue light stimulation of ChR2+ MD axon terminals. B. Total current evoked by MD axon activation was consistent across WT and *DISC1* HET mice but the % GABA current was significantly reduced (***p*<0.01, two-tailed *t*-test)). C. GABA:AMPA ratio is significantly reduced in *DISC1* HET compared to WT (***p*<0.01, two-tailed *t*-test)) *n*= 23, 19 *N*= 8, 7. D. Representative traces for WT and HET with GABA:AMPA ratios. E. Cumulative probability distributions for EPSCs and IPSCs show that IPSCs are significantly smaller in *DISC1* HET mice compared to WT (**p*<0.05, Kolmogorov-Smirnov test). Scale bar = 200 pA, 25 ms

3.3.12 Conclusions

We characterized a projection from the MD thalamus to the ACC that recruits direct excitatory input and feedforward inhibition onto layer III pyramidal neurons. Several results argue that MD-evoked IPSCs are disynaptic and mediated by PV INs.

1) PV INs receive direct excitatory input from the MD; these thalamocortical EPSCs exhibit shorter onset latency and faster kinetics than layer III pyramidal neurons. Furthermore, MD synaptic input is stronger onto PV INs than neighboring PNs.

2) The jitter of onset latency for MD-evoked IPSCs is sufficiently low (~ 0.4 ms) to argue that it is mediated by PV INs that receive direct excitatory input from the MD, rather than polysynaptic recruitment by local PNs.

3) PV INs spike in response to MD axon stimulation. Furthermore, PV spike probability is related to spike onset latency in a manner that is consistent with the IPSC onset delay shift observed between minimal ($< 50\%$ probability) and reliable MD-evoked IPSCs. Furthermore, PV INs spike within a time frame that is consistent with the onset of MD-evoked IPSCs, while all SST INs we recorded spike too late to mediate the short-latency MD-evoked IPSCs.

4) Lastly, and most importantly, optogenetic silencing of PV INs dramatically reduced or abolished MD-evoked IPSCs, while silencing SST INs did not.

As far as I'm aware, the data presented here are the first to demonstrate that MD directly recruits PV INs in the dACC. This data confirms ultrastructural findings (Kuroda *et al.*, 2004; Rotaru *et al.*, 2005), and provides a potential mechanism for MD inhibitory gating of PFC responses to hippocampal stimulation (Floresco & Grace, 2003). In addition, the recruitment of feedforward inhibition from the thalamus to the PFC may have significant implications for the role of the MD-ACC pathway in working memory. Because GABA transmission is important for PFC-dependent cognitive function (Enomoto *et al.*, 2011; Sawaguchi *et al.*, 1989) and MD has been shown to be important for several aspects of executive function, it may follow that optimal processing in the MD-ACC circuit relies on intact feedforward inhibition. In nonhuman primates, MD transmits delay period tuning to the PFC during an oculomotor task (Funahashi

et al., 2004; Watanabe & Funahashi, 2012; Watanabe & Takeda, 2009), and GABA signaling is necessary for the integrity of spatial tuning of delay period neurons in the primate PFC (Rao *et al.*, 2000). Furthermore, neurons in sensory cortices are predicted to amplify tuned input from thalamus (Lien & Scanziani, 2013), and it would be predicted that in the MD-ACC pathway, reduced feedforward inhibition would increase cortical amplification of thalamic input and compromise spatial tuning. In keeping with this idea, introducing PFC disinhibition into a computational model of working memory broadened working memory activity patterns and degraded the precision of stored information during the delay period (Murray *et al.*, 2014). Given that findings from SZ patients suggest that the function of PV INs is impaired in DLPFC (Lewis *et al.*, 2005; Tooney & Chahl, 2004; Woo *et al.*, 1997) and that thalamofrontal connectivity is reduced (Mitelman *et al.*, 2005; Schlosser *et al.*, 2008; Seidman *et al.*, 1994; Zhou *et al.*, 2007), these abnormalities may interact to dysregulate working memory. In addition, adolescent maturation events such as myelination and GABAergic maturation could enhance underlying alterations in the MD-PFC circuit, and thus exacerbate cognitive symptoms during the prodromal phase of SZ.

Optogenetic silencing of PV+ interneurons revealed their function in sharpening layer III pyramidal neuron responses to thalamic input. The duration of EPSCs and PSPs was prolonged when PV interneurons were silenced just prior to MD axon stimulation. The removal of PV mediated feedforward inhibition increased the temporal window during which layer III pyramidal neurons could integrate excitatory input as evidenced by increased EPSC half-width. In one notable case, halorhodopsin activation in PV interneurons caused previously subthreshold stimulation to elicit action potentials. Meanwhile, SST silencing had no effect on integration time, consistent with what is known about the presynaptic properties of thalamic inputs onto PV vs. SST INs: namely, that thalamic synapses onto PV INs rapidly depress while synapses onto SST INs exhibit weak responses that facilitate during repetitive activity *in vitro* (Beierlein *et al.*, 2003; Cruikshank *et al.*, 2010; Tan *et al.*, 2008; Xu *et al.*, 2013) and *in vivo* (Ma *et al.*, 2010). Therefore, the single brief light pulse used in our stimulation protocol was unlikely to drive SST IN firing directly and thus contribute to feedforward inhibitory currents. This is consistent with our data recording cell-attached spikes in PV vs. SST INs: SST spikes occurred

~14 ms after PV spikes, and exhibited more jitter, suggesting that they fired in response to polysynaptic excitatory input rather than direct thalamic input.

In one of my halorhodopsin experiments, I used the *SST-IRES-Cre* line to silence the major non-PV+ inhibitory IN class found in the thalamorecipient cortical layers (constituting 20-30% of GABAergic INs) (Rudy *et al.*, 2010). It was previously discovered that there is a subpopulation of SST INs that overlap with layer IV INs labeled by the X94 transgenic mouse line that have the unique ability to target fast-spiking INs (Xu *et al.*, 2013). Therefore, it's possible that the potentiation of MD-evoked IPSCs that I saw upon silencing SST INs is due to the removal of a source of inhibition onto PV INs. It is still unclear, however, to what extent the organization of the thalamocortical microcircuit is conserved between granular and agranular cortex (like the mPFC). In none of the experiments I've performed thus far have I manipulated SST INs and recorded from a PV IN or vice versa. This type of experiment would shed light on whether SST INs can directly influence the response of PV INs to MD axon stimulation.

While we demonstrate that MD recruits short latency, reliable PV-mediated inhibition onto layer III pyramidal neurons, our PV rabies tracing clearly shows that MD is not the only upstream afferent that recruits PV INs in the mPFC. Ultrastructural studies have demonstrated that both BLA and hippocampal afferents terminate onto PV INs (Gabbott *et al.*, 2002, 2006). Consistent with this finding, it was shown that pharmacological inactivation of ventral hippocampus led to reduced firing rates of inhibitory interneurons in mPFC (Sotres-Bayon *et al.*, 2012). In fact, I have also observed disynaptic inhibition recruited by stimulating BLA terminals under similar conditions see Appendix **Fig. 2A-D**. I observed that the synaptic latencies for BLA-evoked EPSCs and IPSCs were nearly identical to those seen in the MD-BLA pathway **Fig. 2C**. The mean latency of BLA-evoked EPSCs onto layer II/III pyramidal neurons in dACC was $4.8 \pm .19$ ms compared to $4.6 \pm .14$ ms observed for MD-evoked EPSCs onto layer III pyramidal neurons ($p > .05$ two-tailed paired *t*-test; $n = 42, 25$). The mean latency of BLA-evoked IPSCs was $9.7 \pm .27$ ms compared to $9.5 \pm .16$ ms for MD-evoked IPSCs ($p > .05$ two-tailed paired *t*-test; $n = 17, 59$). I also observed that PV INs in layer II/III receive direct excitatory input from BLA afferents **Fig. 2D**. It is difficult to draw comparisons between the BLA and MD stimulation data, as the recording parameters were slightly different (1 ms vs. 0.5

ms light stimulation, Cs-based internal solution vs. K-based internal solution). However, I did notice that the amplitude of BLA-evoked EPSCs onto PV INs were rather small; even with high intensity light stimulation, the average amplitude was -28.8 ± 4.3 pA ($n=5$, $N=2$). Future studies could compare the relative strength of PV input/feedforward inhibition recruitment in different projections, possibly with the use of shifted channelrhodopsins.

The second major finding of this section is that the ratio of GABA : AMPA currents evoked by MD axon stimulation was reduced in the DISC1 HET mice. This is the first physiological demonstration that E/I balance is altered in the DISC1 mouse model. The most consistent findings from DISC1 mouse studies is impaired working memory performance (typically using the DNMS task) and reduced PV expression in the mPFC (Ayhan *et al.*, 2010; Brandon & Sawa, 2011; Clapcote *et al.*, 2007; Hikida *et al.*, 2007; Koike *et al.*, 2006; Kvaajo *et al.*, 2008; Niwa *et al.*, 2010; Shen *et al.*, 2008). Interestingly, reductions in PV staining were observed in models where DISC1 expression was manipulated in pyramidal neurons alone (Hikida *et al.*, 2007; Niwa *et al.*, 2010), suggesting that PV dysfunction may be secondary to primary changes in pyramidal neurons. One possibility is that impaired neuronal differentiation and migration of pyramidal neurons affects PV INs integrate into the local circuit. The DISC1 mouse model that I studied produced a pan neuronal loss of one copy of the DISC1 gene; therefore, different mechanisms may be at play but it should be noted that the DISC1 LI mouse does display characteristic impairments in neuronal proliferation and migration. In the second chapter of my thesis I reported evidence that mIPSC frequency is reduced in the mPFC and PPR of PV-mediated IPSCs is increased in DISC1 HET mice. It is difficult to know what the relationship is between PPR and p_r (Dobrunz & Stevens, 1997) therefore I am cautious in interpreting the observed reduction in GABA : AMPA ratio as a consequence of lower p_r at PV-PN synapses. Regardless of the precise mechanism, the data from three separate experiments suggest that PV-PN transmission is reduced in the DISC1 HET mice and that E/I balance is increased in the mPFC. It would be interesting to test the working memory performance in the DISC1 LI mice, as an outstanding question is whether increased E/I impairs working memory. In the future, *in vivo* recordings in the DISC1 LI mice may shed more light on circuit perturbations.

There are a few caveats of the data presented. I did not record MD-evoked EPSCs onto

PV+ INs and PNs in the presence of TTX + 4-AP, which would be a good additional control to verify that input from MD to these cell-types is monosynaptic as opposed to polysynaptic (Petreanu *et al.*, 2009). Additional recordings of PV and PN pairs using K-gluconate need to be performed to complete the datasets for the EPSC kinetics, PV PPR, and relative response strength. Another experiment that would be informative is paired cell-attached recordings of PV INs and PNs in response to MD stimulation. The data so far would suggest that PV INs will have a lower MD-evoked spike threshold, however it will be interesting to track the curves of light intensity vs. spike probability for PV INs and PNs across genotypes. The initial relative spike thresholds could help clarify if PV INs are normally recruited by MD axon stimulation in the DISC1 HET mice. In addition, the slope of PN spike probability may shed light as to what extent feedforward inhibition curtails PN spikes at low stimulation intensity.

A more general issue with the data may be that we did not standardize the absolute light power across stimulation trials, though we did maintain the diameter of the light source across experiments. My argument for not using a consistent light power is that I believe that the greater source of variability in this type of optogenetic study comes from the viral injection itself: the precise location and infectivity that subsequently affects the distribution of and Chr2 expression within axons. I believe that maintaining light power has the potential to amplify these sources of experimental variability. Instead, we adjusted the stimulation intensity based on each cell's response properties, such that the maximum short-latency single peak IPSC was evoked. Generally the GABA : AMPA ratio does not increase linearly because while AMPA currents increase linearly with light intensity, GABA recruitment is superlinear. Therefore, it's important to compare cells within the same stimulation range. One piece of evidence that we achieved this in our recordings is that the total current evoked by MD stimulation was equal across genotypes. Therefore it is not the case that we sampled within the "low-end" of the GABA : AMPA curve and biased the data towards lower ratios in the DISC1 HET mice.

Chapter 4

Discussion

4.0.13 PV interneuron function in DISC1 LI model

We observed an increase in the paired pulse ratio of PV-evoked IPSCs onto layer III PNs in the DISC1 HET mice. The difference between DISC1 HET and WT mice was largest at the shortest interstimulus intervals tested $\leq 100ms$. This change in PPR is reminiscent of the increased facilitation previously observed in PV-/- mice between INs and Purkinje cells within the cerebellum (Caillard *et al.*, 2000). A similar relationship between PV expression level and IPSC PPR was observed in barrel cortex of whisker trimmed mice. PV expression was reduced within the deprived barrels, and typically robust paired-pulse depression was replaced by weak paired-pulse depression or facilitation (Jiao *et al.*, 2006). Given that reduced parvalbumin expression within PFC has been observed across various DISC1 mutant mouse models (Ayhan *et al.*, 2010; Hikida *et al.*, 2007; Lee *et al.*, 2013b; Niwa *et al.*, 2010; Shen *et al.*, 2008) we are interested in quantifying PV staining in the mPFC of DISC1 HET mice, to determine if lower expression could contribute to altered short-term plasticity at the PV-PN synapse. However, even if PV IPSC PPR increases can be “rescued” by overexpression of parvalbumin, the mechanistic link between DISC1 and parvalbumin is unclear. One hypothesis is that DISC1 deletion could impair neuronal differentiation of PV INs or alter tangential migration of INs in the cortex or interfere with the final stages of PV IN differentiation: parvalbumin protein expression appears in the cortex at postnatal day 10 (del Rio *et al.*, 1994). While our observation

of reduced mIPSC frequency onto pyramidal neurons could be consistent with fewer PV INs rather than changes in the short term dynamics of GABA release, our data from the direct ChR2 activation of PV INs suggest that GABA release dynamics are altered in the DISC1 HET mice. Whether or not parvalbumin expression plays a role in this change remains to be determined. Given that the *PV-IRES-Cre; Ai14* reporter mice “turn on” by even transient expression of parvalbumin at P10 (del Rio *et al.*, 1994), it would be interesting to compare the number of Ai14+ neurons with parvalbumin staining cell counts in adult DISC1 HET and WT mice. This could address the question of whether fewer PV INs are specified early in brain development or whether they lose parvalbumin expression later in life, as is believed to be the case in patients with SZ (Curley *et al.*, 2011).

The unique kinetics of parvalbumin’s Ca^{2+} buffering ability negligibly influences the rise rate of intracellular Ca^{2+} but accelerates the initial decay phase, which limits the buildup of residual Ca^{2+} at presynaptic terminals and shifts short term plasticity towards depression (Muller *et al.*, 2007; Schwaller, 2010). However, a caveat is that the Caillard study was performed in the cerebellum, where PV INs express especially high levels of parvalbumin. A recent study found no functional difference between PV+ and PV-/- to PN synapses in the hippocampus, and concluded from modeling that parvalbumin affects synaptic dynamics only when expressed at high levels (Eggermann & Jonas, 2011).

While facilitation at the PV-PN synapse could suggest an increase in inhibitory transmission, most studies favor the model that reduced PV expression results in a decrease in gamma band power due to asynchronous GABA release. A computational model of a cortical circuit including asynchronous release from GABAergic interneurons found that reducing PV levels – either as a loss of PV interneurons or a constant reduction in PV expression across interneurons – exhibited a decreased level of excitation and reduced gamma-band activity (Volman *et al.*, 2011). It was also observed experimentally that PV-/- mice exhibited greater asynchronous GABA release following high-frequency action potential firing compared to controls (Manseau *et al.*, 2010). The key feature of this network is that PV INs inhibit one another, such that asynchronous GABA release caused by an aberrant increase in presynaptic Ca^{2+} stores would result in desynchronized PV interneuron firing and reduced gamma power. However, another

study in PV knockout mice found that if PV-mediated IPSC decays are constant, an increase in GABA PPR increases gamma power without affecting the dominant frequency or coherence (Vreugdenhil *et al.*, 2003). Our set of findings is consistent with the model of unchanged PV-mediated IPSC decay but increased PPR. Given these conflicting results, it isn't entirely clear if and how gamma oscillations are altered in the DISC1 HET mice. In the future, it would be interesting to apply the method developed by Cardin *et al.* to transduce *DISC1; PV-Cre* mice with Cre-dependent Chr2 and measure the tuning curve of the LFP power ratio across a range of PV stimulation frequencies (Cardin *et al.*, 2009). This method may reveal a more nuanced picture of the ability of PV firing to induce oscillations across frequency bands. This method was used to demonstrate that mice in which NR1 is knocked out of PV INs are impaired in generating oscillations within the gamma band range (Carlen *et al.*, 2012), and will be a useful tool to test the model predictions of altered PV-PN synaptic properties.

A recent study reported that PV interneurons preferentially target the type A subclass of layer V pyramidal neurons in mPFC that project subcortically, compared to type B layer V pyramidal neurons that project to contralateral cortex and striatum (Lee *et al.*, 2014). Our study did not distinguish between type A and type B pyramidal neurons. However, given that we focused our recordings in layer III, we are most likely to have recorded type B neurons (type A are restricted to Vb). In the future it would be interesting to evaluate the contribution of MD-driven feedforward inhibition to distinct subpopulations of pyramidal neurons; for instance to type A vs. type B. The development of new genetic intersection lines that capture subpopulations of pyramidal neurons will aid in this type of study. Another approach would be to use retrograde tracing in combination with Chr2 in MD in order to target recordings from pyramidal neurons that project to MD and ask whether they receive direct excitatory input from MD and compare the GABA:AMPA ratio onto these neurons compared to layer III PNs. Enhanced inhibition from PV INs onto type B neurons might argue for the importance of MD-ACC feedforward projections to synchronize activity across ACC and the MD or other subcortical targets.

Human imaging studies suggest a link between altered MD-PFC functional connectivity and schizophrenia. Analysis of resting-state BOLD MRI suggested reduced functional

connectivity between the MD and prefrontal cortex in patients with SZ. Interestingly, this was accompanied by increased functional connectivity between the somatosensory cortex and the ventral lateral and ventral posterior-lateral thalamus (Woodward *et al.*, 2012). Normally, the thalamus-somatosensory connectivity exhibits an inverted U shape that peaks in adolescence compared to childhood and adult and then decreases from adolescence to adulthood. Therefore, the finding of elevated thalamo-somatosensory connectivity may suggest that there is impaired circuit refinement during late brain maturation, during the time that schizophrenia most often has its onset.

Interestingly, resting-state prefrontal-thalamic functional connectivity is largely absent in children and adolescents and increases from childhood into adulthood (Fair *et al.*, 2010). One explanation may be increasing myelination over that time period. However, intriguingly it has been shown in rodent that the number of synaptic contacts onto mPFC GABAergic interneurons from long-range projections increase 8-fold from juvenile to adulthood (Cunningham *et al.*, 2008). Therefore, another possibility is that the maturation of inhibition in the mPFC shapes the output of MD-projecting layer V and VI neurons in such a way that increases coherent activity across these reciprocally connected brain regions, thus increasing MD-PFC functional connectivity. People diagnosed with SZ have increased fractional anisotropy in white matter tracts connecting MD to DLPFC, suggesting that reduced functional connectivity is due, at least in part, to altered white matter properties (Marenco *et al.*, 2012). However, an appealing explanation that could tie the observed postmortem reductions in markers of inhibitory transmission with reduced functional connectivity between the MD and DLPFC and abnormal oscillations is that altered inhibitory transmission in PFC leads to weakened reverberatory activity between the MD and PFC. Although the topic hasn't been explored very much, at least one study asked whether lesioning the MD of adolescent rats would produce changes in inhibitory markers in PFC (Volk & Lewis, 2003). They found no changes in GABA markers, arguing that impaired GABA transmission in PFC is just as likely a cause as a consequence of altered MD-PFC connectivity. However, it is possible that MD lesion earlier in development may have had an effect. The ability of the thalamus to influence cortical patterning early in development (Pouchelon & Jabaudon, 2014) and its role as a "hub" for information processing

suggest that thalamic disruption early in life could have profound effects on brain function. Notably two recent papers have made interesting findings of aberrant thalamocortical circuitry in genetic models of neurodevelopmental disease (Chun *et al.*, 2014; Normand *et al.*, 2013).

In addition to functional imaging data, postmortem studies report reduced MD thalamic volume (Heckers, 1997; Popken *et al.*, 2000; Young *et al.*, 2000) and cell number (Byrne *et al.*, 2002; Pakkenberg, 1990) in patients with SZ. It is difficult to interpret data collected from a chronically ill patient population, and it is possible that reduced MD volume is related to antipsychotic treatment or other comorbidities from which patients with SZ often suffer. However, in particular, functional imaging studies strongly suggest that communication within the MD-PFC thalamocortical circuit is altered in SZ. Taken with the evidence for impaired GABAergic transmission – particularly from PV INs – in the PFC, an intriguing hypothesis is that PV dysfunction disrupts cortical oscillations in PFC that support cognition. Other higher-order thalamic nuclei such as the pulvinar have been shown to be important for synchronizing activity between cortical regions (Saalmann *et al.*, 2012). This synchronization is a mechanism that could regulate information transfer across brain regions as behavioral or cognitive demands dictate.

Although highly speculative, it’s interesting to note that chemogenetic inhibition of MD reduced coherence of beta oscillations between mPFC and MD during the choice phase of a delayed nonmatch to sample task. It’s been suggested that IN firing in the gamma band range can promote beta band oscillations in excitatory populations as excitatory neurons “skip a beat” of the gamma oscillation (Kopell *et al.*, 1999). While gamma oscillations (40-80 Hz) cannot be transferred across brain regions, oscillations in the lower frequency range such as beta (13-30 Hz), theta (4-12 Hz), and delta (.5-4 Hz) have long conduction delays and are believed to be better suited to transfer information across long distances (Stein *et al.*, 2000). Because we observed that MD relay neurons send a significant projection to PV INs in mPFC, inhibiting MD may alter the strength and/or timing of feedforward inhibition in mPFC and thus alter the synchrony of neuronal firing in PNs that then project back to MD (Singer, 2009). Recently, PV IN dysfunction was proposed as a mechanism underlying altered long-range coordination of delta oscillations during non-REM sleep in the methylazoxymethanol (MAM) E17 mouse

model of schizophrenia (Phillips *et al.*, 2012).

It would be interesting in the future to explore the role that PFC inhibitory INs play in supporting cognitive task-related changes in synchronous activity between connected brain regions. It's known that fast-spiking PV INs play a major role in generating local gamma oscillations, but the mechanism underlying beta frequency oscillations is not yet known. Another possibility is that beta oscillations aren't intrinsic to the MD-mPFC circuit but are driven by brain areas that are upstream of the MD. One such candidate is the globus pallidus, which has GABAergic interneurons that exhibit oscillatory properties (Stanford, 2003). Given that the MD is comprised solely of excitatory projection neurons in the rodent, the MD-ACC-MD could serve as a simplified circuit within which to study the role of local inhibition in the mPFC in inducing or sustaining long-range synchrony. Again, the recurring theme of altered oscillations and reduced inhibitory markers in individuals with SZ highlights the need for understanding the basic mechanisms of rhythm generation in the brain.

4.0.14 Future perspectives

There is debate within the psychiatric research field as to whether a “reverse translational” gene-to-phenotype approach is the best strategy for understanding the biology underlying human brain disorders like schizophrenia. For example, despite having known the single causal gene for Huntington's disease for over 20 years, little progress has been made towards developing therapeutics. Schizophrenia, with its complex, gene-by-environment interaction origins is likely to pose an even greater challenge (Low & Hardy, 2007). Rare schizophrenia risk variants such as DISC1 and NRG1, while not always supported by genome-wide association studies, have been shown to regulate important aspects of brain development and synaptic function. Therefore, from one view, “solving” the puzzle of how DISC1 genomic deletion leads to cognitive dysfunction can only explain a miniscule fraction of SZ cases. However, if we think of DISC1 – a rare, but highly penetrant genetic risk factor for SZ — as a tool to study potential common pathophysiological mechanisms of SZ, then the explanatory power comes not from the gene's specific function but rather the effect it has on neural circuits.

A reduction in parvalbumin mRNA or protein expression is a reproducible finding in the postmortem brains of patients with SZ. PV IN dysfunction, reported as reduced mRNA or protein expression, cell numbers, or physiological readouts is a recurring theme in papers that study psychiatric risk genes or more general environmental stressors such as maternal deprivation, *in utero* MAM administration, or PCP treatment (Deidda *et al.*, 2014; Jiang *et al.*, 2013). These findings suggest that PV INs may be especially sensitive to stress and neurodevelopmental perturbation. Furthermore, PV dysfunction appears to disrupt optimal PFC circuit function that supports working memory and executive function. If PV PFC dysfunction is sufficient to cause PFC-dependent cognitive impairment, then deficits in WM tasks should be present across models, irrespective of the human disease they seek to model. Animal studies that combine genetic risk with environmental stress may be able to enhance the phenotypes caused by genetic liability alone (Abazyan *et al.*, 2011; Niwa *et al.*, 2013).

In this thesis, I've proposed a circuit mechanism by which impaired PV IN function in the ACC could lead to the impaired function connectivity between MD and PFC seen in patients with SZ. In the future, I think it will be crucial to study how PV dysfunction can alter not only the generation of local gamma oscillations, but long range communication across brain regions. Now that we have shown that MD recruits feedforward inhibition in the ACC, the question is what role feedforward inhibition plays in non-sensory cortical areas. What do the receptive fields in the prefrontal cortex represent, and what is the functional consequence of MD-PV IN feedforward inhibition on these representations? The work of Patricia Goldman-Rakic suggests that the PFC serves as temporary storage for spatial representations (or motor plans), however, more recent work suggests that the role of PFC is more complex (Lesh *et al.*, 2010). For instance, it isn't known how the PFC represents objects within different contexts. The MD and PFC are known to be important for flexibly adapting behavior, and the MD appears to have the makings of a comparator, with its reciprocal connections with the PFC and inputs from limbic structures that are involved in motivation, motor planning, and reward.

An important goal in the future will be to bridge the gap between synaptic deficits observed in either environmental or genetic models of psychiatric disease with broad, distributed alterations in brain activity, such as those measured via oscillations. Given the commonly ob-

served change in PV IN function and abnormal oscillatory activity in schizophrenia, it will be crucial to understand the neural substrate of frequency bands that are perturbed in schizophrenia. In addition, I think it will be fascinating to study the link between postnatal brain maturation and oscillation development as it's been shown to develop postnatally (Uhlhaas & Singer, 2011) and require the maturation of inhibitory circuits (Doischer *et al.*, 2008).

Bibliography

- Abazyan, B, Nomura, J, Kannan, G, Ishizuka, K, Tamashiro, K, Nucifora, F, Pogorelov, V, Ladenheim, B, Yang, C, Krasnova, I, Cadet, J, Pardo, C, Mori, S, Kamiya, A, Vogel, M, Sawa, A, Ross, C, & Pletnikov, M. 2011. Prenatal interaction of mutant DISC1 and immune activation produces adult psychopathology. *Biological Psychiatry*, **68**(12), 1172–1181.
- Agmon, A, & Connors, B. 1992. Correlation between synaptic intrinsic firing patterns and thalamocortical synaptic responses of neurons in mouse barrel cortex. *The Journal of Neuroscience*, **12**(1), 319–329.
- Alexander, G, & Fuster, J. 1973. Effects of cooling prefrontal cortex on cell firing in the nucleus medialis dorsalis. *Brain Research*, **26**, 93–105.
- Amann, L, Gandal, M, Halene, T, Ehrlichman, R, White, S, Mccarren, H, & Siegel, S. 2010. Mouse behavioral endophenotypes for schizophrenia. *Brain Research Bulletin*, **83**(3-4), 147–161.
- Ananth, H, Popescu, I, Critchley, H, Good, C, Frackowiak, R, & Dolan, R. 2002. Cortical and subcortical gray matter abnormalities in schizophrenia determined through structural magnetic resonance imaging with optimized volumetric voxel-based morphometry. *Am J Psychiatry*, **159**, 1497–1505.
- Andreasen, N. 1997. The role of the thalamus in schizophrenia. *Canadian Journal of Psychiatry*, **42**, 27–33.
- Arguello, P, & Gogos, J. 2006. Modeling madness in mice: one piece at a time. *Neuron*, **52**, 179–196.
- Arguello, P, & Gogos, J. 2012. Genetic and cognitive windows into circuit mechanisms of psychiatric disease. *Trends in Neurosciences*, **35**(1), 3–13.
- Armbruster, B, Li, X, Pausch, M, Herlitze, S, & Roth, B. 2007. Evolving the lock to fit the key to create a family of G protein-coupled receptors potently activated by an inert ligand. *Proc. Natl. Acad. Sci. USA*, **104**(12), 5163–5168.
- Atallah, B, Bruns, W, Carandini, M, & Scanziani, M. 2012. Parvalbumin-expressing interneurons linearly transform cortical responses to visual stimuli. *Neuron*, **73**(1), 159–170.
- Ayhan, Y, Abazyan, B, Nomura, J, Kim, R, Ladenheim, B, Krasnova, I, Sawa, a, Margolis, R, Cadet, J, Mori, S, Vogel, M, Ross, C, & Pletnikov, M. 2010. Differential effects of prenatal and postnatal expressions of mutant human DISC1 on neurobehavioral phenotypes in transgenic mice: evidence for neurodevelopmental origin of major psychiatric disorders. *Molecular psychiatry*, **1**(Jan.), 1–14.

-
- Barch, DM, & Keefe, RSE. 2010. Anticipating DSM-V: opportunities and challenges for cognition and psychosis. *Schizophrenia Bulletin*, **36**(1), 43–47.
- Bartho, P., Freund, T. F., & Acsady, L. 2002. Selective GABAergic innervation of thalamic nuclei from zona incerta. *European Journal of Neuroscience*, **16**, 999–1014.
- Baxter, MG. 2013. Mediodorsal thalamus and cognition in non-human primates. *Frontiers in Systems Neuroscience*, **7**, 1–5.
- Begleiter, H, & Porjesz, B. 1986. The P300 component of the event-related brain potential in psychiatric patients. *Chap. 49, pages 529–535 of: Evoked Potentials*. New York, NY: Alan R. Liss, Inc.
- Beierlein, M, Gibson, JR, & Connors, BW. 2003. Two dynamically distinct inhibitory networks in layer 4 of the neocortex. *Journal of Neurophysiology*, **90**, 2987–3000.
- Belforte, JE, Zsiros, V, Sklar, ER, Jiang, Z, Yu, G, Li, Y, Quinlan, EM, & Nakazawa, K. 2010. Postnatal NMDA receptor ablation in corticolimbic interneurons confers schizophrenia-like phenotypes. *Nature Neuroscience*, **13**(1), 76–83.
- Benshalom, G, & White, EL. 1986. Quantification of thalamocortical synapses with spiny stellate neurons in layer IV of mouse somatosensory cortex. *The Journal of Comparative Neurology*, **253**, 303–314.
- Blackwood, D H, Fordyce, A, Walker, MT, St Clair, DM, Porteous, DJ, & Muir, WJ. 2001. Schizophrenia and affective disorders—co-segregation with a translocation at chromosome 1q42 that directly disrupts brain-expressed genes: clinical and P300 findings in a family. *American Journal of Human Genetics*, **69**(2), 428–33.
- Blackwood, DH, Glabus, MF, Dunan, J, O’Carroll, RE, Muir, WJ, & Ebmeier, KP. 1999. Altered cerebral perfusion measured by SPECT in relatives of patients with schizophrenia. Correlations with memory and P300. *Br J Psychiatry*, **175**, 357–366.
- Bradshaw, NJ, & Porteous, DJ. 2012. Neuropharmacology DISC1-binding proteins in neural development, signalling and schizophrenia. *Neuropharmacology*, **62**(3), 1230–1241.
- Brandon, NJ, & Sawa, A. 2011. Linking neurodevelopmental and synaptic theories of mental illness through DISC1. *Nature Reviews Neuroscience*, **12**, 707–722.
- Brandon, NJ, Schurov, I, Camargo, LM, Handford, EJ, Duran-Jimeniz, B, Hunt, P, Millar, JK, Porteous, DJ, Shearman, MS, & Whiting, PJ. 2005. Subcellular targeting of DISC1 is dependent on a domain independent from the Nudel binding site. *Molecular and Cellular Neuroscience*, **28**, 613 – 624.
- Brandon, NJ, Millar, JK, Korth, C, Sive, H, Singh, KK, & Sawa, A. 2009. Understanding the role of DISC1 in psychiatric disease and during normal development. *The Journal of Neuroscience*, **29**(41), 12768 –12775.
- Brauns, S, Gollub, RL, Roffman, JL, Yendiki, A, Ho, B, Wassink, TH, Heinz, A, & Ehrlich, S. 2011. DISC1 is associated with cortical thickness and neural efficiency. *NeuroImage*, **57**, 1591–1600.
- Brickman, AM, Buchsbaum, MS, Shihabuddin, L, Byne, W, Newmark, RE, Brand, J, Ahmed, S, Mitelman, SA, & Hazlett, EA. 2004. Thalamus size and outcome in schizophrenia. *Schizophrenia Research*, **71**, 473 – 484.

-
- Bubser, M, De Brabander, J, Timmerman, W, Feenstra, M, Erdtsieck-Ernste, E, Rinkens, A, Van Uum, J, & Westerink, B. 1998. Disinhibition of the mediodorsal thalamus induces fos-like immunoreactivity in both pyramidal and GABA-containing neurons in the medial prefrontal cortex of rats, but does not affect prefrontal extracellular GABA levels. *Synapse*, **165**, 156–165.
- Byne, W, Buchsbaum, MS, Mattiace, LA, Hazlett, EA, Kemether, E, Elhakem, SL, Purohit, DP, Haroutunian, V, & Jones, L. 2002. Postmortem assessment of thalamic nuclear volumes in subjects with schizophrenia. *Am J Psychiatry*, **159**, 59–65.
- Caillard, O, Moreno, H, Schwaller, B, Llano, I, Celio, MR, & Marty, A. 2000. Role of the calcium-binding protein parvalbumin in short-term synaptic plasticity. *Proc. Natl. Acad. Sci. USA*, **106**.
- Callicott, JH, Bertolino, A, Mattay, VS, Langheim, FJP, Duyn, J, Coppola, R, Goldberg, TE, & Weinberger, DR. 2000. Physiological dysfunction of the dorsolateral prefrontal cortex in schizophrenia revisited. *Cerebral Cortex*, **10**, 1078–1092.
- Camargo, LM, Collura, V, Rain, J-C, Mizuguchi, K, Hermjakob, H, Kerrien, S, Bonnert, TP, Whiting, PJ, & Brandon, NJ. 2007. Disrupted in Schizophrenia 1 Interactome: evidence for the close connectivity of risk genes and a potential synaptic basis for schizophrenia. *Molecular Psychiatry*, **12**(Jan.), 74–86.
- Cannon, M, Jones, PB, & Murray, RM. 2002a. Obstetric complications and schizophrenia: historical and meta-analytic review. *Am J Psychiatry*, **159**, 1080–1092.
- Cannon, TD, Theo, QM, Erp, V, Bearden, CE, Loewy, R, Thompson, P, Toga, AW, Huttunen, MO, Keshavan, MS, Seidman, LJ, & Tsuang, MT. 2002b. Early and late neurodevelopmental influences in the prodrome to schizophrenia: contributions of genes, environment, and their interactions. *Schizophrenia*, 653–670.
- Cannon, TD, Hennah, W, van Erp, TGM, Thompson, PM, Lonnqvist, J, Huttunen, M, Gasperoni, T, Tuulio-Henriksson, A, Pirkola, T, Toga, AW, Kaprio, J, Mazziotta, J, & Peltonen, L. 2005. Association of DISC1/TRAX haplotypes with schizophrenia, reduced prefrontal gray matter, and impaired short- and long-term memory. *Arch Gen Psychiatry*, **62**, 1205–1213.
- Cannon, Tyrone D, Huttunen, Matti O, Lonnqvist, Jouko, Tuulio-henriksson, Annamari, Pirkola, Tiia, Glahn, David, Finkelstein, Jennifer, Hietanen, Marja, & Kaprio, Jaakko. 2000. The inheritance of neuropsychological dysfunction in twins discordant for schizophrenia. *Public Health*, 369–382.
- Cardin, JA, Carlen, M, Meletis, K, Knoblich, U, Zhang, F, Deisseroth, K, Tsai, L, & Moore, CI. 2009. Driving fast-spiking cells induces gamma rhythm and controls sensory responses. *Nature*, **459**, 663–668.
- Cardoso-cruz, H, Sousa, M, Vieira, JB, Lima, D, & Galhardo, V. 2013. Prefrontal cortex and mediodorsal thalamus reduced connectivity is associated with spatial working memory impairment in rats with inflammatory pain. *Pain*, **154**, 2397–2406.
- Carlen, M, Meletis, K, Siegle, JH, Cardin, JA, Futai, K, Vierlin-Claassen, D, Ruhlmann, C, Jones, SR, Deisseroth, K, Moore, CI, & Tsai, L-H. 2012. A critical role for NMDA receptors in parvalbumin interneurons for gamma rhythm induction and behavior. *Molecular Psychiatry*, **17**, 537–548.

-
- Carless, MA, Glahn, DC, Johnson, MP, Curran, JE, Bozaoglu, K, Dyer, TD, Winkler, AM, & Cole, SA. 2011. Impact of DISC1 variation on neuroanatomical and neurocognitive phenotypes. *Molecular Psychiatry*, **16**, 1096–1104.
- Carlisle, HJ, Luong, TN, Medina-marino, A, Schenker, L, Khorosheva, E, Indersmitten, T, Gunapala, KM, Steele, AD, O'Dell, TJ, Patterson, PH, & Kennedy, MB. 2011. Deletion of densin-180 results in abnormal behaviors associated with mental illness and reduces mGluR5 and DISC1 in the postsynaptic density fraction. *The Journal of Neuroscience*, **31**(45), 16194–16207.
- Carpenter, WT, & Koenig, JI. 2008. The evolution of drug development in schizophrenia: past issues and future opportunities. *Neuropsychopharmacology*, **33**, 2061–2079.
- Carter, CS, Barch, DM, Buchanan, RW, Bullmore, E, Krystal, JH, Cohen, J, Geyer, M, Green, M, Nuechterlein, KH, Robbins, T, Silverstein, S, Smith, EE, Strauss, M, Wykes, T, & Heinssen, R. 2008. Identifying cognitive mechanisms targeted for treatment development in schizophrenia: an overview of the first meeting of the cognitive neuroscience treatment research to improve cognition in schizophrenia initiative. *Biological Psychiatry*, **64**, 4–10.
- Castner, SA, Goldman-Rakic, PS, & Williams, GV. 2004. Animal models of working memory: insights for targeting cognitive dysfunction in schizophrenia. *Psychopharmacology*, **174**(1), 111–25.
- Chang, MC, Park, JM, Pelkey, KA, Grabenstatter, HL, Xu, D, Linden, DJ, Sutula, TP, Mcbain, CJ, & Worley, PF. 2010. Narp regulates homeostatic scaling of excitatory synapses on parvalbumin-expressing interneurons. *Nature Neuroscience*, **13**(9), 1090–1097.
- Chen, CA, Stanford, AD, Mao, X, Abi-dargham, A, Shungu, DC, Lisanby, H, Schroeder, CE, & Kegeles, LS. 2014. GABA level, gamma oscillation, and working memory performance in schizophrenia. *NeuroImage: Clinical*, **4**, 531–539.
- Chittajallu, R, & Isaac, JTR. 2010. Emergence of cortical inhibition by coordinated sensory-driven plasticity at distinct synaptic loci. *Nature Neuroscience*, **13**(10), 1240–1248.
- Cho, J-H, Deisseroth, K, & Bolshakov, VY. 2013. Synaptic encoding of fear extinction in mPFC-amygdala circuits. *Neuron*, **80**, 1491–1507.
- Cho, RY, Konecky, RO, & Carter, CS. 2006. Impairments in frontal cortical gamma synchrony and cognitive control in schizophrenia. *Proc. Natl. Acad. Sci. USA*, **103**(52), 19878–19883.
- Chubb, JE, Bradshaw, NJ, Soares, DC, Porteous, DJ, & Millar, JK. 2008. The DISC locus in psychiatric illness. *Molecular Psychiatry*, **13**(Jan.), 36–64.
- Chun, S, Westmoreland, J, Bayazitov, I, Eddins, D, Pani, AK, Smeyne, RJ, Yu, J, Blundon, JA, & Zakharenko, SS. 2014. Specific disruption of thalamic inputs to the auditory cortex in schizophrenia models. *Science*, **344**(6188), 1178–1182.
- Churchill, L, Zahm, DS, & Kalivas, PW. 1996. The mediodorsal nucleus of the thalamus in rats- I. forebrain GABAergic innervation. *Neuroscience*, **70**(1), 93–102.
- Clapcote, SJ, Lipina, TV, Millar, JK, Mackie, S, Christie, S, Ogawa, F, Lerch, JP, Trimble, K, Uchiyama, M, Sakuraba, Y, Kaneda, H, Shiroishi, T, Houslay, MD, Henkelman, RM, Sled, JG, Gondo, Y, Porteous, DJ, & Roder, JC. 2007. Behavioral phenotypes of Disc1 missense mutations in mice. *Neuron*, **54**, 387–402.

-
- Consortium. 2009. Common variants conferring risk of schizophrenia. *Nature*, **460**(6), 744–748.
- Consortium, Cross-Disorder Group of the Psychiatric Genomics. 2013. Identification of risk loci with shared effects on five major psychiatric disorders: a genome-wide analysis. *Lancet*, **381**(9875), 1371–1379.
- Cross, Laura, Brown, Malcolm W, Aggleton, John P, & Warburton, E Clea. 2013. The medial dorsal thalamic nucleus and the medial prefrontal cortex of the rat function together to support associative recognition and recency but not item recognition. *Learning & Memory*, 41 –50.
- Cruikshank, SJ, Lewis, TJ, & Connors, BW. 2007. Synaptic basis for intense thalamocortical activation of feedforward inhibitory cells in neocortex. *Nature Neuroscience*, **10**(4), 462–468.
- Cruikshank, SJ, Urabe, H, Nurmikko, AV, & Connors, BW. 2010. Pathway-specific feedforward circuits between thalamus and neocortex revealed by selective optical stimulation of axons. *Neuron*, **65**(Jan.), 230–45.
- Cruikshank, SJ, Ahmed, OJ, Stevens, TR, Patrick, SL, Gonzalez, AN, Elmaleh, M, & Connors, BW. 2012. Thalamic control of layer 1 circuits in prefrontal cortex. *The Journal of Neuroscience*, **32**(49), 17813–17823.
- Cunningham, MG, Bhattacharyya, S, & Benes, FM. 2008. Increasing interaction of amygdalar afferents with GABAergic interneurons between birth and adulthood. *Cerebral Cortex*, **18**, 1529–1535.
- Curley, AA, Arion, D, Volk, DW, Asafu-adjei, JK, Sampson, AR, Fish, KN, & Lewis, DA. 2011. Cortical deficits of glutamic acid decarboxylase 67 expression in schizophrenia: clinical, protein, and cell type-specific features. *Am J Psychiatry*, **168**, 921–929.
- Cuthbert, BN, & Insel, TR. 2013. Toward the future of psychiatric diagnosis: the seven pillars of RDoC. *BMC Medicine*, **11**(126), 1–8.
- Danos, P, Schmidt, A, Baumann, B, Bernstein, H-G, Northoff, G, Stauch, R, Krell, D, & Bogerts, B. 2005. Volume and neuron number of the mediodorsal thalamic nucleus in schizophrenia: a replication study. *Psychiatry Research: Neuroimaging*, **140**, 281 – 289.
- Davies, EJ. 2007. Developmental aspects of schizophrenia and related disorders: possible implications for treatment strategies. *Advances in Psychiatric Treatment*, **13**, 384–391.
- Daw, Michael I, Ashby, Michael C, & Isaac, John T R. 2007. Coordinated developmental recruitment of latent fast spiking interneurons in layer IV barrel cortex. *Nature neuroscience*, **10**(4), 453–61.
- DeFelipe, J, & Farinas, I. 1992. The pyramidal neuron of the cerebral cortex: morphological and chemical characteristics of the synaptic inputs. *Prog Neurobiol*, **39**, 563–607.
- Deidda, G, Bozarth, IF, & Cancedda, L. 2014. Modulation of GABAergic transmission in development and neurodevelopmental disorders: investigating physiology and pathology to gain therapeutic perspectives. *Frontiers in Cellular Neuroscience*, **8**(May), 1–23.
- del Rio, JA, de Lecea, L, Ferrer, I, & Soriano, E. 1994. The development of parvalbumin-immunoreactivity in the neocortex of the mouse. *Brain Res Dev Brain Res.*, **81**(2), 247–259.

-
- Diamond, ME, Armstrong-James, M, Budway, MJ, & Ebner, FF. 1992. Somatic sensory responses in the rostral sector of the posterior group (POm) and in the ventral posterior medial nucleus (VPM) of the rat thalamus: dependence on the barrel field cortex. *The Journal of Comparative Neurology*, **319**, 66–84.
- Divac, I. 1993. Cortical projections of the thalamic mediodorsal nucleus in the rat. Definition of the prefrontal cortex. *Acta Neurobiol. Exp.*, **53**, 425–429.
- Dobrunz, LE, & Stevens, CF. 1997. Heterogeneity of release probability, facilitation, and depletion at central synapses. *Cell*, **18**, 995–1008.
- Doischer, D, Hosp, JA, Yanagawa, Y, Obata, K, Jonas, P, Vida, I, & Bartos, M. 2008. Postnatal differentiation of basket cells from slow to fast signaling devices. *The Journal of Neuroscience*, **28**(48), 12956–12968.
- Duan, X, Chang, JH, Ge, S, Faulkner, RL, Kim, JY, Kitabatake, Y, Liu, X-B, Yang, C-H, Jordan, JD, Ma, DK, Liu, CY, Ganesan, S, Cheng, H-J, Ming, G-L, Lu, B, & Song, H. 2007. Disrupted-In-Schizophrenia 1 regulates integration of newly generated neurons in the adult brain. *Cell*, **130**(Sept.), 1146–58.
- Duff, BJ, Macritchie, KAN, Moorhead, TWJ, Lawrie, SM, & Blackwood, DHR. 2013. Human brain imaging studies of DISC1 in schizophrenia, bipolar disorder and depression: A systematic review. *Schizophrenia Research*, **147**, 1–13.
- Eggermann, E, & Jonas, P. 2011. release in nanodomain-coupling regimes. *Nature Neuroscience*, **15**(1), 20–22.
- Ekelund, J, Hennah, W, Hiekkalinna, T, Parker, A, Meyer, J, Lonnqvist, J, & Peltonen, L. 2004. Replication of 1q42 linkage in Finnish schizophrenia pedigrees. *Molecular Psychiatry*, **9**, 1037–1041.
- Engel, AK, & Singer, W. 2001. Temporal binding and the neural correlates of sensory awareness. *Trends in Cognitive Sciences*, **5**(1), 10749–10753.
- Enomoto, A, Asai, N, Namba, T, Wang, Y, Kato, T, Tanaka, M, Tatsumi, H, Taya, S, Tsuboi, D, Kuroda, K, Kaneko, N, Sawamoto, K, Miyamoto, R, Jijiwa, M, Murakumo, Y, Sokabe, M, Seki, T, & Kaibuchi, K. 2009. Roles of Disrupted-In-Schizophrenia 1-interacting protein girdin in postnatal development of the dentate gyrus. *Neuron*, **63**, 774–787.
- Enomoto, T, Tse, MT, & Floresco, SB. 2011. Reducing prefrontal gamma-aminobutyric acid activity induces cognitive, behavioral, and dopaminergic abnormalities that resemble schizophrenia. *Biological Psychiatry*, **69**, 432–441.
- Erlenmeyer-Kimling, L, Rock, D, Roberts, SA, Janal, M, Kestenbaum, C, Cornblatt, B, Adamo, UH, & Gottesman, II. 2000. Attention, memory, and motor skills as childhood predictors of schizophrenia-related psychoses: the New York high-risk project. *Am J Psychiatry*, **157**, 1416–1422.
- Fair, DA, Bathula, D, Mills, KL, Costa Dias, TG, Blythe, MS, Zhang, D, Snyder, AZ, Raichel, ME, Stevens, AA, Nigg, JT, & Nagel, BJ. 2010. Maturing thalamocortical functional connectivity across development. *Frontiers in Systems Neuroscience*, **4**(10), 1–10.
- Fatemi, SH, & Folsom, TD. 2009. The neurodevelopmental hypothesis of schizophrenia, revisited. *Schizophrenia Bulletin*, **35**(3), 528–548.

-
- Flores, R, Hirota, Y, Armstrong, B, Sawa, A, & Tomoda, T. 2011. DISC1 regulates synaptic vesicle transport via a lithium-sensitive pathway. *Neuroscience Research*, **71**, 71–77.
- Floresco, SB, & Grace, AA. 2003. Gating of hippocampal-evoked activity in prefrontal cortical neurons by inputs from the mediodorsal thalamus and ventral tegmental area. *The Journal of Neuroscience*, **23**(9), 3930–3943.
- Floresco, SB, Braaksma, DN, & Phillips, AG. 1999. Thalamic-cortical-striatal circuitry subserves working memory during delayed responding on a radial arm maze. *The Journal of Neuroscience*, **19**(24), 11061–11071.
- Fornito, A, Yucel, M, Dean, B, Wood, SJ, & Pantelis, C. 2009. Anatomical abnormalities of the anterior cingulate cortex in schizophrenia: bridging the gap between neuroimaging and neuropathology. *Schizophrenia Bulletin*, **35**(5), 973–993.
- Funahashi, S, Bruce, CJ, & Goldman-Rakic, PS. 1989. Mnemonic coding of visual space in the monkeys dorsolateral prefrontal cortex. *Journal of Neurophysiology*, **61**(2), 331–349.
- Funahashi, S, Takeda, K, & Watanabe, Y. 2004. Neural mechanisms of spatial working memory : Contributions of the dorsolateral prefrontal cortex and the thalamic mediodorsal nucleus. *Cognitive, Affective, & Behavioral Neuroscience*, **4**(4), 409–420.
- Gabbott, P, Headlam, A, & Busby, S. 2002. Morphological evidence that CA1 hippocampal afferents monosynaptically innervate PV-containing neurons and NADPH-diaphorase reactive cells in the medial prefrontal cortex (Areas 25/32) of the rat. *Brain Research*, **946**, 314–322.
- Gabbott, PLA, Warner, TA, & Busby, SJ. 2006. Amygdala input monosynaptically innervates parvalbumin immunoreactive local circuit neurons in rat medial prefrontal cortex. *Neuroscience*, **139**(Jan.), 1039–48.
- Gabernet, L, Jadhav, SP, Feldman, DE, Carandini, M, & Scanziani, M. 2005. Somatosensory integration controlled by dynamic thalamocortical feed-forward inhibition. *Neuron*, **48**, 315–327.
- Gao, W-J, Wang, Y, & Goldman-Rakic, PS. 2003. Dopamine modulation of perisomatic and peridendritic inhibition in prefrontal cortex. *The Journal of Neuroscience*, **23**(5), 1622–1630.
- Gaser, C, Nenadic, I, Hazlett, EA, & Buchsbaum, MS. 2004. Ventricular enlargement in schizophrenia related to volume reduction of the thalamus, striatum, and superior temporal cortex. *Am J Psychiatry*, **161**, 154–156.
- Gentet, LJ, Kremer, Y, Taniguchi, H, Huang, ZJ, Staiger, JF, & Petersen, CCH. 2012. Unique functional properties of somatostatin-expressing GABAergic neurons in mouse barrel cortex. *Nature Neuroscience*, **15**(4), 607–612.
- Gigg, J, Tan, AM, & Finch, DM. 1994. Glutamatergic hippocampal formation projections to prefrontal cortex in the rat are regulated by GABAergic inhibition and show convergence with glutamatergic projections from the limbic thalamus. *Hippocampus*, **4**(2), 189–198.
- Gil, Z, & Amitai, Y. 1996. Properties of convergent thalamocortical and intracortical synaptic potentials in single neurons of neocortex. *The Journal of Neuroscience*, **16**(20), 6567–6578.
- Goldman-Rakic, PS, & Selemon, LD. 1997. Functional and anatomical aspects of prefrontal pathology in schizophrenia. *Schizophrenia Bulletin*, 437–458.

-
- González-burgos, G, Krimer, LS, Povysheva, NV, Barrionuevo, G, & Lewis, David A. 2005. Functional properties of fast spiking interneurons and their synaptic connections with pyramidal cells in primate dorsolateral prefrontal cortex. *Journal of Neurophysiology*, **93**, 942–953.
- Gonzalez-Burgos, G, Fish, KN, & Lewis, DA. 2011. GABA neuron alterations, cortical circuit dysfunction, and cognitive deficits in schizophrenia. *Neural Plasticity*, **2011**, 723184.
- Gordon, JA, & Moore, H. 2012. Charting a course toward an understanding of schizophrenia. *Neuron*, **76**, 465–467.
- Gottesman, II, & Gould, TD. 2003. The endophenotype concept in psychiatry: etymology and strategic intentions. *Am J Psychiatry*, **160**, 636–645.
- Gradinaru, Viviana, Zhang, Feng, Ramakrishnan, Charu, Mattis, Joanna, Prakash, Rohit, Diester, Ilka, Goshen, Inbal, Thompson, Kimberly R, & Deisseroth, Karl. 2010. Molecular and cellular approaches for diversifying and extending optogenetics. *Cell*, **141**(1), 154–165.
- Green, MF, Kern, RS, Braff, DL, & Mintz, J. 2000. Neurocognitive deficits and functional outcome in schizophrenia: are we measuring the "right stuff"? *Schizophrenia bulletin*, **26**(1), 119–36.
- Groenewegen, HJ. 1988. Organization of the afferent connections of the mediodorsal thalamic nucleus in rat, related to the mediodorsal-prefrontal topography. *Neuroscience*, **24**(2), 379–431.
- Guillery, RW. 2003. Branching thalamic afferents link action and perception. *Journal of Neurophysiology*, **90**, 539–548.
- Haenschel, C, Bittner, RA, Waltz, J, Haertling, F, Wibrall, M, Singer, W, Linden, DEJ, & Rodriguez, E. 2009. Cortical oscillatory activity is critical for working memory as revealed by deficits in early-onset schizophrenia. *The Journal of Neuroscience*, **29**(30), 9481–9489.
- Han, J, Lee, JH, Kim, MJ, & Jung, MW. 2013. Neural activity in mediodorsal nucleus of thalamus in rats performing a working memory task. *Frontiers in Neural Circuits*, **7**, 1–10.
- Hannesson, DK, Howland, JG, & Phillips, AG. 2004. Interaction between perirhinal and medial prefrontal cortex is required for temporal order but not recognition memory for objects in rats. *The Journal of Neuroscience*, **24**(19), 4596 – 4604.
- Hashimoto, T, Volk, DW, Eggan, SM, Mirnics, K, Pierri, JN, Sun, Z, Sampson, AR, & Lewis, DA. 2003. Gene expression deficits in a subclass of GABA neurons in the prefrontal cortex of subjects with schizophrenia. *The Journal of Neuroscience*, **23**(15), 6315– 6326.
- Hashimoto, T, Arion, D, Unger, T, Maldonado-Aviles, JG, Morris, HM, Volk, DW, Mirnics, K, & Lewis, DA. 2008. Alterations in GABA-related transcriptome in the dorsolateral prefrontal cortex of subjects with schizophrenia. *Molecular Psychiatry*, **13**, 147–161.
- Hattori, T, Shimizu, S, Koyama, Y, Yamada, K, Kuwahara, R, Kumamoto, N, Matsuzaki, S, Ito, a, Katayama, T, & Tohyama, M. 2010. DISC1 regulates cell-cell adhesion, cell-matrix adhesion and neurite outgrowth. *Molecular psychiatry*, May, 1–12.
- Hayashi-Takagi, A, Takaki, M, Graziane, N, Seshadri, S, Murdoch, H, Dunlop, AJ, Makino, Y, Seshadri, AJ, Ishizuka, K, Srivastava, DP, Xie, Z, Baraban, JM, Houslay, MD, Tomoda, T, Brandon, NJ, Kamiya, A, Yan, Z, Penzes, P, & Sawa, A. 2010. Disrupted-in-Schizophrenia

-
- 1 (DISC1) regulates spines of the glutamate synapse via Rac1. *Nature Neuroscience*, **13**(3), 327–32.
- Hayes, RD, Chang, C-K, Fernandes, AC, Begum, A, To, D, Broadbent, M, Hotopf, M, & Stewart, R. 2012. Functional status and all-cause mortality in serious mental illness. *Plos One*, **7**(9), 1–9.
- Heckers, S. 1997. Neuropathology of schizophrenia: cortex, thalamus, basal ganglia, and neurotransmitter-specific projection systems. *Schizophrenia Bulletin*, **23**(3), 403–421.
- Hefft, S, & Jonas, P. 2005. Asynchronous GABA release generates long-lasting inhibition at a hippocampal interneuron-principal neuron synapse. *Nature Neuroscience*, **8**(10), 1319–1328.
- Heidbreder, CA, & Groenewegen, HJ. 2003. The medial prefrontal cortex in the rat: evidence for a dorso-ventral distinction based upon functional and anatomical characteristics. *Neuroscience and Biobehavioral Reviews*, **27**, 555–579.
- Hennah, W, Paunio, T, Ekelund, J, Varilo, T, Partonen, T, & Cannon, TD. 2005. A haplotype within the DISC1 gene is associated with visual memory functions in families with a high density of schizophrenia. *Molecular Psychiatry*, **10**, 1097–1103.
- Hensch, TK. 2005. Critical period plasticity in local cortical circuits. *Nature Reviews Neuroscience*, **6**(Nov.), 877–88.
- Herry, C, & Garcia, R. 2002. Prefrontal cortex long-term potentiation, but not long-term depression, is associated with the maintenance of extinction of learned fear in mice. *The Journal of Neuroscience*, **22**(2), 577–583.
- Hikida, T, Jaaro-peled, H, Seshadri, S, Oishi, K, Hookway, C, Kong, S, Wu, D, Xue, R, Andrade, M, Tankou, S, Mori, S, Gallagher, M, Ishizuka, K, Pletnikov, M, Kida, S, & Sawa, A. 2007. Dominant-negative DISC1 transgenic mice display schizophrenia-associated phenotypes detected by measures translatable to humans. *Proc. Natl. Acad. Sci. USA*, **104**(36), 14501–14506.
- Hippenmeyer, S, Vrieseling, E, Sigrist, M, Portmann, T, Laengle, C, Ladle, DR, & Arber, S. 2005. A developmental switch in the response of DRG neurons to ETS transcription factor signaling. *PLoS Biology*, **3**(5), 878–890.
- Holley, SM, Wang, EA, Cepeda, C, Jentsch, JD, Ross, CA, Pletnikov, MV, & Levine, MS. 2013. Frontal cortical synaptic communication is abnormal in Disc1 genetic mouse models of schizophrenia. *Schizophrenia Research*, **146**, 264–272.
- Hooks, BM, Mao, T, Gutnisky, D, Yamawaki, N, Svoboda, K, & Shepherd, G. 2013. Organization of cortical and thalamic input to pyramidal neurons in mouse motor cortex. *Journal of Neuroscience*, **33**(2), 748–760.
- Hor, K, & Taylor, M. 2010. Suicide and schizophrenia: a systematic review of rates and risk factors. *Journal of Psychopharmacology*, **24**(11), 81–90.
- Howard, Al, Tamas, G, & Soltesz, I. 2005. Lighting the chandelier: new vistas for axo-axonic cells. *Trends in Neurosciences*, **28**(6), 310–316.
- Howard, MW, Rizzuto, DS, Caplan, JB, Madsen, JR, Lisman, J, Aschenbrenner-Scheibe, R, Schulze-Bonhage, A, & Kahana, MJ. 2003. Gamma oscillations correlate with working memory load in humans. *Cerebral Cortex*, **13**, 1369–1374.

-
- Hugues, S, & Garcia, R. 2007. Reorganization of learning-associated prefrontal synaptic plasticity between the recall of recent and remote fear extinction memory. *Learning & Memory*, **14**, 520–524.
- Ibi, D, Nagai, T, Koike, H, Kitahara, Y, Mizoguchi, H, Niwa, M, Jaaro-peled, H, Nitta, A, Yoneda, Y, Nabeshima, T, Sawa, A, & Yamada, K. 2010. Combined effect of neonatal immune activation and mutant DISC1 on phenotypic changes in adulthood. *Behavioural Brain Research*, **206**, 32–37.
- Insel, TR. 2010. Rethinking schizophrenia. *Nature*, **468**(7321), 187–193.
- Ishizuka, K, Kamiya, A, Oh, EC, Kanki, H, Seshadri, S, Robinson, JF, Murdoch, H, Dunlop, AJ, Kubo, K-I, Furukori, K, Huang, B, Zeledon, M, Hayashi-Takagi, A, Okano, H, Nakajima, K, Houslay, MD, Katsanis, N, & Sawa, A. 2011. DISC1-dependent switch from progenitor proliferation to migration in the developing cortex. *Nature*, **473**(Apr.), 92–96.
- Jaaro-peled, H, Hayashi-takagi, A, Seshadri, S, Kamiya, A, Brandon, NJ, & Sawa, A. 2009. Neurodevelopmental mechanisms of schizophrenia: understanding disturbed postnatal brain maturation through neuregulin-1-ErbB4 and DISC1. *Trends in Neurosciences*, **32**(9), 485–495.
- Jacobs, PA, Brunton, M, Frackiewicz, A, Newton, M, Cook, PJJ, & Robson, EB. 1970. Studies on a family with three cytogenetic markers. *Ann. Hum. Genet., London*, **33**, 325–336.
- James, R, Adams, RR, Christie, S, Buchanan, SR, Porteous, DJ, & Millar, JK. 2004. Disrupted in Schizophrenia 1 (DISC1) is a multicompartimentalized protein that predominantly localizes to mitochondria. *Molecular and Cellular Neuroscience*, **26**, 112 – 122.
- Jiang, Z, Cowell, RM, & Nakazawa, K. 2013. Convergence of genetic and environmental factors on parvalbumin-positive interneurons in schizophrenia. *Frontiers in Behavioral Neuroscience*, **7**, 1–18.
- Jiao, Y, Zhang, C, Yanagawa, Y, & Sun, Q-Q. 2006. Major effects of sensory experiences on the neocortical inhibitory circuits. *The Journal of Neuroscience*, **26**(34), 8691– 8701.
- Jung, WH, Kim, JS, Jang, JH, Choi, J-S, Jung, MH, Park, J-Y, Han, JY, Choi, C-H, Kang, D-H, Chung, CK, & Kwon, JS. 2011. Cortical thickness reduction in individuals at ultra-high-risk for psychosis. *Schizophrenia Bulletin*, **37**(4), 839–849.
- Kamiya, A, Kubo, K-I, Tomoda, T, Takaki, M, Youn, R, Ozeki, Y, Sawamura, N, Park, U, Kudo, C, Okawa, M, Ross, CA, Hatten, ME, Nakajima, K, & Sawa, A. 2005. A schizophrenia-associated mutation of DISC1 perturbs cerebral cortex development. *Nature Cell Biology*, **7**(12), 1167–78.
- Kanichay, RT, & Silver, RA. 2008. Synaptic and cellular properties of the feed-forward inhibitory circuit within the input layer of the cerebellar cortex. *The Journal of Neuroscience*, **28**(36), 8955–8967.
- Kawaguchi, Y. 1996. Physiological and morphological identification of Somatostatin-Vasoactive Intestinal Polypeptide-containing cells among GABAergic cell subtypes in rat frontal cortex. *The Journal of Neuroscience*, **76**(8), 2701–2715.
- Keefe, RSE, Bilder, RM, Davis, SM, Harvey, PD, Rosenheck, RA, Perkins, DO, Davis, CE, &

-
- Hsiao, JK. 2007. Neurocognitive effects of antipsychotic medications in patients With chronic schizophrenia in the CATIE trial. *Arch Gen Psychiatry*, **64**, 633–647.
- Kellendonk, C, Simpson, EH, & Kandel, ER. 2009. Modeling cognitive endophenotypes of schizophrenia in mice. *Trends in Neurosciences*, **32**(6), 347–358.
- Kelly, C, & McCreddie, R. 2000. Cigarette smoking and schizophrenia. *Advances in Psychiatric Treatment*, **6**, 327–331.
- Kim, JC, Cook, MN, Carey, MR, Shen, C, Regehr, WG, & Dymecki, SM. 2009. Neurotechnique linking genetically defined neurons to behavior through a broadly applicable silencing allele. *Neuron*, **63**(3), 305–315.
- Kirkpatrick, B, Xu, Leyan, Cascella, N, Ozeki, Y, Sawa, A, & Roberts, RC. 2006. DISC1 immunoreactivity at the light and ultrastructural level in the human neocortex. *The Journal of Comparative Neurology*, **497**, 436 – 450.
- Knickmeyer, RC, Wang, J, Zhu, H, Geng, X, Woolson, S, Hamer, RM, Konneker, T, Lin, W, Styner, M, & Gilmore, JH. 2013. Common variants in psychiatric risk genes predict brain structure at birth. *Cerebral Cortex*, **5**, 1230–46.
- Kobayashi, M, Koyanagi, Y, Yamamoto, K, Oi, Y, Koshikawa, N, & Kobayashi, M. 2010. Presynaptic interneuron subtype- and age-dependent modulation of GABAergic synaptic transmission by β -adrenoceptors in rat insular cortex. *Journal of Neurophysiology*, **103**, 2876–2888.
- Koike, H, Arguello, PA, Kvajo, M, Karayiorgou, M, & Gogos, JA. 2006. Disc1 is mutated in the 129S6 SvEv strain and modulates working memory in mice. *Proc. Natl. Acad. Sci. USA*, **103**(10), 3693–3697.
- Kopell, N, Ermentrout, GB, Whittington, MA, & Traub, RD. 1999. Gamma rhythms and beta rhythms have different synchronization properties. *Proc. Natl. Acad. Sci. USA*, **97**(4), 1867–1872.
- Korotkova, T, Fuchs, EC, Ponomarenko, A, von Engelhardt, J, & Monyer, H. 2010. NMDA receptor ablation on parvalbumin-positive interneurons impairs hippocampal synchrony, spatial representations, and working memory. *Neuron*, **68**(3), 557–569.
- Kremen, WS, Vinogradov, S, Poole, JH, Schaefer, CA, Deicken, RF, Factor-Litvak, P, & Brown, AS. 2010. Cognitive decline in schizophrenia from childhood to midlife: A 33-year longitudinal birth cohort study. *Schizophrenia Research*, **118**(1-3), 1–5.
- Kubo, K-I, Tomita, K, Uto, A, Kuroda, K, Seshadri, S, Cohen, J, Kaibuchi, K, Kamiya, A, & Nakajima, K. 2010. Migration defects by DISC1 knockdown in C57BL/6, 129X1/SvJ, and ICR strains via in utero gene transfer and virus-mediated RNAi. *Biochemical and biophysical research communications*, **400**(4), 631–7.
- Kuhlman, SH, & Huang, ZJ. 2008. High-resolution labeling and functional manipulation of specific neuron types in mouse brain by Cre-activated viral gene expression. *Plos One*, **3**(4), 1–11.
- Kuroda, K, Yamada, S, Tanaka, M, Iizuka, M, Yano, H, Mori, D, Tsuboi, D, Nishioka, T, Namba, T, Iizuka, Y, Kubota, S, Nagai, T, Ibi, D, Wang, R, Enomoto, A, Isotani-sakakibara, M, Asai, N, Kimura, K, Kiyonari, H, Abe, T, Mizoguchi, A, Sokabe, M, Takahashi, M, &

-
- Yamada, K. 2011. Behavioral alterations associated with targeted disruption of exons 2 and 3 of the *Disc1* gene in the mouse. *Human Molecular Genetics*, **20**(23), 4666–4683.
- Kuroda, M, & Price, JL. 1991a. Synaptic organization of projections from basal forebrain structures to the mediodorsal thalamic nucleus of the rat. *Journal of Comparative Neurology*, **303**(4), 513–533.
- Kuroda, M, & Price, JL. 1991b. Ultrastructural and synaptic organization of brainstem structures to the mediodorsal thalamic nucleus of the rat. *Journal of Comparative Neurology*, **313**(3), 539–552.
- Kuroda, M, Murakami, K, Oda, S, Shinkai, M, & Kishi, Kiyoshi. 1993. Direct synaptic connections between thalamocortical axon terminals for the mediodorsal thalamic nucleus (MD) and corticothalamic neurons to MD in the prefrontal cortex. *Brain Research*, **612**(1-2), 339–344.
- Kuroda, M, Murakami, K, Shinkai, M, Ojima, H, & Kishi, K. 1995a. Electron microscopic evidence that axon terminals from the mediodorsal thalamic nucleus make direct synaptic contacts with callosal cells in the prelimbic cortex of the rat. *Brain Research*, **677**, 348–353.
- Kuroda, M, Murakami, K, Kishi, K, & Price, JL. 1995b. Thalamocortical synapses between axons from the mediodorsal thalamic nucleus and pyramidal cells in the prelimbic cortex of the rat. *Journal of Comparative Neurology*, 143–151.
- Kuroda, M, Yokofujita, J, & Murakami, K. 1998. An ultrastructural study of the neural circuit between prefrontal cortex and the mediodorsal nucleus of the thalamus. *Progress in Neurobiology*, **54**(97), 417–458.
- Kuroda, M, Yokofujita, J, Oda, S, & Price, JL. 2004. Synaptic relationships between axon terminals from the mediodorsal thalamic nucleus and gamma-aminobutyric acidergic cortical cells in the prelimbic cortex of the rat. *Journal of Comparative Neurology*, **477**, 220–234.
- Kuroda, Masaru, Ojima, Hisayuki, Igarashi, Hiroaki, Murakami, Kunio, & Okada, Akiko. 1996. Synaptic relationships between axon terminals from the mediodorsal thalamic nucleus and layer III pyramidal cells in the prelimbic cortex of the rat. *Brain Research*, **708**, 185–190.
- Kvajo, M, McKellar, H, Arguello, PA, Drew, LJ, Moore, H, MacDermott, AB, Karayiorgou, M, & Gogos, JA. 2008. A mutation in mouse *Disc1* that models a schizophrenia risk allele leads to specific alterations in neuronal architecture and cognition. *Proc. Natl. Acad. Sci. USA*, **105**(19), 7076–81.
- Kvajo, M, McKellar, H, Drew, LJ, Lepagnol-bestel, A-M, Xiao, L, Levy, RL, Blazeki, R, Arguello, PA, Lacefield, CO, Mason, CA, Simonneau, M, O'Donnell, JM, MacDermott, AB, Karayiorgou, M, & Gogos, JA. 2011. Altered axonal targeting and short-term plasticity in the hippocampus of *Disc1* mutant mice. *Proc. Natl. Acad. Sci. USA*, **108**(49), 1349–58.
- Lavin, A, & Grace, AA. 1998. Dopamine modulates the responsivity of mediodorsal thalamic cells recorded in vitro. *The Journal of Neuroscience*, **18**(24), 10566–10578.
- Lee, AT, Gee, SM, Vogt, D, Patel, T, Rubenstein, JL, & Sohal, VS. 2014. Pyramidal neurons in prefrontal cortex receive subtype-specific forms of excitation and inhibition. *Neuron*, **81**(1), 61–8.
- Lee, FHF, Fadel, MP, Preston-Maher, K, Cordes, SP, Clapcote, SJ, Price, DJ, Roder, JC, &

-
- Wong, AHC. 2011. Disc1 point mutations in mice affect development of the cerebral cortex. *The Journal of Neuroscience*, **31**(9), 3197–3206.
- Lee, FHF, Zai, CC, Cordes, SP, Roder, JC, & Wong, AHC. 2013a. Abnormal interneuron development in disrupted-in-schizophrenia-1 L100P mutant mice. *Molecular Brain*, **6**(20), 1–10.
- Lee, Soohyun, Kruglikov, Ilya, Huang, Z Josh, Fishell, Gord, & Rudy, Bernardo. 2013b. A disinhibitory circuit mediates motor integration in the somatosensory cortex. *Nature Neuroscience*, **11**, 1–11.
- Lesh, TA, Niendam, TA, Minzenberg, MJ, & Carter, CS. 2010. Cognitive control deficits in schizophrenia: mechanisms and meaning. *Neuropsychopharmacology Reviews*, **36**(1), 316–338.
- Lewis, DA. 2009. Neuroplasticity of excitatory and inhibitory cortical circuits in schizophrenia. *Dialogues in Clinical Neuroscience*, **11**, 269–280.
- Lewis, DA, & Gonzalez-Burgos, G. 2008. Neuroplasticity of neocortical circuits in schizophrenia. *Neuropsychopharmacology*, **33**, 141–165.
- Lewis, DA, & Lieberman, JA. 2000. Catching up on schizophrenia: natural history and neurobiology. *Neuron*, **28**, 325–334.
- Lewis, DA, & Sweet, RA. 2009. Schizophrenia from a neural circuitry perspective: advancing toward rational pharmacological therapies. *The Journal of Clinical Investigation*, **119**(4), 706–716.
- Lewis, DA, Hashimoto, T, & Volk, DW. 2005. Cortical inhibitory neurons and schizophrenia. *Nature Reviews Neuroscience*, **6**(4), 312–24.
- Lewis, DA, Curley, AA, Glausier, JR, & Volk, DW. 2012. Cortical parvalbumin interneurons and cognitive dysfunction in schizophrenia. *Trends in Neurosciences*, **35**(1), 57–67.
- Li, H, Penzo, MA, Taniguchi, H, Kopec, CD, Huang, ZJ, & Li, B. 2013. Experience-dependent modification of a central amygdala fear circuit. *Nature Neuroscience*, **16**(3), 332–339.
- Li, W, Zhou, Y, Jentsch, JD, Brown, RM, Tian, X, Ehninger, D, Hennah, W, Peltonen, L, Lönnqvist, J, Huttunen, MO, Kaprio, J, Trachtenberg, JT, Silva, AJ, & Cannon, TD. 2007. Specific developmental disruption of disrupted-in-schizophrenia-1 function results in schizophrenia-related phenotypes in mice. *Proc. Natl. Acad. Sci. USA*, **104**(46), 18280–5.
- Lien, AD, & Scanziani, M. 2013. Tuned thalamic excitation is amplified by visual cortical circuits. *Nature Neuroscience*, **16**(9), 1315–1323.
- Lipina, TV, Niwa, M, Fletcher, PJ, Seeman, P, Sawa, A, & Roder, JC. 2010. Enhanced dopamine function in DISC1-L100P mutant mice: implications for schizophrenia. *Genes, Brain, and Behavior*, **9**, 777–789.
- Lipska, Barbara K, Peters, Tricia, Hyde, Thomas M, Halim, Nader, Horowitz, Cara, Mitkus, Shruti, Weickert, Cynthia Shannon, Matsumoto, Mitsuyuki, Sawa, Akira, Straub, Richard E, Vakkalanka, Radhakrishna, Herman, Mary M, Weinberger, Daniel R, & Kleinman, Joel E. 2006. Expression of DISC1 binding partners is reduced in schizophrenia and associated with DISC1 SNPs. *Access*, **15**(8), 1245–1258.

-
- Liu, B, Fan, L, Cui, Y, Zhang, X, Hou, B, Li, Y, Qin, W, Wang, D, Yu, C, & Jang, T. 2013. DISC1 Ser704Cys impacts thalamic-prefrontal connectivity. *Brain Structure Function*, 1–10.
- Lodge, Daniel J, Behrens, Margarita M, & Grace, Anthony A. 2009. A loss of parvalbumin-containing interneurons is associated with diminished oscillatory activity in an animal model of schizophrenia. *The Journal of Neuroscience*, **29**(8), 2344–2354.
- Lodge, DJ, & Grace, AA. 2010. Hippocampal dysfunction and disruption of dopamine system regulation in an animal model of schizophrenia. *Neurotox. Res.*, **14**, 97–104.
- Low, NC, & Hardy, J. 2007. What is a schizophrenic mouse? *Neuron*, **54**, 348–349.
- Ma, W-P, Liu, B-H, Li, Y-T, Huang, ZJ, Zhang, LI, & Tao, HW. 2010. Visual representations by cortical somatostatin inhibitory neurons selective but with weak and delayed responses. *The Journal of Neuroscience*, **30**(43), 14371–14379.
- Ma, Y, Hu, H, & Agmon, A. 2012. Short-term plasticity of unitary inhibitory-to-inhibitory synapses depends on presynaptic interneuron subtype. *The Journal of Neuroscience*, **32**(3), 983–988.
- Madisen, L, Zwingman, TA, Sunkin, SM, Oh, SW, Zariwala, HA, Gu, H, Ng, LL, Palmiter, RD, Hawrylycz, MJ, Jones, AR, Lein, ES, & Zeng, H. 2010. A robust and high-throughput Cre reporting and characterization system for the whole mouse brain. *Nature Neuroscience*, **13**(1), 133–140.
- Maher, BJ, & Loturco, JJ. 2012. Disrupted-in-Schizophrenia (DISC1) functions presynaptically at glutamatergic synapses. *Plos One*, **7**(3), 1–9.
- Manoach, DS. 2003. Prefrontal cortex dysfunction during working memory performance in schizophrenia: reconciling discrepant findings. *Schizophrenia Research*, **60**, 285 – 298.
- Manseau, F, Marinelli, S, Mendez, P, Schwaller, B, Prince, DA, Huguenard, JR, & Bacci, A. 2010. Desynchronization of neocortical networks by asynchronous release of GABA at autaptic and synaptic contacts from fast-spiking interneurons. *Plos Biology*, **8**(9), 1–16.
- Mao, Y, Ge, X, Frank, CL, Madison, JM, Koehler, AN, Doud, MK, Tassa, C, Berry, EM, Soda, T, Singh, KK, Biechele, T, Petryshen, TL, Moon, RT, Haggarty, SJ, & Tsai, L-H. 2009. Disrupted in schizophrenia 1 regulates neuronal progenitor proliferation via modulation of GSK3beta/beta-catenin signaling. *Cell*, **136**(6), 1017–31.
- Marenco, S, Stein, JL, Savostyanova, AA, Sambataro, F, Tan, H-Y, Goldman, AL, Verchinski, BA, Barnett, AS, Dickinson, D, Callicott, JH, Meyer-lindenberg, A, & Weinberger, DR. 2012. Investigation of anatomical thalamo-cortical connectivity and fMRI activation in schizophrenia. *Neuropsychopharmacology*, **37**, 499–507.
- Marín, Oscar. 2012. Interneuron dysfunction in psychiatric disorders. *Nature Reviews Neuroscience*, 107–120.
- Markram, H, Toledo-rodriguez, M, Wang, Y, & Gupta, A. 2004. Interneurons of the neocortical inhibitory system. *Nature Reviews Neuroscience*, **5**, 793–807.
- Mason, A, Nicoll, A, & Stratford, K. 1991. Synaptic transmission between individual pyramidal neurons of the rat visual cortex in vitro. *Journal of Neuroscience*, **11**(1), 72–84.

-
- Mata, I, Perez-Iglesias, R, Roiz-Santiañez, R, Tordesillas-Gutierrez, D, Gonzalez-Mandly, A, Berja, A, Vazquez-Barquero, JL, & Crespo-Facorro, B. 2010. Additive effect of NRG1 and DISC1 genes on lateral ventricle enlargement in first episode schizophrenia. *NeuroImage*, **53**(3), 1016–1022.
- Matyas, F, Lee, J, Shin, H-S, & Acsady, L. 2014. The fear circuit of the mouse forebrain: connections between the mediodorsal thalamus, frontal cortices and basolateral amygdala. *European Journal of Neuroscience*, **39**, 1810–1823.
- Mcintosh, AM, Job, DE, Moorhead, TWJ, Harrison, LK, Forrester, K, Lawrie, SM, & Johnstone, EC. 2004. Voxel-based morphometry of patients with schizophrenia or bipolar disorder and their unaffected relatives. *Biological Psychiatry*, **56**, 544–552.
- Meyer, KD, & Morris, JA. 2008. Immunohistochemical analysis of Disc1 expression in the developing and adult hippocampus. *Gene Expression Patterns*, **8**(7-8), 494–501.
- Meyer, KD, & Morris, JA. 2009. Disc1 regulates granule cell migration in the developing hippocampus. *Human Molecular Genetics*, **18**(17), 3286–3297.
- Millar, JK, Wilson-Annan, JC, Anderson, S, Christie, S, Taylor, MS, Semple, CA, Devon, RS, St Clair, D M, Muir, W J, Blackwood, D H, & Porteous, D J. 2000. Disruption of two novel genes by a translocation co-segregating with schizophrenia. *Human molecular genetics*, **9**(9), 1415–23.
- Millar, JK, Christie, S, & Porteous, DJ. 2003. Yeast two-hybrid screens implicate DISC1 in brain development and function. *Biochemical and Biophysical Research Communications*, **311**, 1019–1025.
- Millar, JK, Pickard, BS, Mackie, S, James, R, Christie, S, Buchanan, SR, Malloy, MP, Chubb, JE, Huston, E, Baillie, GS, Thomson, PA, Hill, EV, Brandon, NJ, Rain, J-C, Camargo, LM, Whiting, PM, Houslay, MD, Blackwood, DHR, Muir, WJ, & Porteous, DJ. 2005. DISC1 and PDE4B are interacting genetic factors in schizophrenia that regulate cAMP signaling. *Science*, **310**(Nov.), 1187–1191.
- Miller, KD, Pinto, DJ, & Simons, DJ. 2001. Processing in layer 4 of the neocortical circuit: new insights from visual and somatosensory cortex. *Current Opinion in Neurobiology*, **11**, 488–497.
- Minzenberg, Michael J, Firl, Alana J, Yoon, Jong H, Gomes, Glenn C, Reinking, Celeste, & Carter, Cameron S. 2010. Gamma oscillatory power is impaired during cognitive control independent of medication status in first-episode schizophrenia. *Neuropsychopharmacology*, **35**(13), 2590–2599.
- Minzenberg, MJ, Laird, AR, Thelen, S, Carter, CS, & Glahn, DC. 2009. Meta-analysis of 41 functional neuroimaging studies of executive function in schizophrenia. *Arch Gen Psychiatry*, **66**(8), 811–822.
- Mitchell, AS, & Chakraborty, S. 2013. What does the mediodorsal thalamus do? *Frontiers in Systems Neuroscience*, **7**, 1–19.
- Mitchell, AS, & Dalrymple-Alford, JC. 2005. Dissociable memory effects after medial thalamus lesions in the rat. *European Journal of Neuroscience*, **22**, 973–985.
- Mitchell, KJ. 2012. What is complex about complex disorders? *Genome Biology*, **13**(1), 1–11.

-
- Mitelman, SA, Byne, W, Kemether, EM, Hazlett, EA, & Buchsbaum, MS. 2005. Metabolic disconnection between the mediodorsal nucleus of the thalamus and cortical Brodmanns areas of the left hemisphere in schizophrenia. *Am J Psychiatry*, **162**, 1733–1735.
- Mittmann, Wolfgang, Koch, Ursula, & Michael, H. 2005. Feed-forward inhibition shapes the spike output of cerebellar Purkinje cells. *J Physiol*, **563**, 369–378.
- Miyoshi, K, Honda, A, Baba, K, Taniguchi, M, Oono, K, Fujita, T, Kuroda, S, & Katayama, T. 2003. Disrupted-In-Schizophrenia 1, a candidate gene for schizophrenia, participates in neurite outgrowth. *Molecular Psychiatry*, 685–694.
- Moriarty, O, Mcguire, BE, & Finn, DP. 2011. The effect of pain on cognitive function: a review of clinical and preclinical research. *Progress in Neurobiology*, **93**(3), 385–404.
- Morris, JA, Kandpal, G, Ma, L, & Austin, CP. 2003. DISC1 (Disrupted-In-Schizophrenia 1) is a centrosome-associated protein that interacts regulation and loss of interaction with mutation. *Human Molecular Genetics*, **12**(13), 1591–1608.
- Muller, M, Felmy, F, Schwaller, B, & Schneggenburger, R. 2007. Parvalbumin is a mobile presynaptic Ca²⁺ buffer in the calyx of Held that accelerates the decay of Ca²⁺ and short-term facilitation. *The Journal of Neuroscience*, **27**(9), 2261–2271.
- Murray, JD, Anticevic, A, Gancsos, M, Ichinose, M, Corlett, PR, Krystal, JH, & Wang, X-J. 2014. Linking microcircuit dysfunction to cognitive impairment: effects of disinhibition associated with schizophrenia in a cortical working memory model. *Cerebral Cortex*, **24**, 859–872.
- Myles-Worsley, M, & Park, S. 2002. Spatial working memory deficits in schizophrenia patients and their first degree relatives from Palau, Micronesia. *American Journal of Medical Genetics*, **114**, 609– 615.
- Nakata, K, Lipska, BK, Hyde, TM, Ye, T, Newburn, EN, Morita, Y, Vakkalanka, R, Barenboim, M, Sei, Y, Weinberger, DR, & Kleinman, JE. 2009. DISC1 splice variants are upregulated in schizophrenia and associated with risk polymorphisms. *Proc. Natl. Acad. Sci. USA*, **106**(37), 15873–15878.
- Niwa, M, Kamiya, A, Murai, R, Kubo, K, Grubor, AJ, Tomita, K, Lu, L, Tomisato, S, Jaaro-Peled, H, Seshadri, S, Hiyama, H, Huang, B, Kohda, K, Noda, Y, O'Donnell, P, Nakajima, K, Sawa, A, & Nabeshima, T. 2010. Knockdown of DISC1 by in utero gene transfer disturbs postnatal dopaminergic maturation in the frontal cortex and leads to adult behavioral deficits. *Neuron*, **65**, 480–489.
- Niwa, M, Jaaro-peled, H, Tankou, S, Seshadri, S, Matsumoto, Y, Cascella, NG, Kano, S, Ozaki, N, Nabeshima, T, & Sawa, A. 2013. Adolescent stress-induced epigenetic control of dopaminergic neurons via glucocorticoids. *Science*, **339**(6117), 335–339.
- Normand, EA, Crandall, SR, Thorn, CA, Murphy, EM, Voelcker, B, Browning, C, Machan, JT, Moore, CI, Connors, BW, & Zervas, M. 2013. Temporal and mosaic Tsc1 deletion in the developing thalamus disrupts thalamocortical circuitry, neural function, and behavior. *Neuron*, **78**(5), 895–909.
- Öngür, D, & Price, J L. 2000. The organization of networks within the orbital and medial prefrontal cortex of rats, monkeys and humans. *Cerebral Cortex*, **10**, 206–219.

-
- Owen, SF, Tuncdemir, SN, Bader, PL, Tirko, NN, Fishell, G, & Tsien, RW. 2013. Oxytocin enhances hippocampal spike transmission by modulating fast-spiking interneurons. *Nature*, **500**(7463), 458–462.
- Oyoshi, T, Nishijo, H, Asakura, T, Takamura, Y, & Ono, T. 1996. Emotional and behavioral correlates of mediodorsal thalamic neurons during associative learning in rats. *The Journal of Neuroscience*, **16**(18), 5812–5829.
- Ozeki, Y, Tomoda, T, Kleiderlein, J, Kamiya, A, Bord, L, Fujii, K, Okawa, M, Yamada, N, Hatten, M, Snyder, SH, Ross, CA, & Sawa, A. 2003. Disrupted-in-Schizophrenia-1 (DISC1-1): Mutant truncation prevents binding to Nude-like (NUDEL) and inhibits neurite outgrowth. *Proc. Natl. Acad. Sci. USA*, **100**(1), 289–294.
- Pakkenberg, B. 1990. Pronounced reduction of total neuron number in mediodorsal thalamic nucleus and nucleus accumbens in schizophrenics. *Arch Gen Psychiatry*, **47**(11), 1023–1028.
- Palo, OM, Antila, M, Silander, K, Hennah, W, Kilpinen, H, Soronen, P, Partonen, T, Lonnqvist, J, Peltonen, L, & Paunio, T. 2007. Association of distinct allelic haplotypes of DISC1 with psychotic and bipolar spectrum disorders and with underlying cognitive impairments. *Human Molecular Genetics*, **16**(20), 2517–2528.
- Parnaudeau, S, O'Neill, P-K, Bolkan, SS, Ward, RD, Abbas, AI, Roth, BL, Balsam, PD, Gordon, JA, & Kellendonk, C. 2013. Inhibition of mediodorsal thalamus disrupts thalamofrontal connectivity and cognition. *Neuron*, **77**(6), 1151–1162.
- Parnaudeau, S, Taylor, K, Bolkan, SS, Ward, RD, & Balsam, PD. 2014. Mediodorsal thalamus hypofunction impairs flexible goal-directed behavior. *Biological Psychiatry*, 1–9.
- Paspalas, CD, Wang, M, & Arnsten, AFT. 2013. Constellation of HCN channels and cAMP regulating proteins in dendritic spines of the primate prefrontal cortex: potential substrate for working memory deficits in schizophrenia. *Cerebral Cortex*, **23**(7), 1643–1654.
- Penzes, P, & Jones, KA. 2008. Dendritic spine dynamics - a key role for kalirin-7. *Trends in Neurosciences*, 419–427.
- Petreaanu, L, Huber, D, Sobczyk, A, & Svoboda, K. 2007. Channelrhodopsin-2 assisted circuit mapping of long-range callosal projections. *Nature Neuroscience*, **10**(5), 663–668.
- Petreaanu, L, Mao, T, Sternson, SM, & Svoboda, K. 2009. The subcellular organization of neocortical excitatory connections. *Nature*, **457**(7233), 1142–1145.
- Phillips, KG, Bartsch, U, McCarthy, AP, Edgar, DM, Tricklebank, MD, & Wafford, KA. 2012. Decoupling of sleep-dependent cortical and hippocampal interactions in a neurodevelopmental model of schizophrenia. *Neuron*, **76**(3), 526–533.
- Pletnikov, MV, Ayhan, Y, Nikolskaia, O, Xu, Y, Ovanesov, MV, Huang, H, Mori, S, & Moran, TH. 2008. Inducible expression of mutant human DISC1 in mice is associated with brain and behavioral abnormalities reminiscent of schizophrenia. *Molecular Psychiatry*, **1**, 173–186.
- Popken, GJ, Bunney, WE, Potkin, SG, & Jones, EG. 2000. Subnucleus-specific loss of neurons in medial thalamus of schizophrenics. *Proc. Natl. Acad. Sci. USA*, **97**(16), 9276–9280.
- Porteous, DJ, Thomson, PA, Millar, JK, Evans, KL, Hennah, W, Soares, DC, McCarthy, S, McCombie, WR, Clapcote, SJ, Korth, C, Brandon, NJ, Sawa, A, Kamiya, A, Roder, JC, Lawrie, SM, McIntosh, AM, St. Clair, D, & Blackwood, DH. 2014. DISC1 as a genetic risk

-
- factor for schizophrenia and related major mental illness: response to Sullivan. *Molecular Psychiatry*, **19**(2), 141–143.
- Porter, JT, Johnson, CK, & Agmon, A. 2001. Diverse types of interneurons generate thalamus-evoked feedforward inhibition in the mouse barrel cortex. *The Journal of Neuroscience*, **21**(8), 2699–2710.
- Pouchelon, G, & Jabaudon, D. 2014. Nurturing the cortex’s thalamic nature. *Current Opinion Neurology*, **27**(2), 142–148.
- Pouille, F, & Scanziani, M. 2001. Enforcement of temporal fidelity in pyramidal cells by somatic feed-forward inhibition. *Science*, **1159**(2001), 1159–1163.
- Rampino, A, Walker, RM, Torrance, HS, Anderson, SM, Fazio, L, Giorgio, AD, Taurisano, P, Gelao, B, Romano, R, Masellis, R, Ursini, G, Caforio, G, Blasi, G, Millar, JK, Porteous, DJ, Thomson, PA, Bertolino, A, & Evans, KL. 2014. Expression of DISC1-interactome members correlates with cognitive phenotypes related to schizophrenia. *Plos One*, **9**(6), 1–8.
- Rao, SG, Williams, GG, & Goldman-Rakic, PS. 2000. Destruction and creation of spatial tuning by disinhibition: GABAA blockade of prefrontal cortical neurons engaged by working memory. *The Journal of Neuroscience*, **20**(1), 485–494.
- Ray, JP, & Price, JL. 1992. The organization of the thalamocortical connections of the mediodorsal thalamic nucleus in the rat, related to the ventral forebrain-prefrontal cortex topography. *The Journal of Comparative Neurology*, **323**, 167–197.
- Rogan, SC, & Roth, BL. 2011. Remote control of neuronal signaling. *Pharmacological Reviews*, **63**(2), 291–315.
- Romanides, AJ, Duffy, P, & Kalivas, PW. 1999. Glutamatergic and dopaminergic afferents to the prefrontal cortex regulate spatial working memory in rats. *Neuroscience*, **92**(1), 97–106.
- Rose, JE, & Woolsey, CN. 1948. Structure and relations of limbic cortex and anterior thalamic nuclei in rabbit and cat. *Journal of Comparative Neurology*, **89**(3), 279–347.
- Rose, SE, Chalk, JB, Janke, AL, Strudwick, MW, Windus, LC, Hannah, DE, Mcgrath, JJ, Pantelis, C, Wood, SJ, & Mowry, BJ. 2006. Evidence of altered prefrontal thalamic circuitry in schizophrenia: an optimized diffusion MRI study. *NeuroImage*, **32**, 16 – 22.
- Rotaru, DiC, Barrionuevo, G, & Sesack, SR. 2005. Mediodorsal thalamic afferents to layer III of the rat prefrontal cortex: synaptic relationships to subclasses of interneurons. *Journal of Comparative Neurology*, **238**(May), 220 – 238.
- Rudy, B, Fishell, G, Lee, S, & Hjerling-leffler, J. 2010. Three groups of interneurons account for nearly 100% of neocortical GABAergic neurons. *Developmental Neurobiology*, **71**, 45–61.
- Saalmann, YB, Pinsk, M, Wang, L, Li, X, & Kastner, S. 2012. The pulvinar regulates information transmission between cortical areas based on attention demands. *Science*, **337**, 753–756.
- Sawaguchi, T, Matsumura, M, & Kubota, K. 1989. Delayed response deficits produced by local injection of bicuculine into the dorsolateral prefrontal cortex in Japanese macaque monkeys. *Exp Brain Res*, **75**, 457–469.

-
- Sawamura, N, Sawamura-Yamamoto, T, Ozeki, Y, Ross, CA, & Sawa, A. 2005. A form of DISC1 enriched in nucleus : Altered subcellular distribution in orbitofrontal cortex in psychosis and substance/alcohol abuse. *Proc. Natl. Acad. Sci. USA*, **102**(4), 1187–1192.
- Schlosser, RGM, Koch, K, Wagner, G, Nenadic, I, Roebel, M, Schachtzabel, C, Axer, M, & Schultz, C. 2008. Inefficient executive cognitive control in schizophrenia is preceded by altered functional activation during information encoding: an fMRI study. *Neuropsychologia*, **46**, 336–347.
- Schurov, I L, Handford, E J, Brandon, N J, & Whiting, P J. 2004. Expression of disrupted in schizophrenia 1 (DISC1) protein in the adult and developing mouse brain indicates its role in neurodevelopment. *Molecular Psychiatry*, **9**(12), 1100–10.
- Schwaller, B. 2010. Cytosolic Ca²⁺ buffers. *Cold Spring Harb Perspect Biol*, **2**, 1–20.
- Schwindel, CD, Ali, K, Mcnaughton, BL, & Tatsuno, M. 2014. Long-term recordings improve the detection of weak excitatory-excitatory connections in rat prefrontal cortex. *The Journal of Neuroscience*, **34**(16), 5454–5467.
- Seidman, LJ, Yurgelun-Todd, D, Kremen, WS, Woods, BT, Goldstein, JM, Faraone, SV, & Tsuang, MT. 1994. Relationship of prefrontal and temporal lobe MRI measures to neuropsychological performance in chronic schizophrenia. *Biological Psychiatry*, **35**(4), 235–246.
- Selemon, LD. 2013. A role for synaptic plasticity in the adolescent development of executive function. *Translational Psychiatry*, **3**, 1–9.
- Shen, S, Lang, B, Nakamoto, C, Zhang, F, Pu, J, Kuan, S-L, Chatzi, C, He, S, Mackie, I, Brandon, NJ, Marquis, KL, Day, M, Hurko, O, Mccaig, CD, Riedel, G, & St. Clair, D. 2008. Schizophrenia-related neural and behavioral phenotypes in transgenic mice expressing truncated Disc1. *The Journal of Neuroscience*, **28**(43), 10893–10904.
- Shepherd, GMG. 2013. Corticostriatal connectivity and its role in disease. *Nature Review Neuroscience*, **14**, 278–291.
- Sherman, SM, & Guillery, RW. 2002. The role of the thalamus in the flow of information to the cortex. *Phil. Trans. R. Soc. Lond.*, **357**, 1695–1708.
- Sicras-Mainar, A, Navarro-Artieda, R, Rejas-Gutiérrez, J, & Blanca-Tamayo, M. 2008. Relationship between obesity and antipsychotic drug use in the adult population: A longitudinal, retrospective claim database study in Primary Care settings. *Neuropsychiatric Disease and Treatment*, **4**(1), 219–226.
- Sikes, W, & Vogt, Brent A. 1992. Nociceptive neurons in area 24 of rabbit cingulate cortex. *Journal of Neurophysiology*, **68**(5), 1720–1732.
- Silberberg, G, & Markram, H. 2007. Disynaptic inhibition between neocortical pyramidal cells mediated by Martinotti cells. *Neuron*, **53**, 735–746.
- Singer, W. 2009. Distributed processing and temporal codes in neuronal networks. *Cogn Neurodyn*, **3**, 189–196.
- Singh, KK, Ge, X, Mao, Y, Drane, L, Meletis, K, Samuels, BA, & Tsai, L-H. 2010. Dixdc1 Is a critical regulator of DISC1 and embryonic cortical development. *Neuron*, **67**(1), 33–48.

-
- Snitz, BE, MacDonald III, AW, & Carter, CS. 2006. Cognitive deficits in unaffected first-degree relatives of schizophrenia patients: a meta-analytic review of putative endophenotypes. *Schizophrenia Bulletin*, **32**(1), 179–194.
- Sohal, VS, Zhang, F, Yizhar, O, & Deisseroth, K. 2009. Parvalbumin neurons and gamma rhythms enhance cortical circuit performance. *Nature*, **459**(7247), 698–702.
- Song, W, Li, W, Feng, J, Heston, LL, Scaringe, WA, & Sommer, SS. 2008. Identification of high risk DISC1 structural variants with a 2 % attributable risk for schizophrenia. *Biochemical and Biophysical Research Communications*, **367**, 700–706.
- Sotres-Bayon, F, Sierra-Mercado, D, Pardilla-Delgado, E, & Quirk, GJ. 2012. Gating of fear in prelimbic cortex by hippocampal and amygdala inputs. *Neuron*, **76**(4), 804–812.
- St. Clair, D, Blackwood, D, Muir, W, Carothers, A, Walker, M, Spowart, G, Gosden, C, & Evans, HJ. 1990. Association within a family of a balanced autosomal translocation with major mental illness. *Lancet*, **336**, 13–16.
- Stanford, IM. 2003. Independent neuronal oscillators of the rat globus pallidus. *Journal of Neurophysiology*, **89**, 1713–1717.
- Stein, AV, Chiang, C, & Ko, P. 2000. Top-down processing mediated by interareal synchronization. *Proc. Natl. Acad. Sci. USA*, **97**(48), 14748–14753.
- Steinecke, A, Gampe, C, Valkova, C, Kaether, C, & Bolz, J. 2012. Disrupted-in-Schizophrenia 1 (DISC1) is necessary for the correct migration of cortical interneurons. *The Journal of Neuroscience*, **32**(2), 738–745.
- Sullivan, PF. 2013. Questions about DISC1 as a genetic risk factor for schizophrenia. *Molecular Psychiatry*, **18**(10), 1050–1052.
- Sun, Q-Q, Huguenard, JR, & Prince, DA. 2006. Barrel cortex microcircuits: thalamocortical feedforward inhibition in spiny stellate cells is mediated by a small number of fast-spiking interneurons. *The Journal of Neuroscience*, **26**(4), 1219–30.
- Swadlow, HA. 2002. Thalamocortical control of feed-forward inhibition in awake somatosensory barrel cortex. *Phil. Trans. R. Soc. Lond.*, **357**, 1717–1727.
- Tan, Z, Hu, H, Huang, ZJ, & Agmon, A. 2008. Robust but delayed thalamocortical activation of dendritic-targeting inhibitory interneurons. *Proc. Natl. Acad. Sci. USA*, **105**(6), 2187–2192.
- Tandon, R, Gaebel, W, Barch, DM, Bustillo, J, Gur, RE, Heckers, S, Malaspina, D, Owen, MJ, Schultz, S, Tsuang, M, Os, JV, & Carpenter, W. 2013. Definition and description of schizophrenia in the DSM-5. *Schizophrenia Research*, **150**(1), 3–10.
- Taniguchi, Hiroki, He, Miao, Wu, Priscilla, Kim, Sangyong, Paik, Raehum, Sugino, Ken, Kvit-sani, Duda, Fu, Yu, Lu, Jiangteng, Lin, Ying, Miyoshi, Goichi, Shima, Yasuyuki, Fishell, Gord, Nelson, Sacha B, & Huang, Z Josh. 2011. A Resource of Cre driver lines for genetic targeting of GABAergic neurons in cerebral cortex. *Neuron*, 995–1013.
- Taya, S, Shinoda, T, Tsuboi, D, Asaki, J, Nagai, K, Hikita, T, Kuroda, S, Kuroda, K, Shimizu, M, Hirotsune, S, Iwamatsu, A, & Kaibuchi, K. 2007. DISC1 regulates the transport of the NUDEL/LIS1/14-3-3 epsilon complex through Kinesin-1. *The Journal of Neuroscience*, **27**(1), 15–26.

-
- Tomita, K, Kubo, K-I, Ishii, K, & Nakajima, K. 2011. Disrupted-in-Schizophrenia-1 (Disc1) is necessary for migration of the pyramidal neurons during mouse hippocampal development. *Human Molecular Genetics*, **20**(14), 2834–2845.
- Tooney, PA, & Chahl, LA. 2004. Neurons expressing calcium-binding proteins in the prefrontal cortex in schizophrenia. *Progress in Neuro-Psychopharmacology & Biological Psychiatry*, **28**, 273–278.
- Torborg, CL, Nakashiba, T, Tonegawa, S, & McBain, CJ. 2011. Control of CA3 output by feedforward inhibition despite developmental changes in the excitation-inhibition balance. *The Journal of Neuroscience*, **30**(46), 15628–15637.
- Trost, S, Platz, B, Usher, J, Scherk, H, Wobrock, T, Ekawardhani, S, Meyer, J, Reith, W, Falkai, P, & Gruber, O. 2013. DISC1 (disrupted-in-schizophrenia 1) is associated with cortical grey matter volumes in the human brain : A voxel-based morphometry (VBM) study. *Journal of Psychiatric Research*, **47**(2), 188–196.
- Uhlhaas, PJ, & Singer, W. 2011. The development of neural synchrony and large-scale cortical networks during adolescence: relevance for the pathophysiology of schizophrenia and neurodevelopmental hypothesis. *Schizophrenia Bulletin*, **37**(3), 514–523.
- Van De Werd, HJJM, Rajkowska, G, Evers, P, & Uylings, HBM. 2010. Cytoarchitectonic and chemoarchitectonic characterization of the prefrontal cortical areas in the mouse. *Brain Structure Function*, **214**, 339–353.
- Vogt, B, & Vogt, L. 2004. Cingulate cortex and disease models. *Chap. In Paxinos, pages 705–727 of: The Rat Nervous System*, 3rd edn edn. San Diego: Elsevier Academic Press.
- Vogt, BA, Rosene, DL, & Peters, A. 1981. Synaptic termination of thalamic and callosal afferents in cingulate cortex of the rat. *The Journal of Comparative Neurology*, **201**, 265–283.
- Volk, DW, & Lewis, DA. 2003. Effects of a mediodorsal thalamus lesion on prefrontal inhibitory circuitry: implications for schizophrenia. *Biological Psychiatry*, **53**, 385–389.
- Volman, V, Behrens, MM, & Sejnowski, TJ. 2011. Downregulation of parvalbumin at cortical GABA synapses reduces network gamma oscillatory activity. *The Journal of Neuroscience*, **31**(49), 18137–18148.
- Vreugdenhil, M, Jefferys, JGR, Celio, MR, & Schwaller, B. 2003. Parvalbumin-deficiency facilitates repetitive IPSCs and gamma oscillations in the hippocampus. *Journal of Neurophysiology*, **89**, 1414–1422.
- Wagner, G, Koch, K, Schachtzabel, C, Schultz, CC, Gaser, C, Reichenbach, JR, Sauer, H, Bär, K-J, & Schlösser, RG. 2013. Structural basis of the fronto-thalamic dysconnectivity in schizophrenia: A combined DCM-VBM study. *NeuroImage: Clinical*, **3**, 95–105.
- Wahlbeck, K, Westman, J, Nordentoft, M, Gissler, M, & Laursen, TM. 2011. Outcomes of Nordic mental health systems: life expectancy of patients with mental disorders. *The British Journal of Psychiatry*, **199**, 453–458.
- Wall, NR, Wickersham, IR, Cetin, A, La, MD, & Callaway, EM. 2010. Monosynaptic circuit tracing in vivo through Cre-dependent targeting and complementation of modified rabies virus. *Proc. Natl. Acad. Sci. USA*, **107**(50), 21848–21853.

-
- Walsh, T, McClellan, JM, McCarthy, SE, Addington, AM, Pierce, SB, Cooper, GM, Nord, AS, Kusenda, M, Malhotra, D, Bhandari, A, Stray, SM, Rippey, CF, Roccanova, P, Makarov, V, Lakshmi, B, Findling, RL, Sikich, L, Stromberg, T, Merriman, B, Gogtay, N, Butler, P, Eckstrand, K, Noory, L, Gochman, P, Long, R, Chen, Z, Davis, S, Baker, C, Eichler, EE, Meltzer, PS, Nelson, SF, Singleton, AB, Lee, MK, Rapoport, JL, King, M-C, & Sebat, J. 2014. Rare structural variants disrupt multiple genes in neurodevelopmental pathways in schizophrenia. *Science*, **320**(2008), 539–543.
- Wang, C-C, & Shyu, B-C. 2004. Differential projections from the mediodorsal and centrolateral thalamic nuclei to the frontal cortex in rats. *Brain Research*, **995**, 226 – 235.
- Wang, J-Y, Luo, F, Chang, J-Y, Woodward, DJ, & Han, Ji-S. 2003. Parallel pain processing in freely moving rats revealed by distributed neuron recording. *Brain Research*, **992**, 263 – 271.
- Wang, Q, Charych, E I, Pulito, V L, Lee, J B, Graziane, N M, Crozier, R a, Revilla-Sanchez, R, Kelly, M P, Dunlop, a J, Murdoch, H, Taylor, N, Xie, Y, Pausch, M, Hayashi-Takagi, a, Ishizuka, K, Seshadri, S, Bates, B, Kariya, K, Sawa, a, Weinberg, R J, Moss, S J, Houslay, M D, Yan, Z, & Brandon, N J. 2010. The psychiatric disease risk factors DISC1 and TNIK interact to regulate synapse composition and function. *Molecular psychiatry*, Sept., 1–18.
- Wang, Y, Markram, H, Goodman, PH, Berger, TK, Ma, J, & Goldman-Rakic, PS. 2006. Heterogeneity in the pyramidal network of the medial prefrontal cortex. *Nature Neuroscience*, **9**(4), 534–542.
- Watanabe, Y, & Funahashi, S. 2012. Thalamic mediodorsal nucleus and working memory. *Neuroscience and Biobehavioral Reviews*, **36**(1), 134–142.
- Watanabe, Yumiko, & Takeda, Kazuyoshi. 2009. *Population vector analysis of primate mediodorsal thalamic activity during oculomotor delayed-response performance*. Vol. 19.
- Wehr, M, & Zador, AM. 2003. Balanced inhibition underlies tuning and sharpens spike timing in auditory cortex. *Nature*, **426**(Nov.), 442–446.
- Whitt, JL, Masri, R, Pulimood, NS, & Keller, A. 2013. Pathological activity in mediodorsal thalamus of rats with spinal cord injury pain. *The Journal of Neuroscience*, **33**(9), 3915–3926.
- Winklbaur, B, Ebner, N, Sachs, G, Thau, K, & Fischer, G. 2006. Substance abuse in patients with schizophrenia. *Dialogues in Clinical Neuroscience*, **8**(1), 37–43.
- Woo, T-U, Miller, JL, & Lewis, DA. 1997. Schizophrenia and the parvalbumin-containing class of cortical local circuit neurons. *Am J Psychiatry*, **154**(7), 1013–1015.
- Woodruff, AR, McGarry, LM, Vogels, TP, Inan, M, Anderson, SA, & Yuste, R. 2011. State-dependent function of neocortical chandelier cells. *The Journal of Neuroscience*, **31**(49), 17872–17886.
- Woods, BT. 1998. Is schizophrenia a progressive neurodevelopmental disorder? Toward a unitary pathogenetic mechanism. *Am J Psychiatry*, **155**(12), 1661–1670.
- Woodward, N, Karbasforoushan, H, & Heckers, S. 2012. Thalamocortical dysconnectivity in schizophrenia. *Am J Psychiatry*, **169**(10), 1092–1099.
- Xu, H, Jeong, H-Y, Tremblay, R, & Rudy, B. 2013. Neocortical somatostatin-expressing GABAergic interneurons disinhibit the thalamorecipient layer 4. *Neuron*, **77**(1), 155–167.

-
- Xu, Q, Cobos, I, De La Cruz, E, Rubenstein, JL, & Anderson, SA. 2004. Origins of cortical interneuron subtypes. *The Journal of Neuroscience*, **24**(11), 2612–2622.
- Xu, W, & Südhof, TC. 2013. A neural circuit for memory. *Science*, **339**, 1290–1295.
- Xue, M, Atallah, BV, & Scanziani, M. 2014. Equalizing excitation-inhibition ratios across visual cortical neurons. *Nature*, **511**(7511), 596–600.
- Yizhar, O, Fenno, LE, Prigge, M, Schneider, F, Davidson, TJ, Shea, DJO, Sohal, VS, Goshen, I, Finkelstein, J, Paz, JT, Stehfest, K, Fudim, R, Ramakrishnan, C, Huguenard, JR, Hegemann, P, & Deisseroth, K. 2011. Neocortical excitation/inhibition balance in information processing and social dysfunction. *Nature*, **477**(7363), 171–178.
- Young, KA, Manaye, KF, Liang, C-L, Hicks, PB, & German, DC. 2000. Reduced number of mediodorsal and anterior thalamic neurons in schizophrenia. *Biological Psychiatry*, **47**, 944–953.
- Yu, C, Fan, D, Lopez, A, & Yin, HH. 2012. Dynamic changes in single unit activity and gamma oscillations in a thalamocortical circuit during rapid instrumental learning. *Plos One*, **7**(11), 1–10.
- Zhang, F, Wang, L, Boyden, ES, & Deisseroth, K. 2006. Channelrhodopsin-2 and optical control of excitable cells. *Nature Methods*, **3**(10), 785–792.
- Zhou, Y, Liang, M, Jiang, T, Tian, L, & Liu, Y. 2007. Functional dysconnectivity of the dorso-lateral prefrontal cortex in first-episode schizophrenia using resting-state fMRI. *Neuroscience Letters*, **417**, 297–302.

.1 Supplementary figures

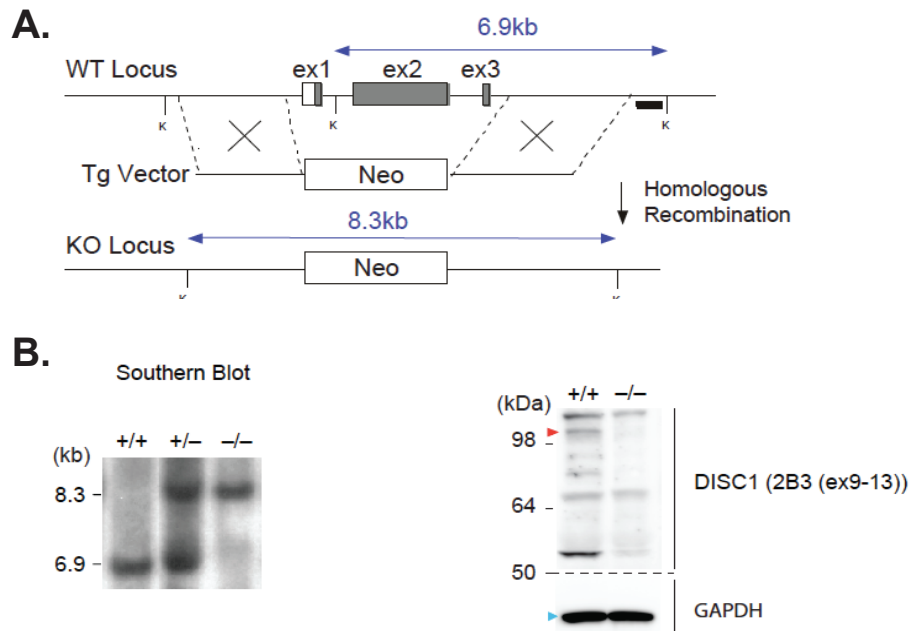


Figure 1: Generation of Disc1 locus impairment mice. A. Schematic diagram of exon targeting and deletion strategy. The genomic regions flanking Disc1 exon 1 and 3 were used as homology arms to replace the exons 1 to 3 with a neomycin cassette. B. Southern blotting confirms successful targeting of Disc1 in homozygous mutant (-/-) mice. C. Western blotting using mouse Disc1 antibodies raised against exons 9-13 (2B3) confirms depletion of the immunoreactivity corresponding to full-length Disc1 isoform.

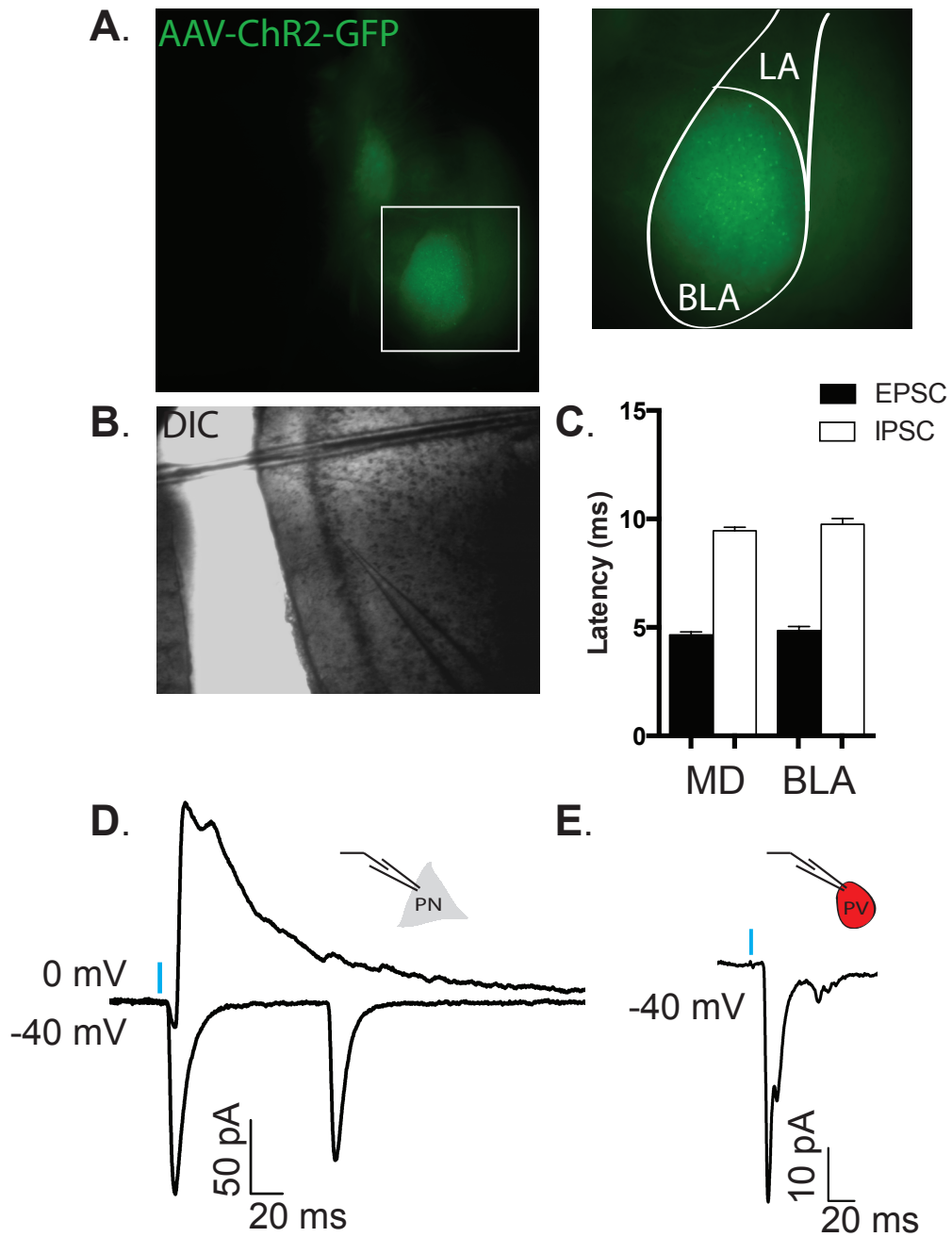


Figure 2: BLA inputs to ACC recruit IPSCs with the same latency seen in the MD-ACC projection. A. Sample AAV-ChR2-GFP injection into the BLA. B. Image of recorded PN in layer II/II. C. EPSC and IPSC onset latencies are consistent between the MD-ACC and BLA-ACC projection pathways $p > .05$. D. Sample trace of BLA-evoked EPSC and IPSC. E. Sample trace of BLA-evoked EPSC onto superficial PV IN.

.2 List of abbreviations

AAV	adeno-associated virus
ACC	anterior cingulate cortex
ACSF	artificial cerebral spinal fluid
AMPA	α -Amino-3-hydroxy-5-methyl-4-isoxazolepropionic acid
ANOVA	analysis of variance
AP-5	DL-2-Amino-5-phosphonopentanoic acid
BLA	basolateral amygdala
Cdk5	cyclin-dependent kinase 5
Cg	cingulate
ChR2	channelrhodopsin-2
CL	centrolateral nucleus of the thalamus
CNO	8-Chloro-11-(4-methyl-1-piperazinyl)-5H-dibenzo[b,e](1,4)diazepine N-oxide
CNQX	6-Cyano-7-nitroquinoxaline-2,3-dione
Cre	Cre-recombinase
CTB	cholera toxin B (conjugated to Alexa-Flour-555)
DIO-	double floxed inverse open reading frame
DISC1	Disrupted-in-Schizophrenia 1
DISC1 LI	DISC1 locus impairment
Dixdc1	DIX domain containing 1
DLPFC	dorsolateral prefrontal cortex
DNMS	delayed nonmatch-to-sample working memory task
DNMTP	delayed nonmatch-to-place working memory task
DREADD	designer receptor exclusively activated by designer drug
DSM-5	fifth edition of the Diagnostic and Statistical Manual of Mental Disorders
E#	embryonic day
E/I	excitation : inhibition
EnvA	avian sarcoma leucosis virus glycoprotein EnvA
EPSC	excitatory postsynaptic current
G#	gestational day
GABA	γ -aminobutyric acid

GDP	guanine diphosphate
GTP	guanine triphosphate
Glur1	glutamate receptor subunit 1
GFP	green fluorescent protein
GSK3β	glycogen synthase kinase 3 beta
hDISC1	truncated form of human DISC1
HET	heterozygous, referring to mice with loss of 1 copy of DISC1
IL	infralimbic cortex
IN	interneuron
IMD	intermediodorsal nucleus of the thalamus
IPSC	inhibitory postsynaptic current
IT	intratelencephalic
KD	knockdown
LFS	low frequency stimulation
LO	lateral orbital frontal cortex
LTD	long term depression
MAM	methylazoxymethanol
M2	secondary motor cortex
MD	mediodorsal nucleus of the thalamus
mPFC	medial prefrontal cortex
mEPSC	miniature excitatory postsynaptic current
mIPSC	miniature inhibitory postsynaptic current
MRS	magnetic resonance spectroscopy
NDEL1	NudE nuclear distribution E homolog (A. nidulans)-like 1
NMDA	<i>N</i> -methyl-D-aspartate
NpHR3.0	halorhodopsin 3.0
P#	postnatal day
PFC	prefrontal cortex
PIT	Pavlovian-to-instrumental transfer
PN	pyramidal neuron
PPR	paired pulse ratio
PrL	prelimbic Cortex

PSD95	post synaptic density 95
PT	pyramidal tract
PV	parvalbumin
TC	thalamocortical
TRE	tetracycline response element
VPM	ventral posteromedial nucleus of the thalamus
shRNA	short hairpin RNA
SNP	single nucleotide polymorphism
SZ	schizophrenia
t(1;11)	chromosomal translocation between chromosome 1 and 11
TNIK	TRAF2 and NCK interacting kinase
TTX	tetrodotoxin
TRN	thalamic reticular nucleus
TVA	avian tumor virus receptor A
vHipp	ventral hippocampus
VO	ventral orbital frontal cortex
WT	wildtype
ZI	zona incerta